

*Max-Planck Institut für
molekulare Physiologie*



*Technische Universität
Dortmund*

Development of Contractive Synthesis of Cyclobutanes from Pyrrolidines

Dissertation

For the achievement of the academic degree of the

Doctor in Natural Science

(Dr. rer. nat.)

Submitted to

The Faculty of Chemistry and Chemical Biology

Technical University of Dortmund

By

M.Sc. Chun-Ngai Hui

from Hong Kong, China

Dortmund 2021

1. Gutachter: Prof. Dr. Dr. h.c. Herbert Waldmann
2. Gutachter: Prof. Dr. Andrey P. Antonchick

The present dissertation was written in the period from September 2018 to September 2021 under the supervision and guidance of Prof. Dr. Dr. h.c. Herbert Waldmann at Faculty of Chemistry and Chemical Biology at the Technical University of Dortmund and the Max-Planck-Institute for Molecular Physiology in Dortmund.

Results presented in this thesis contributed to the following publication:

1. C. Hui, L. Brieger, C. Strohmann, A. P. Antonchick*

Stereoselective synthesis of cyclobutanes by contraction of pyrrolidines. *J. Am. Chem. Soc.*

Manuscript submitted and under review.

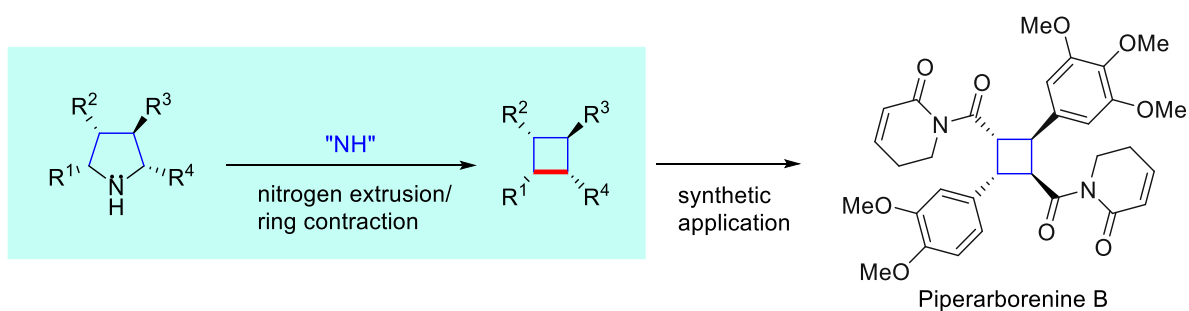
Contents

Abstract.....	6
1. Introduction.....	8
1.1 Contractive synthesis of carbocycle.....	10
1.1.1 Semi-pinacol rearrangement.....	11
1.1.2 Benzilic acid rearrangement	13
1.1.3 Wolff rearrangement	14
1.2 Nitrogen extrusion	17
1.2.1 Cyclopropane formation from 1,2-diazene	19
1.2.2 Dimerization via 1,2-diazene fragmentation.....	21
1.2.3 Trimethylenemethane diyl [3+2] cycloaddition.....	25
1.3 The development of iodonitrene chemistry and its applications	27
1.3.1 Direct <i>N-H</i> transfer to sulfoxides and sulfonamides	29
1.3.2 Terminal diazirine from amino acid through tandem decarboxylation/iodonitrene transfer	30
1.4 Summary.....	32
2. Aim of the Thesis.....	33
3. Stereoselective synthesis of cyclobutanes by contraction of pyrrolidines	34
3.1 Introduction.....	34
3.2 Reported synthesis of cyclobutanes <i>via</i> nitrogen extrusion.....	36
3.3 Preliminary study.....	38
3.4 Optimization of condition.....	40
3.4.1 Screening of solvent	40
3.4.2 Screening of oxidant.....	41
3.4.3 Screening of nitrogen source	43
3.4.4 Screening of reaction temperature	44
3.4.5 Screening of equivalence of reagents.....	45
3.5 Study of the substrate scope.....	46
3.6 Investigation of reaction mechanism.....	49
3.7 Cytotoxic cyclobutane natural product Piperarborenine B.....	51
3.8 Reported synthesis of cytotoxic natural product Piperarborenine B.....	52
3.9 Retrosynthetic analysis of piperarborenine B	54
3.9 Formal synthesis of piperarborenine B using ring contraction approach	55
3.10 Improvement of ring contraction step of piperarborenine B's synthesis.....	56
4 Summary of the thesis	58
5. Experimental section	59
5.1 General Information	59
5.2 General Procedure for the preparation of pyrrolidines	61

General Procedure A	61
General Procedure B	61
5.3 General Procedure for the synthesis of cyclobutanes from pyrrolidines.	62
General procedure C	62
General procedure D	62
5.5 Characterization data for pyrrolidines	63
5.6 Characterization data for cyclobutanes	78
5.7 Further investigation of contractive synthesis of cyclobutanes from pyrrolidines	93
5.71 Ring contraction using enantioenriched pyrrolidine	93
5.72 Ring contraction of <i>N</i>-aminopyrrolidine	96
5.73 Oxidation of pyrrolidine as side reaction	98
5.8 Formal synthesis of piperarborenine B	100
5.9 Synthesis and characterization of synthetic intermediates	101
5.91 Observation of olefinic side products using general procedure C	104
5.92 Synthesis of <i>N</i>-aminopyrrolidine	106
5.10 X-ray diffraction (XRD) analysis	107
6. Reference	126
7. Appendix	132
7.1 List of abbreviations	132
7.2 Acknowledgement	135

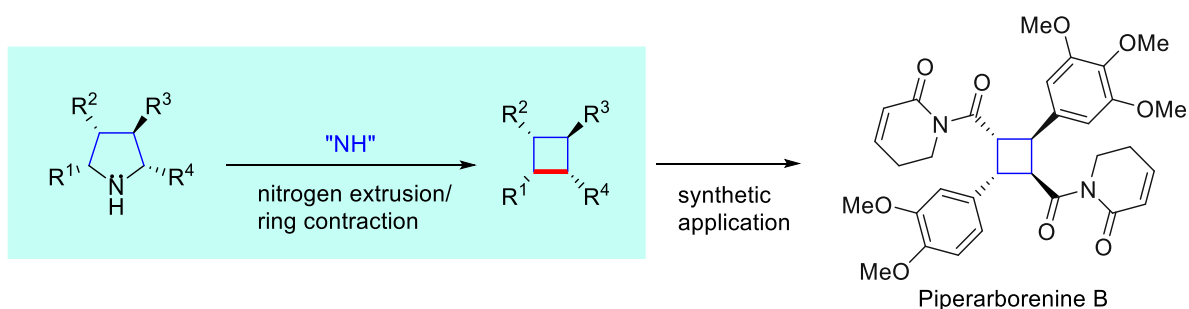
Abstract

Carbocycles are omnipresent in chemical pharmaceuticals, biologically active natural products and organic functional materials. Construction of structurally intriguing, highly functionalized small carbocycles with congested stereocenters remain to be an intricate task in organic chemistry. Consistent endeavor such as innovation of chemical methodology and development of synthetic tactics has been made to improve the synthetic efficiency to these complex structures. In particular, the synthesis of carbocycle through ring contraction, which complies with the concept of synthetic efficiency in modern organic chemistry, has been widely applied in organic synthesis of complex architectures. In this thesis, the unprecedented, stereospecific and contractive synthesis of multi-substituted cyclobutanes from corresponding pyrrolidines is discussed. The reaction mechanism is investigated and the reaction was applied to the synthesis of cytotoxic natural product piperarborenine B.



Kurzzusammenfassung

Carbocycles sind in chemischen Pharmazeutika, biologisch aktiven Naturstoffen und organischen Funktionsmaterialien allgegenwärtig. Der Aufbau strukturell faszinierender, hoch funktionalisierter kleiner Carbocyclen mit überfüllten Stereozentren bleibt eine schwierige Aufgabe in der organischen Chemie. Konsequente Bemühungen wie die Innovation der chemischen Methodik und die Entwicklung von Synthesetaktiken wurden unternommen, um die Syntheseeffizienz dieser komplexen Strukturen zu verbessern. Insbesondere die Synthese von Carbocyclen durch Ringkontraktion, die dem Konzept der Syntheseeffizienz in der modernen organischen Chemie entspricht, findet breite Anwendung in der organischen Synthese komplexer Architekturen. In dieser Arbeit wird die beispiellose stereospezifische und kontraktive Synthese von mehrfach substituierten Cyclobutanen aus entsprechenden Pyrrolidinen diskutiert. Der Reaktionsmechanismus wird untersucht und die Reaktion auf die Synthese des zytotoxischen Naturstoffs Piperarborenin B angewendet.

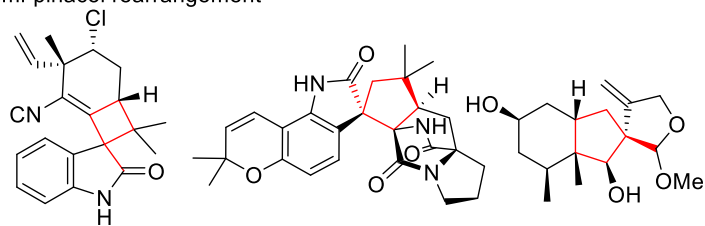


1. Introduction

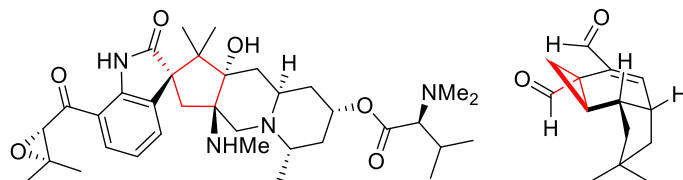
Carbocycles are omnipresence in chemical pharmaceuticals, biologically active natural products and organic functional materials. Construction of structurally intriguing carbocycles such as highly-strained fused ring^{1, 2}, spirocycles³ and/or highly-functionalized carbocycles with congested stereocenters^{4, 5} remain to be a daunting task in organic chemistry. Therefore, the efficient synthesis of these practically useful and synthetically demanding small-size carbocycles is of uttermost importance to satisfy the demand from the synthetic communities.⁶ Various strategies and/or logics, including step economy⁷, chemoselectivity⁸, protecting group free synthesis⁹, atom economy¹⁰ and redox economy¹¹, were proposed to improve the efficiency of synthetic design.⁷⁻¹⁵ The contractive synthesis of carbocycle, which usually complies with these values, has been widely applied in complex natural product synthesis. **(Figure 1.1)** Synthetic methods, such as cycloaddition¹⁶⁻²⁰, cyclization²¹⁻²⁸ and cascade reaction²⁹⁻³⁵, are used routinely to build the carbocyclic structure. Alternatively, ring contraction methods including *rearrangement reaction* or *gas extrusion reaction* generates smaller carbocycle with highly-condensed functionalities and/or stereocentres from the parental skeleton. Compared to routine methods, ring contraction usually require the preparation of precursor carrying necessary functionalities. Fascinated by the contemporary advancements and the prospect of contractive synthesis of carbocycle, the contractive synthesis appears as an important synthetic strategy to forge congested and highly functionalized carbocycles. Contractive synthesis of carbocycle and its role in organic synthesis are illustrated and could provide insights to yet addressed synthetic dilemma, for instance, the rapid construction of highly functionalized core skeleton of bioactive natural product and the dead-end total synthesis.

In this section, the methods of contractive synthesis of carbocycles in organic synthesis are illustrated. Ring contraction based on nitrogen extrusion, which may involve the generation of biradical intermediate, are elaborated and discussed in the next section.

A. Semi-pinacol rearrangement



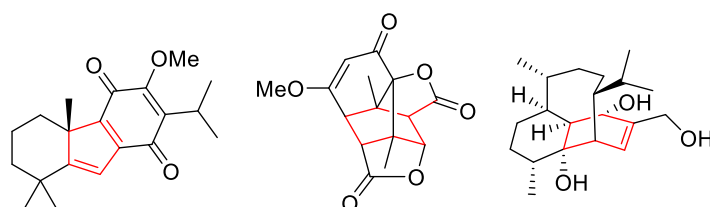
(+)-Welwitindolinone A (1) (+)-Notoamide B (2) (-)-Peribysin E (3)



Citrinadin A (4)

Isovelleral (5)

B. Benzilic acid rearrangement

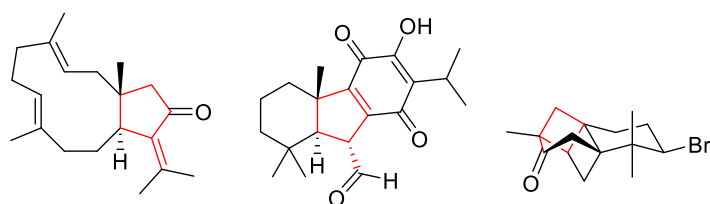


(-)-Taiwaniaquinone H (6)

Preisolactone A (7)

(-)-Vinigrol (8)

C. Wolff rearrangement

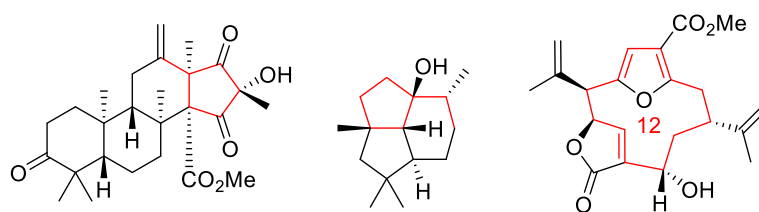


Taiwaniaquinone A (10)

Dolabellatrienone (9)

Aplydactone (11)

D. Other rearrangement methods



Terrenoid (12)

Presilphiperfolan-1-ol (13)

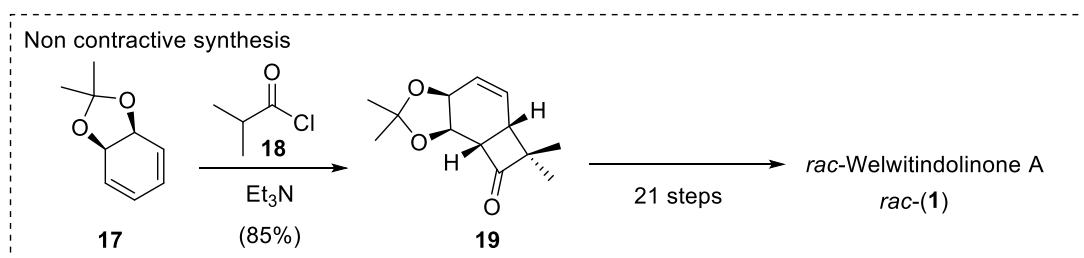
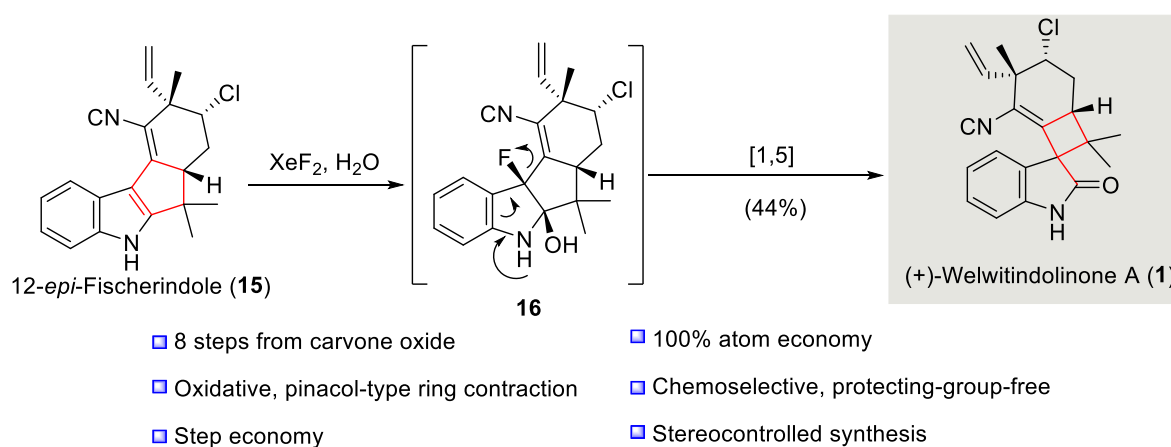
11-Gorgiacerol (14)

Figure 1.1 Selected examples of natural product synthesis achieved by contractive synthesis of carbocycle. **A.** Semipinacol rearrangement. **B.** Benzilic acid type rearrangement. **C.** Wolff rearrangement. **D.** Other rearrangement methods

1.1 Contractive synthesis of carbocycle

Ring contraction based on 1,2-rearrangement has been applied widely in organic synthesis. In particular, the use of semi-pinacol rearrangement, benzylic acid rearrangement including its variants α -ketol rearrangement, Wolff rearrangement and miscellaneous 1,2-rearrangement reactions in natural product synthesis are discussed.

The protecting-group-free synthesis of (+)-welwitindolinone A (**1**) features oxidative, pinacol-type rearrangement to construct the cyclobutane structure from cyclopropentane moiety of 12-*epi*-fischerindole I (**15**)³⁶ (**Scheme 1.1**). Fluorohydroxylation of indole **15** was facilitated by XeF₂/H₂O and subsequent pinacol rearrangement resulted in 1,2-carbon migration through [1,5] sigmatropic shift to give an oxindole (**1**) in 44 % yield. Alternatively, the first total synthesis of *rac*-**1** required 22 steps³⁷⁻³⁹, which involved the early construction of cyclobutane **19** followed by a sequence of functional group transformations. The oxidative pinacol-type reaction-based ring contraction of (**15**) showed perfect atom-economy, good chemoselectivity without no protecting group and was under stereocontrol.



Scheme 1.1 An oxidative pinacol-type rearrangement is used to convert 12-*epi*-fischerindole (**15**) to an oxindole (+)-welwitindolinone A (**1**)³⁶ (inset, non-contractive synthesis of *rac*-welwitindolinone A *rac*-**1**)).³⁷⁻³⁹

1.1.1 Semi-pinacol rearrangement

The 1,2-carbon migration between two vicinal atoms creates structural complexity *via* skeletal rearrangement, which is the principal mechanism of numerous classical named rearrangement reactions. Semi-pinacol rearrangement is an organic transformation that involves a 1,2-migration of a C-C or C-H bond that is centered on the oxygen containing carbon and that occurs towards the vicinal electrophilic carbon center, generating a carbonyl group at the end of the process.⁴⁰ Semi-pinacol rearrangement allows the contractive synthesis of smaller carbocycle and are applied widely in organic synthesis (**Scheme 1.2**).⁴¹⁻⁴³

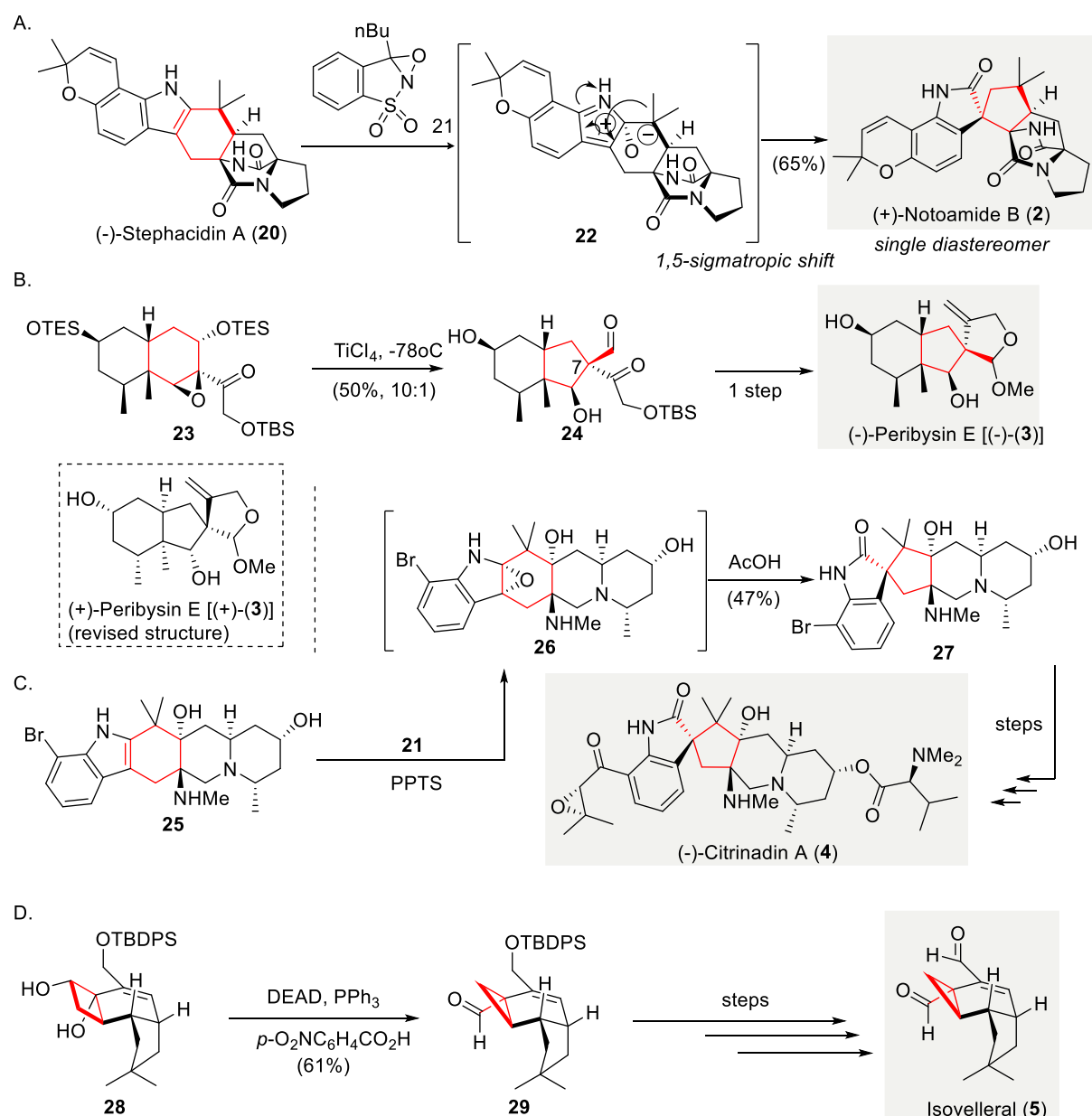
The synthesis of oxindole (+)-notoamide B (**2**) is accomplished by a biomimetic, oxidative semipinacol rearrangement using Davis' oxaziridine **21**^{44 45, 46} (**Scheme 1.2A**). Regioselective epoxidation of the (-)-stephacidin A (**20**) at sterically less-hindered α -face and subsequent epoxide opening gave intermediate **22**. Ring contraction at α -face of **22** *via* a [1,5] sigmatropic shift successfully afforded (+)-notoamide B (**2**) in 65% yield as a single diastereomer. This biomimetic maneuver converting an indole structure to corresponding oxindole using Davis' oxaziridine were reported thereafter.⁴⁷⁻⁵⁰

The synthesis of (-)-peribysine E [(-)-**3**] uses semipinacol-type rearrangement to facilitate the contractive synthesis of C7 quaternary center-bearing fused cyclopentane **24**.^{51, 52} (**Scheme 1.2B**) Treatment of epoxide **23** with titanium chloride afforded cyclopentane **24** in 50% yield, which was converted to (-)-peribysine E [(-)-**3**] in one step.⁵³ The revised structure was proved to be (+)-peribysine E [(+)-**3**] and was mis-assigned as (-)-peribysine E [(-)-**3**].

The enantioselective synthesis of (-)-citrinadin A (**4**) features a substrate-controlled, oxidative semipinacol rearrangement of indole **25** to oxindole **27** by using William's approach⁴⁶⁻⁴⁸ (**Scheme 1.2C**). Amino groups on indole **25** were protected upon treatment with pyridine *p*-toluenesulfonate, and subsequent exposure to excessive amount of Davis' oxaziridine **21** afforded epoxide **26** as intermediate, which was subjected to semi-pinacol rearrangement effecting by acetic acid to give **27** in 47% yield. A variety of oxidants besides Davis' oxaziridine **21**, such as *tert*-BuOCl, OsO₄, and NBS, failed to give oxindole **26**.⁵⁴

The synthesis of sesquiterpenoid isovelleral (**5**) reveals the preparation of cyclopropane **29** through an unexpected semi-pinacol type rearrangement⁵⁵ (**Scheme 1.2D**). When cyclobutanediol **28** was subjected to Mitsunobu's condition (i.e. DEAD, PPh₃ and *p*-O₂NC₆H₄CO₂H), an unexpected semi-pinacol rearrangement occurred to give cyclopropane **29**

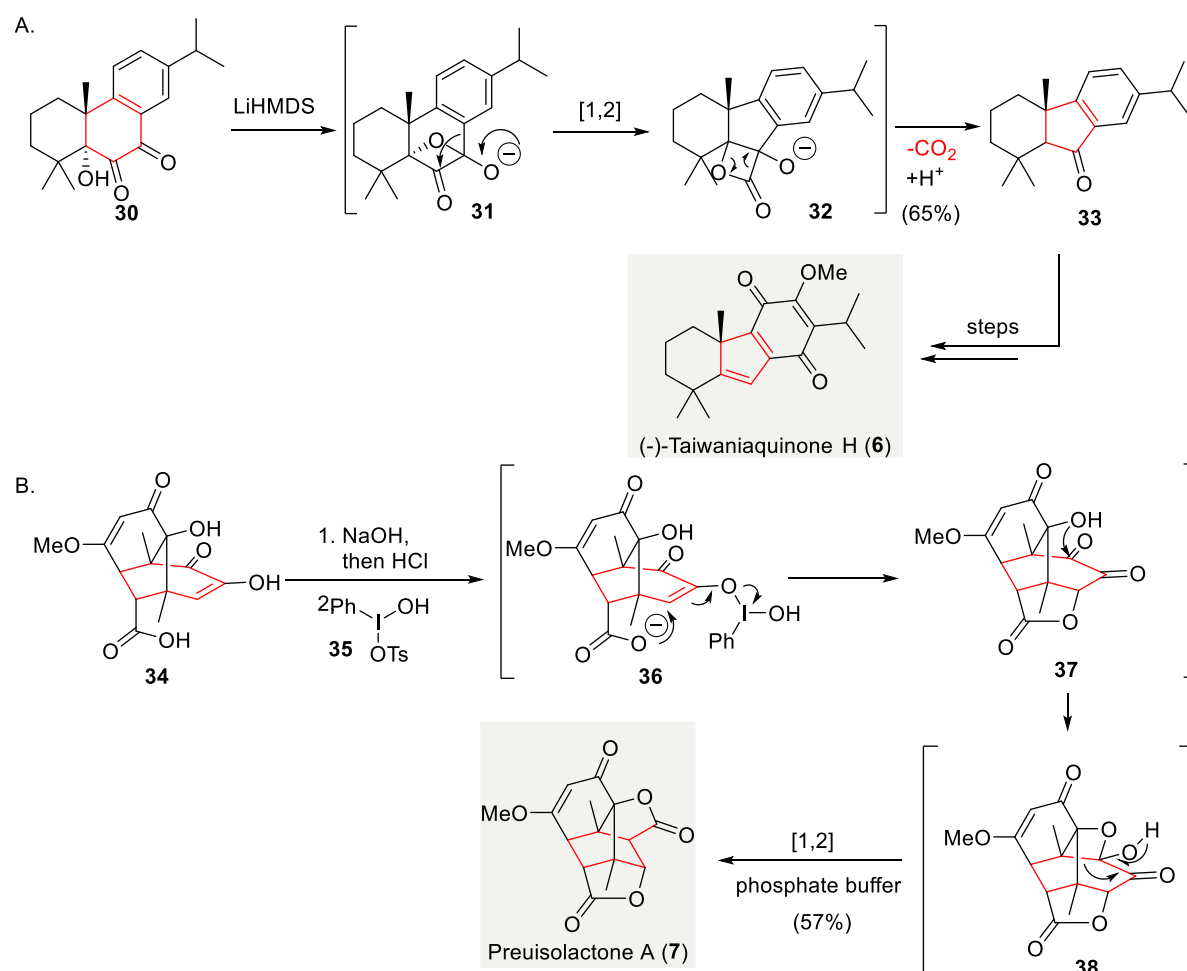
in 61% yield without observing the expected stereo-inverted product (not described). Ring contraction of cyclobutanediol to quaternary carbon containing cyclopropane could be used as an efficient strategy to prepare fused cyclopropane.⁵⁶



Scheme 1.2 Semi-pinacol rearrangement in organic synthesis. **A.** Biomimetic, oxidative semipinacol rearrangement facilitates conversion of (-)-stephacidin A (**20**) to (+)-notoamide B (**2**).^{45, 46, 57} **B.** The synthesis of (-)-peribysin E [(-)-(3)] involves a semipinacol type reaction to build the [6,5] fused ring structural skeleton **24** from **23** with [6,6] fused ring⁵¹. **C.** Diastereoselective epoxidation with Davis' oxaziridine **21** and subsequent acid-promoted rearrangement accesses to oxindole precursor **70** in the enantioselective synthesis of (-)-citrinadin A (**4**)⁴⁷. **D.** An unexpected semipinacol-type reaction occurs under Mitsunobu's condition in the preparation of isovelleral (**5**)⁵⁸

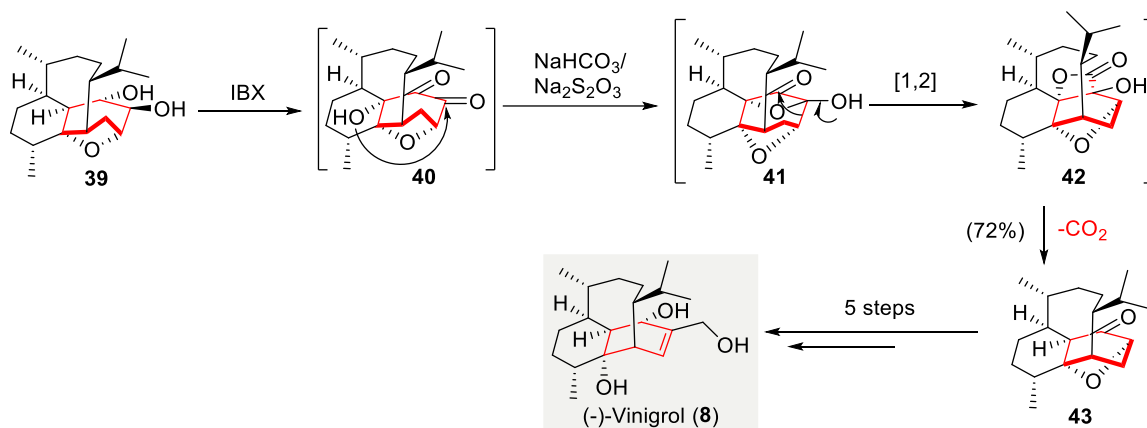
1.1.2 Benzylic acid rearrangement

The synthesis of (-)-taiwaniaquinone H (**6**) features benzylic acid rearrangement as key reaction to forge the 6-5-6 tricycle **33**.⁵⁹ (Scheme 1.3A) Treatment of 1,2-diketone **30** with LiHMDS resulted in the formation of oxetane intermediate **31**, which underwent 1,2-carbon migration of the aryl group to give an intermediate lactone **32**. Successive decarboxylation and protonation of **32** afforded the desired tricyclic ketone **33**, which is the precursor of (-)-taiwaniaquinone H (**6**). Ring contraction *via* benzylic acid rearrangement completes the synthesis of preisolactone A (**7**)⁶⁰ (Scheme 1.3B). Under alkaline condition, Koser's reagent **35** oxidized enol **34** resulted in the formation of lactone **37**. In this process, enolized 1,2-diketone **34** was activated to give hypervalent iodine (III) species **36**. The resultant 1,2-diketone **37** was converted to an oxetane **38** followed by a 1,2-carbon migration upon workup with aqueous phosphate buffer (pH = 8) to afford preisolactone A (**7**) in 57% yield.



Scheme 1.3 Ring contraction enabled by Benzylic acid rearrangement in organic synthesis. **A.** Benzylic acid rearrangement *en route* to (-)-taiwaniaquinone H (**6**).⁵⁹ **B.** A late-stage benzylic acid rearrangement *en route* to preisolactone A (**7**).⁶⁰

The synthesis of (-)-vinigrol (**8**) features an unexpected decarboxylative ring contraction to afford the 1,5-butanodecahydronaphthalene **43** as a synthetic precursor.⁶¹ (**Scheme 1.4**) An IBX oxidation of diol **39** gave 1,2-diketone **40**, in which the α -hydroxy group attacked the less hindered ketone to give oxetanone **41** followed by 1,2-carbon migration to give an unstable β -lactone **42**. This β -lactone **42**, which was isolated and characterized, underwent spontaneous decarboxylation and epimerization to give the desired **43** in 72% yield.



Scheme 1.4 An unexpected decarboxylative ring contraction is used in the synthesis of (-)-vinigrol (**8**).⁶¹

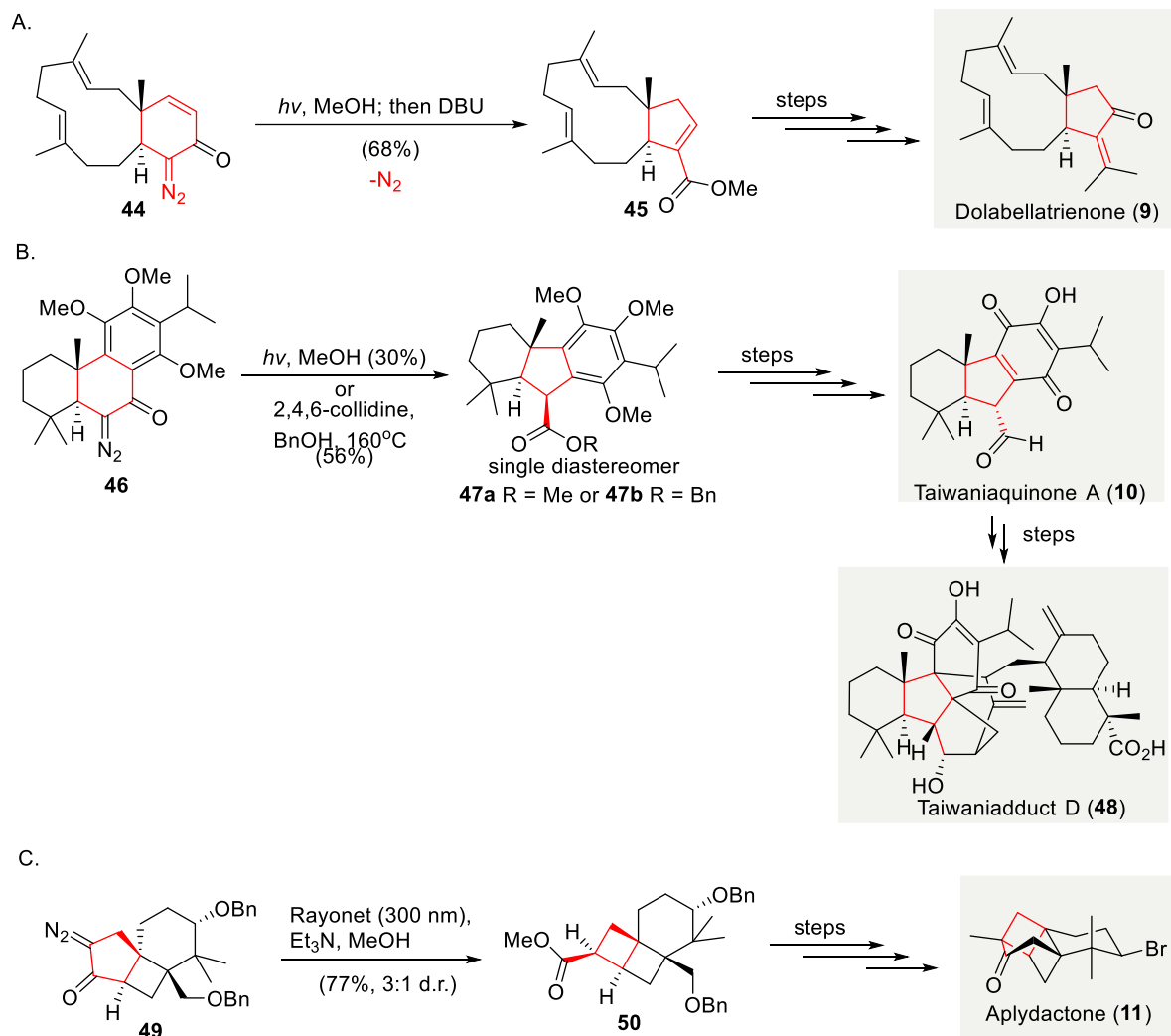
1.1.3 Wolff rearrangement

The synthesis of dolabellatrienone (**9**) relies on Wolff rearrangement to produce chiral dolabellane derivative **45** in 68% yield.⁶² (**Scheme 1.5A**) Upon photoirradiation of α,β -unsaturated diazoketone **44** followed by heating in neat DBU, the ring-contracted ester **45** was furnished through an α -keto carbene intermediate.

The synthesis of taiwaniaquinone A (**10**)⁶³ and taiwaniadduct D (**48**)⁶⁴ adopts a Wolff rearrangement as key reaction to prepare the 6-5-6 tricyclic core **47a** or **47b** from 6-6-6 tricyclic diazo compound **46**. (**Scheme 1.5B**) Irradiation of diazo compound **46** with mercury lamp in methanol afforded the desired product **47a** in 30% yield as single diastereomer. Due to the decreased efficiency on scale-up reaction under photoirradiation, thermal condition (BnOH, 2,4,6-collidine, 160°C) was attempted and the desired benzyl ester **47b** was isolated in 56% yield as single diastereomer.

Trauner's synthesis of aplydactone (**11**) features a Wolff rearrangement-oriented synthesis of fused cyclobutane **50**.⁶⁵ (**Scheme 1.5C**) Upon photoirradiation of α -diazo cyclopentanone **49**, the ladderane **50** was formed in 77% yield with a 3:1 d.r.. Later, the same strategy was adopted

to prepare fused cyclobutane by Zhang⁶⁶ in their total synthesis of aplydactone (**11**) (synthesis not described).

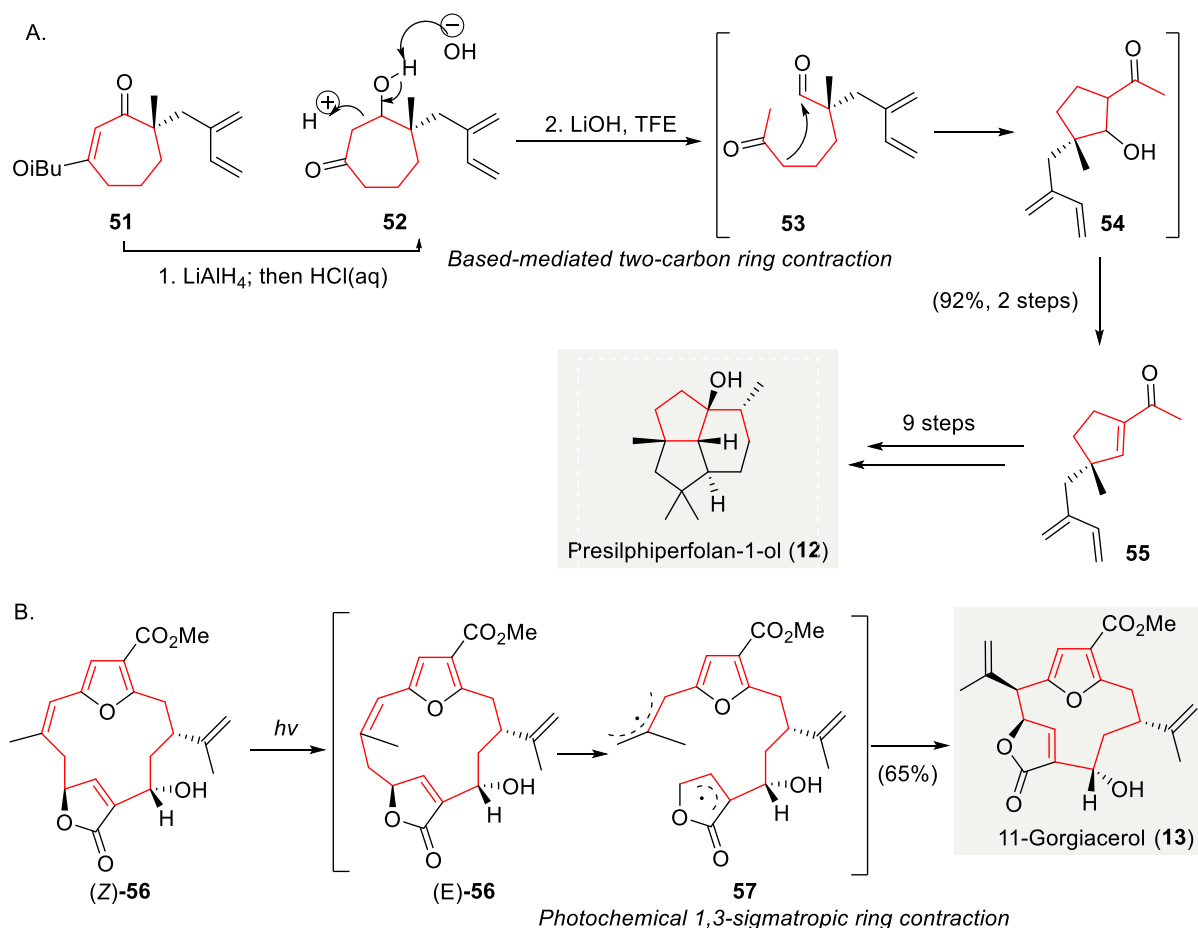


Scheme 1.5 Ring contraction enabled by Wolff rearrangement in organic synthesis. **A.** Wolff rearrangement features as key reaction in the synthesis of dolabellatrienone (**9**).⁶² **B.** Synthesis of taiwaniaquinone A (**10**) and taiwaniadduct D (**48**) reveal a conversion of [6.6.6]-tricyclic fused ring **46** to [6.5.6] tricyclic fused ring **47a** or **47b**.^{63, 64} **C.** Synthesis of aplydactone (**11**) demonstrates the preparation of [4.4.6] tricyclic fused ring **50**.^{65, 66}

1.1.4 Miscellaneous 1,2-carbon migration methods

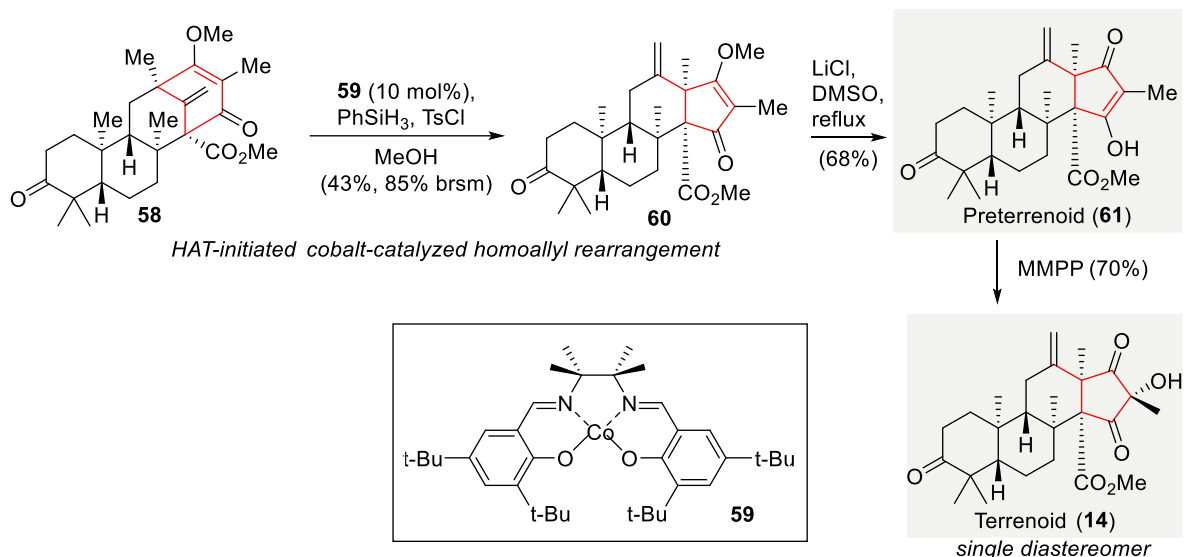
The synthesis of presilphiperfolan-1-ol (**12**) makes use of a base-mediated two-carbon ring contraction to give acylcyclopentene **55**^{67, 68} (**Scheme 1.5A**). Reduction of α -quaternary vinylogous ester **51** by LiAlH_4 gave intermediate β -hydroxyketone **52**, which was exposed to lithium hydroxide in 2,2,2-trifluoroethanol to give the desired densely functionalized chiral acylcyclopentene **55** in 92% yield over two steps. The synthesis of presilphiperfolan-1-ol (**12**) requires a 9-step synthesis from **55**.

The synthesis of 11-gorgiacerol (**13**) features a photochemical 1,3-sigmatropic ring contraction^{69, 70} as a synthetic key step⁷¹ (**Scheme 1.5B**). Photoirradiation of **56** led to olefin *Z*-to-*E* isomerization followed by a [1,3]-sigmatropic shift to give 11-gorgiacerol (**13**) in 65% yield.



Scheme 1.6 Ring contraction enabled by miscellaneous rearrangement reactions in organic synthesis. **A.** A base-mediated two-carbon ring contraction⁷² allows efficient access to acylcyclopentene **55** as key intermediate in the synthesis of presilphiperfolan-1-ol (**12**)^{67, 68}. **B.** An photochemical 1,3-sigmatropic ring contraction *en route* to 11-gorgiacerol (**13**).⁷¹

The synthesis of terretonin meroterpenes (e.g. terrenoid (**14**)) harnesses hydrogen atom transfer-initiated homoallyl rearrangement⁷² (**Scheme 1.5C**). Treatment of **57** with 10 mol% of cobalt (II) catalyst **58** and phenylsilane in the presence of tosyl chloride⁷³ afforded **59** in 43% yield. Demethylation of **59** with lithium chloride under reflux afforded preterrenoid (**60**), which was subjected to stereoselective oxidation with magnesium monoperoxyphthalate to give terrenoid (**14**).



Scheme 1.7 Ring contraction enabled by miscellaneous rearrangement reactions in organic synthesis. HAT-initiated cobalt-catalyzed homoallyl rearrangement *en route* to terrenoid (**14**)⁷²

1.2 Nitrogen extrusion

Nitrogen extrusion reaction has been widely applied in complex natural product synthesis. With less exception such as rhodium-catalyzed nitrenoid insertion, most of the nitrogen extrusion reaction facilitate C-C bond formation involving a possible radical-based mechanism. In general, there are three types of radical based nitrogen extrusion reaction that are applied to synthesis of carbocycles (**Figure 1.2**), namely (i) cyclopropane formation from 1,2-diazene, (ii) dimerization *via* 1,2-diazene fragmentation, and (iii) trimethylenemethane-diyl [3+2] cycloaddition (*aka.* TMM diyl [3+2] cycloaddition).

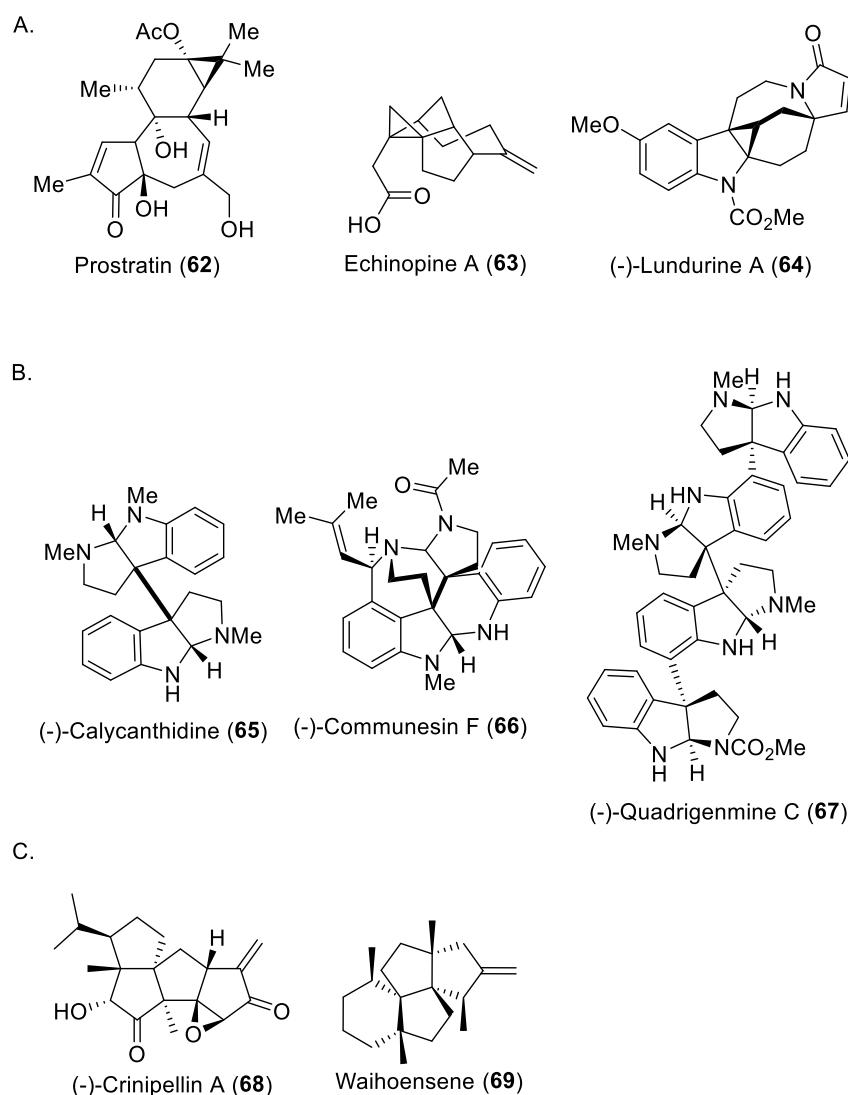
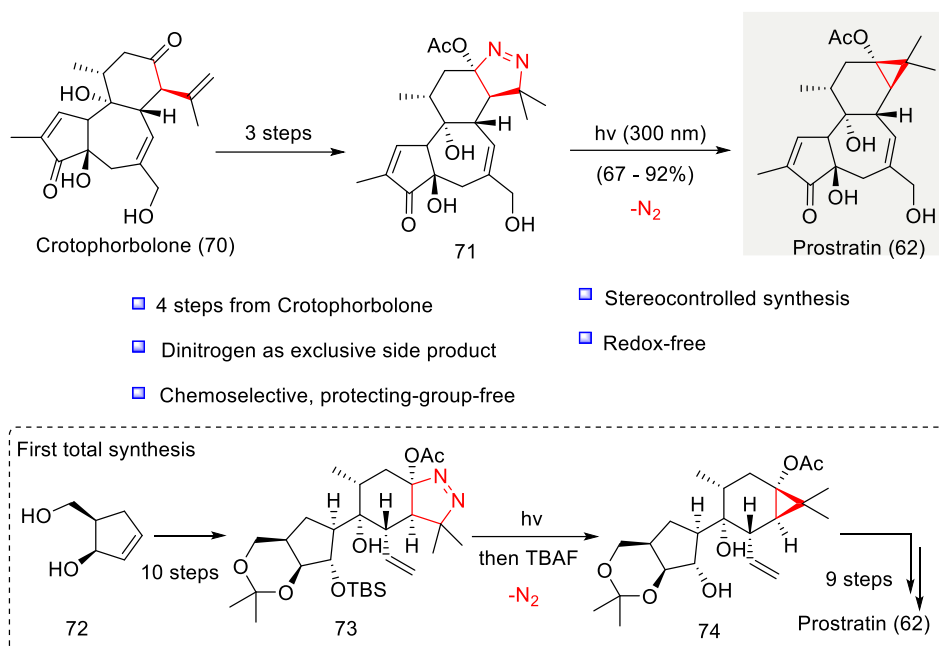


Figure 1.2 Selected examples of natural product synthesis achieved by nitrogen extrusion. **A.** cyclopropane formation from 1,2-diazene, **B.** dimerization via 1,2-diazene fragmentation, and **C.** trimethylenemethane-diyl [3+2] cycloaddition

A representative example is the 4-step synthesis of prostratin (**62**) from crotophorbolone (**70**).⁷⁴ (**Scheme 1.6**) Dinitrogen extrusion was performed on pyrazoline **71** under UV irradiation to give the desired cyclopropane on prostratin (**62**). Wender's elegant approach of using highly-chemoselective dinitrogen-extrusion left the cyclopropane synthesis to the last step. The dinitrogen extrusion process not only is a stereocontrolled process but also requires neither prior protection of reactive hydroxy groups nor redox chemistry. Introduction of heteroatom (i.e. nitrogen atom) at the earlier stage that is not present on the final product can serve as a latent transformable group, could be eliminated *via* gas extrusion reaction to give the desired ring-contraction product. (i.e. 5-membered pyrazoline to cyclopropane) Same reaction was also adopted in the first, 20-step total synthesis of prostratin (**62**).⁷⁵

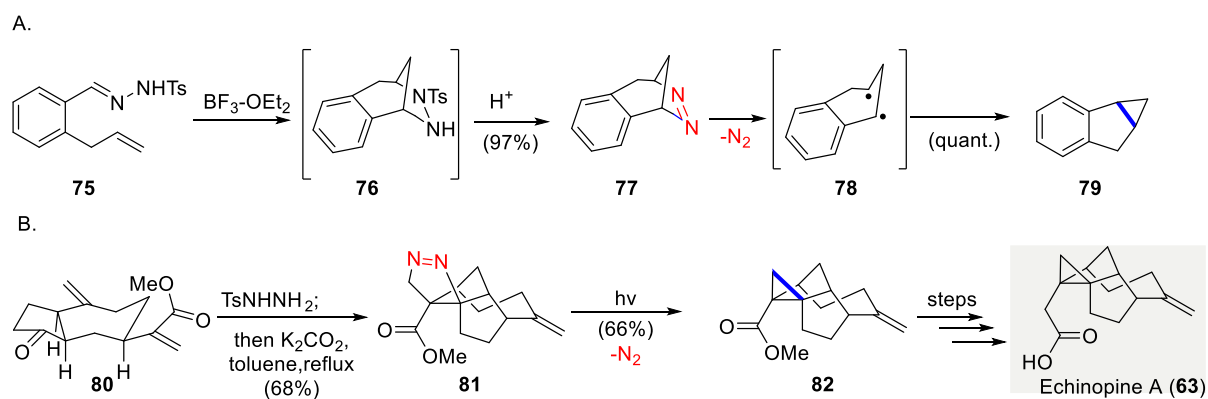


Scheme 1.8 Photoinduced dinitrogen extrusion-ring contraction of pyrazoline **70** *en route* to prostratin (**62**)⁷⁴, same approach was adopted in the first total synthesis of prostratin (**62**)⁷⁵.

1.2.1 Cyclopropane formation from 1,2-diazene

Pioneer study from Padwa and co-workers on intramolecular cycloaddition reactions of olefinic tosylhydrazones was reported in 1980⁷⁶ (**Scheme 1.9A**). Exposure of tosylhydrazone **75** to boron trifluoride etherate afforded benzodiazepine **77** as exclusive product in 97% yield *via* intramolecular cyclization intermediate **76**. Heating of the freshly prepared **77** led to nitrogen extrusion to give **79** in quantitative yield, presumably involves the formation of biradical **78**.

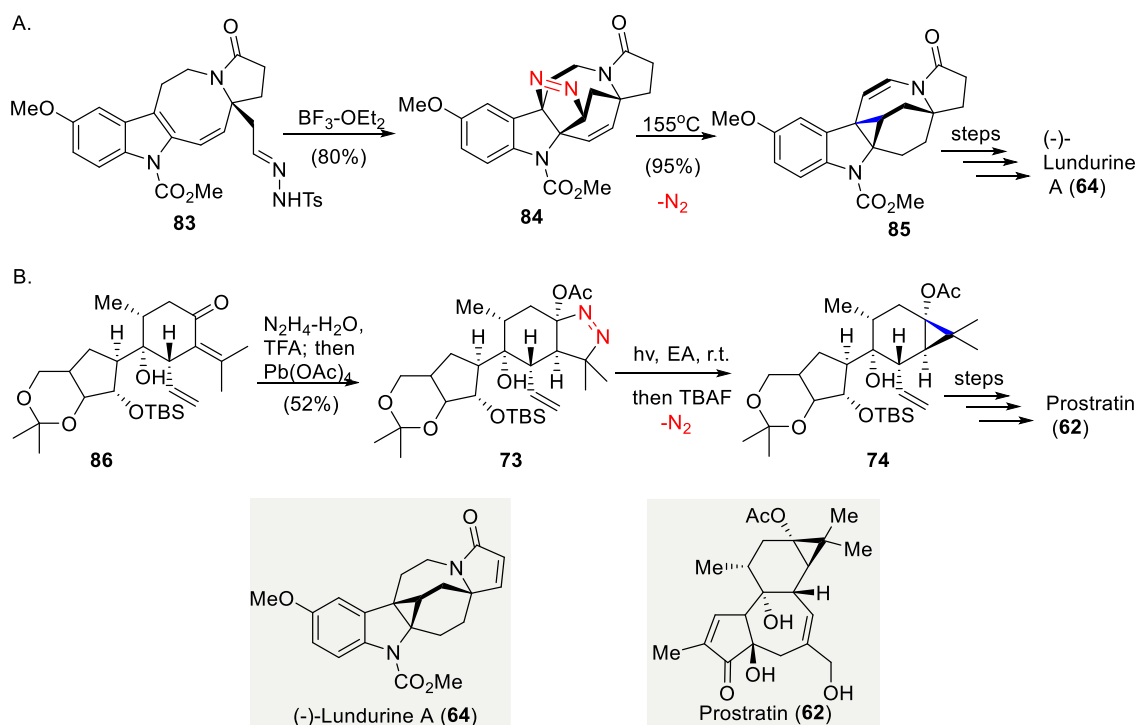
In 2013, Liang and co-workers synthesized the cyclopropane moiety of echinopine A (**63**) utilizing a nitrogen extrusion reaction (**Scheme 1.9B**). Treatment of ketone **80** with tosylhydrazine gave corresponding tosylhydrazone, which underwent cross-ring 1,3-dipolar cycloaddition upon heating in the presence of potassium carbonate to give the desired pyrazoline **81** in 68% yield. Irradiation of the freshly prepared pyrazoline **81** afforded cyclopropane **82** in 66% yield. Conversion of cyclopropane **82** to echinopine A (**62**) was accomplished in steps.



Scheme 1.9 Cyclopropane formation from 1,2-diazene in organic synthesis. **A.** Synthetic studies of radical-based nitrogen extrusion from 1,2-diazene reported by Padwa in 1980.⁷⁶ **B.** Photolysis of pyrazoline **81** gives cyclopropane **82** in the synthesis of echinopine A (**63**) (Liang 2013).⁷⁷

In 2016, Echavarren's synthesis of (-)-lundurine A (**64**) featured a cyclopropanation via formal [3+2] cycloaddition/nitrogen extrusion as a synthetic critical step (**Scheme 1.10A**). Treatment of tosyl hydrazone **83** with $\text{BF}_3\text{-OEt}_2$ as the Lewis acid produced cycloaddition product **84** in 80% yield. Heating of pyrazoline **84** to 155°C resulted in a cyclopropanation *via* nitrogen extrusion concomitant with the migration of olefin presumably *via* a homodienyl *retro-ene/ene* rearrangement to generate **85** in 95% yield.

In 2019, Li and co-workers completed the total synthesis of prostratin (**62**) applying pyrazoline formation/nitrogen extrusion approach (**Scheme 1.10B**). Condensation of enone **86** with hydrazine hydrate in the presence of trifluoroacetic acid generated a pyrrolozoline intermediate with the desired 8,14-*cis* configuration, which was exposed to lead(IV) acetate to give corresponding pyrazoline **73** in 52% yield. Photolysis of **73** followed by desilylation gave cyclopropane **74** in 79% yield.



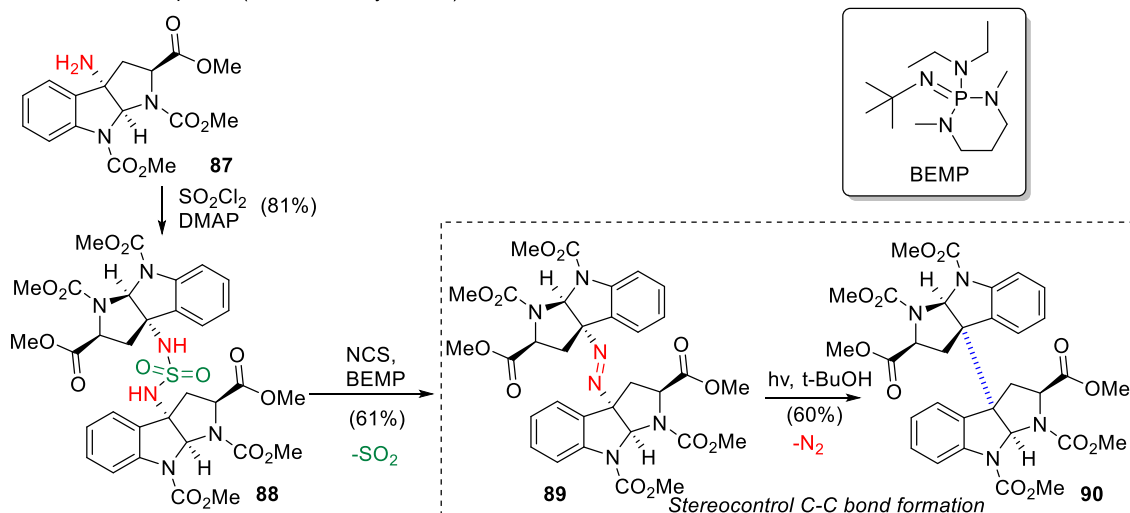
Scheme 1.10 Cyclopropane formation from 1,2-diazene in organic synthesis. **A.** Thermolysis of pyrazoline **84** results in a cyclopropanation/alkene isomerization cascade to give **85** in the synthesis of (-)-lundurine A (**64**) (Echavarren 2016).⁷⁸ **B.** Synthesis of prostratin (**62**) makes use of photolysis of 1,2-diazene to construct cyclopropane **74** (Li 2019).⁷⁵

1.2.2 Dimerization via 1,2-diazene fragmentation

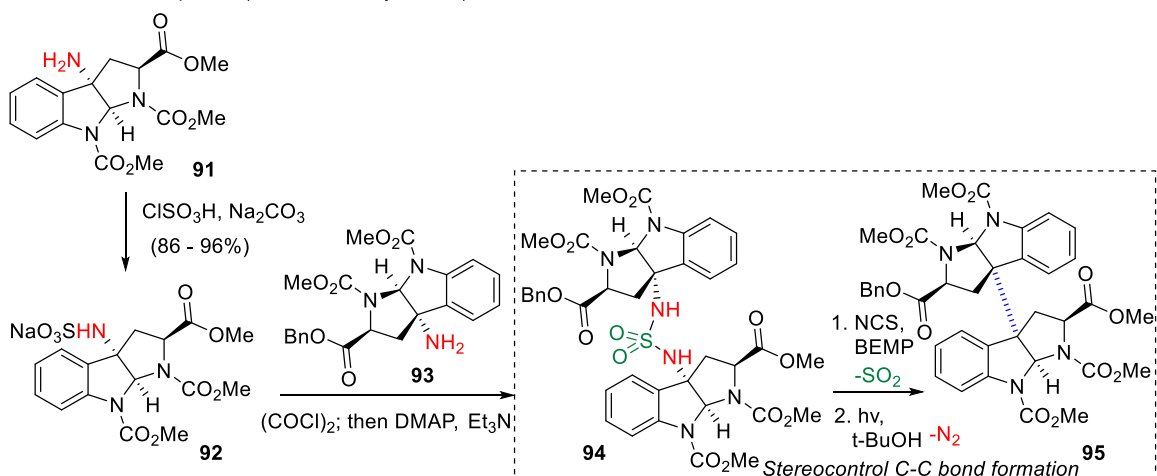
In 2011, Movassaghi and co-workers disclosed a directed and stereocontrolled assembly of carbon-carbon linked *homo*- and *hetero*-dimeric hexahydropyrroloindoles (**Scheme 1.11**). Homodimer synthesis from corresponding monomeric amine **87** was conducted (**Scheme 1.11 A**). Treatment of amine **87** with sulfuryl chloride and DMAP gave sulfamide **88** in 81% yield. Oxidation of sulfamide **88** with NCS and BEMP afforded the desired 1,2-diazene **89** in 61% yield. Photolysis of freshly prepared 1,2-diazene **89** in *tert*-butanol resulted in the stereocontrol C-C bond formation and produced homodimer **90**.

After the successful preparation of homodimer **90**, this elegant synthetic strategy was applied to the preparation of heterodimer **95** (**Scheme 1.11B**). Stepwise sulfonylation strategy including treatment of **91** with chlorosulfonic acid in the presence of sodium carbonate provided sodium sulfamide salt **92**. Exposure of this newly prepared sodium sulfamide **92** with **93** in the presence of oxalyl chloride and DMAP and triethyl amine afforded the unsymmetrical sulfamide **94**. Conversion of the sulfamide **94** to corresponding diazene was achieved by using NCS and BEMP, in which the photolysis of this diazene provided heterodimeric hexahydropyrroloindoles **95** though a stereocontrol C-C bond formation.

A. Method development (Homodimer synthesis)



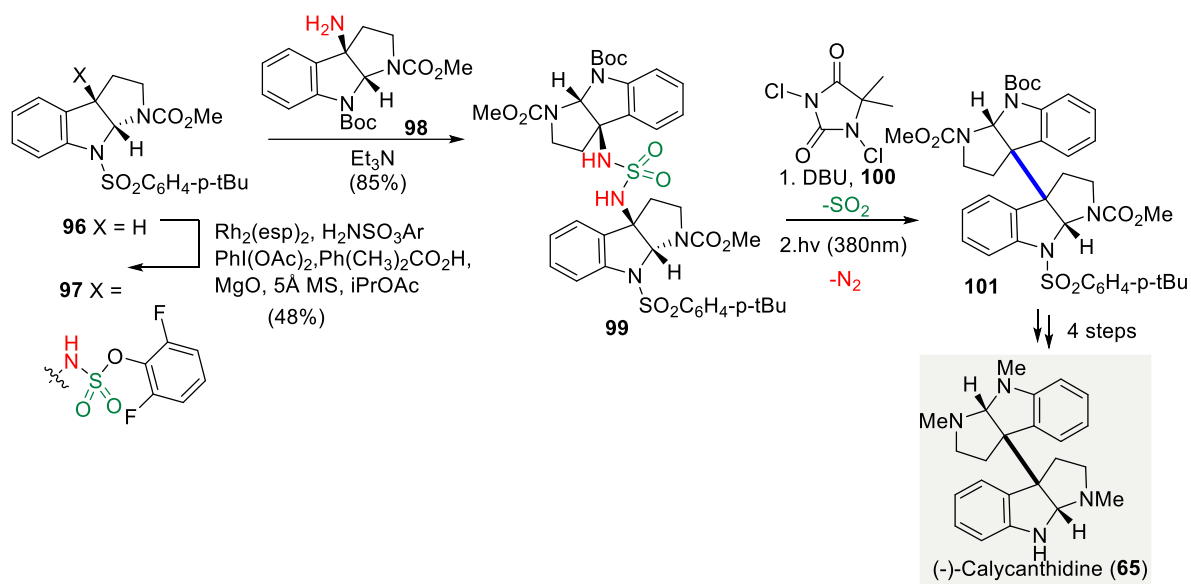
B. Method development (Heterodimer synthesis)



Scheme 1.11 Stereocontrolled homo- and hetero-dimerization of hexahydropyrroloindoles *via* 1,2-diazene fragmentation. (Movassaghi, 2011).⁷⁹

After the report of an innovative approach of the directed and stereocontrolled assembly of carbon-carbon linked homodimeric and heterodimeric hexahydropyrroloindole by Movassaghi and co-workers, the application of this approach in organic synthesis was reported by the same research group (**Scheme 1.12**). The synthesis of (-)-calycanthidine (**65**) employed the direct catalytic C-H amination of protected cyclotryptamine **96** to give the arylsulfamate **97**, which is an important intermediate toward the preparation of unsymmetrical sulfamide **99**⁸⁰. Compared to the previous approach involving the preparation of a more sensitive sulfamoyl chloride (*see* **Scheme 1.11**), this modified approach requires less equivalent (i.e. 1.2 eq.) of **96** to provide a sterically hindered arylsulfamide **97** with decent reactivity, that is readily convertible to the desired sulfamide **99** in 85% yield by treatment with **98** in the presence of

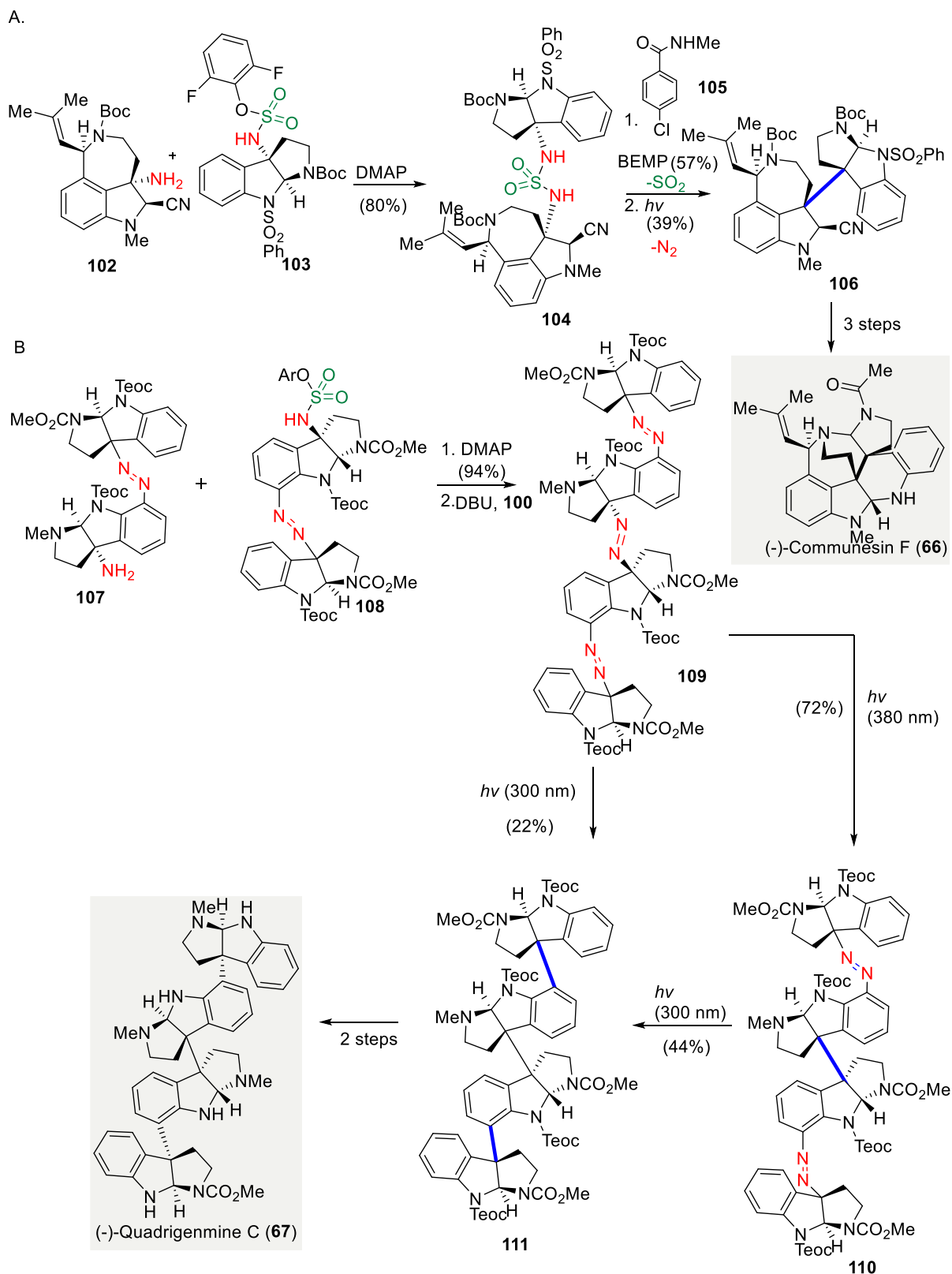
triethyl amine. A two-step synthesis from sulfamide **99** including the formation of diazene followed by photolysis resulted in stereocontrol C-C bond formation and gave **101**. The synthesis of (-)-calycanthidine (**65**) was accomplished in four steps.



Scheme 1.12 The application of stereocontrolled heterodimerization in the synthesis of (-)-calycanthidine (**65**) (Movassaghi 2014).⁸⁰

In 2016, Movassaghi and co-workers reported a biomimetic enantioselective total synthesis of (-)-communesin F (**66**) featuring a diazene synthesis from unsymmetric sulfamide/photolysis approach as key reaction⁸¹ (**Scheme 1.13A**). Arylsulfamate **103**, which was prepared using catalytic C-H amination, was reacted with aminonitrile **102** effected by DMAP to give unsymmetrical sulfamide **104** in 80% yield. Successive diazene formation from **104** and photolysis gave **106**, which was converted to (-)-communesin F (**66**) in three steps.

Later, the same research group disclosed an elegant synthesis of (-)-quadrigemine C (**67**) employing a multiple photo-extrusion of nitrogen from a *tris*-diazene intermediate **109** as a synthetic key step⁸² (**Scheme 1.13B**). Sulfonylation of amine **107** with **108** effected by DMAP provided a sulfamide, which was treated with DBU and NCS to give a *tris*-diazene **109**. Photoirradiation of this freshly prepared *tris*-diazene **109** at 300 nm led to triple nitrogen extrusion and provided **111** in 22% yield. An additional two-step synthesis from **111** afforded quadrigemine C (**67**). Alternatively, the preparation of **111** from **109** can be achieved through a stepwise photolysis. Photoirradiation of *tris*-diazene **109** with 380 nm provided a *bis*-diazene **110** in 72% yield. Further photolysis of this newly prepared *bis*-diazene **110** with 300 nm irradiation gave **111** in 44% yield.



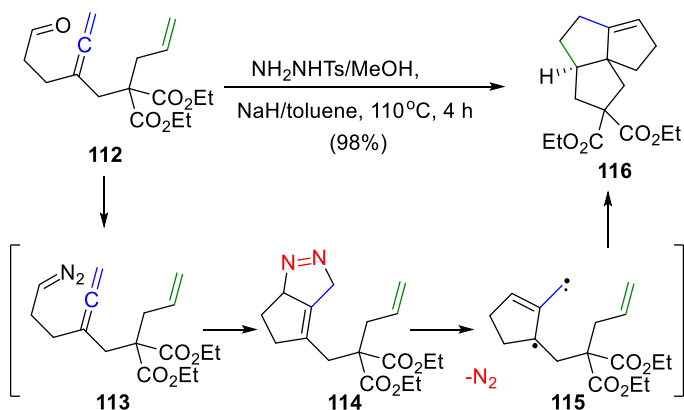
1.2.3 Trimethylenemethane diyl [3+2] cycloaddition

In the late 1970s, Berson and Little reported the intramolecular trimethylenemethane diyl [3 + 2] cycloaddition reaction (*also abbreviated as* TMM-diyl [3+2] cycloaddition), independently.^{83, 84} In 2011, Lee and co-workers reported an intramolecular TMM diyl [3 + 2] cycloaddition of **113** gave angular fused triquinane **116** in 98% yield⁸⁵ (**Scheme 1.14**). Later, Lee's group completed the synthesis of (-)-crinipellin A (**68**) and waihoensene (**69**) using TMM diyl [3 + 2] cycloaddition as key step.^{86, 87}

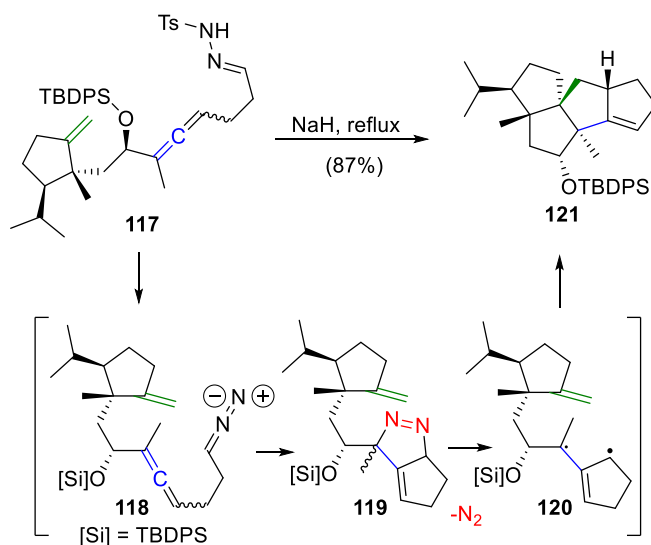
The allenyl diazo compound **113**, which was generated from the reaction between aldehyde **112** and p-toluene-sulfonylhydrazide in the presence of sodium hydride upon heating, to produce diazene **114**. Heating of **114** generated diyl **115** via nitrogen extrusion led to intramolecular TMM diyl [3 + 2] cycloaddition to give angular fused triquinane **116**.⁸⁵ (**Scheme 1.14 (A)**). Based on the above successful synthetic model, the synthesis of (-)-crinipellin A (**68**) and waihoensene (**69**) applied this reaction as synthetic critical step. The synthesis of (-)-crinipellin A (**68**) commenced with treatment of hydrazone **117** with sodium hydride under reflux to afford the tetraquinane **121** in 87% yield⁸⁶ (**Scheme 1.14B**). The diazo compound **118** formed underwent an intramolecular [3+2] cycloaddition to give **119**. Freshly prepared **119** was converted to diyl **120** followed by another [3+2] cycloaddition to give the tetraquinane **121**. The synthesis of (-)-crinipellin A (**68**) was achieved from tetraquinane **121**.

Lee's synthesis of waihoensene (**69**) began with the preparation of hydrazone **122b**, which was treated with sodium hydride under reflux to give **126** in 83% yield over two steps⁸⁷ (**Scheme 1.14C**). The author proposed that freshly prepared **122b** was converted to diazo **123**, which was subjected to an intramolecular [3 + 2] cycloaddition to give adduct **124**. Formation of diyl **125** from **124** and subsequent [3 + 2] cycloaddition produced the tetracycle **126**. Waihoensene (**69**) was prepared from the precursor **126**.

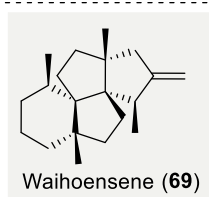
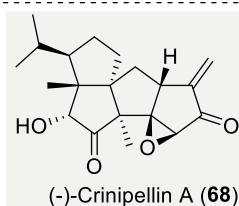
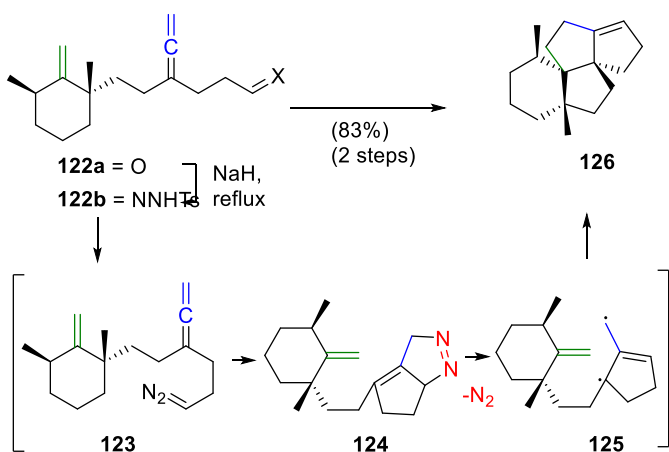
A. Method development (Lee 2011)



B. (-)-Crinipellin A (Lee 2014)



C. Waihoensene (Lee 2017)



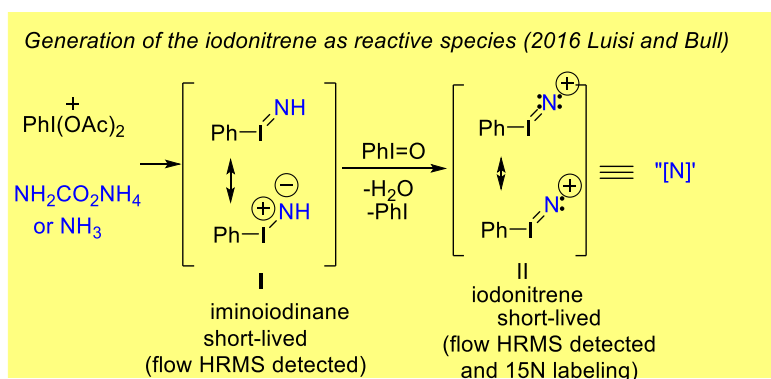
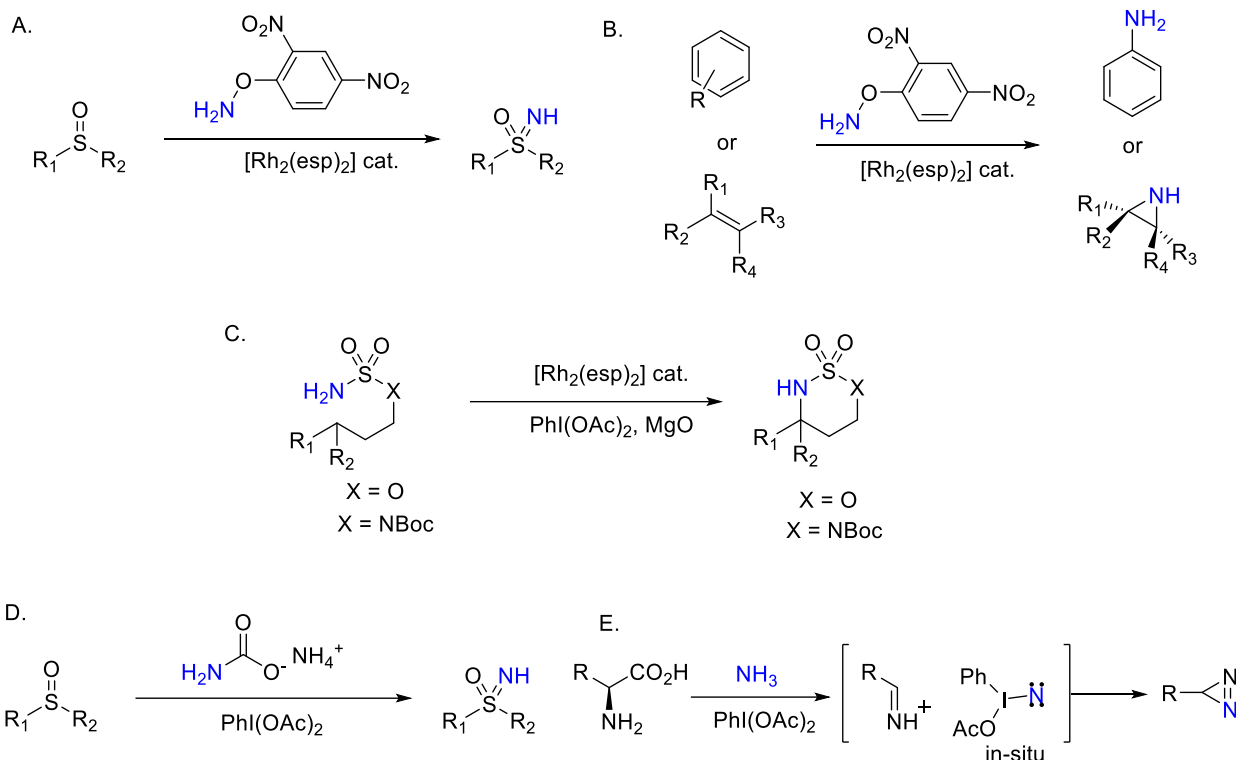
Scheme 1.14 Trimethylenemethane diyl [3+2] cycloaddition with diradicals generated from diazene precursor. **A.** An intramolecular trimethylenemethane diyl [3+2] cycloaddition with allenyl diazo compound **113** as a key intermediate to give angular fused triquinane **116** (Lee, 2011)⁸⁵. **B.** Synthesis of (-)-crinipellin A (**68**) (Lee, 2014)⁸⁶. **C.** Synthesis of waihoensene (**69**) (Lee, 2017)⁸⁷.

1.3 The development of iodonitrene chemistry and its applications

Direct access to nitrogen-containing function group is extremely valuable in the preparation of biological important molecules. Various amination methods such as nucleophilic substitution, reductive amination and metal-catalyzed amination reactions (e.g. allylic substitution, hydroamination and C–N cross-coupling reactions) are general and widely used strategies for amine synthesis.^{88, 89} Electrophilic amination, which required electrophilic aminating reagents, metal–nitrene equivalents, or oxaziridines as nitrogen source, is the net addition of an amino group to the compounds containing electron-rich functionalities. Noteworthy, the advance of dirhodium-nitrene chemistry enables the synthesis of *NH*-sulfoximine⁹⁰, direct preparation of *NH*-aziridine and aniline^{91, 92}, intramolecular amination of inert C_{sp3}-H bond⁹³, and has been broadly applied in natural product synthesis.⁹⁴ (**Scheme 1.15A – 1.15C**).

Iodonitrene⁹⁵, which is generated *in-situ* from reaction between hypervalent iodine (III) reagent and ammonia or its surrogate, has recently prompts as a promising electrophilic aminating reagent for synthetic transformations, such as synthesis of *NH*-sulfoximine⁹⁵. (**Scheme 1.15D**) Moreover, iodonitrene shows reactivities that is complementary to that of dirhodium-nitrene. For instance, the synthesis of diazirines from unprotected amino acid provides novel reactivity of iodonitrene from the precedent metal-nitrene chemistry⁹⁶ (**Scheme 1.15E**). Electrophilic amination using iodonitrene not only provide a convenient and reactive nitrene species for different reactions but also circumvents the use of metal and avoids the use of activated and/or explosive reagent, such as *O*-(mesitylsulfonyl)-hydroxylamine (MSH) or *O*-(2,4-dinitrophenyl)-hydroxylamine (DPH).

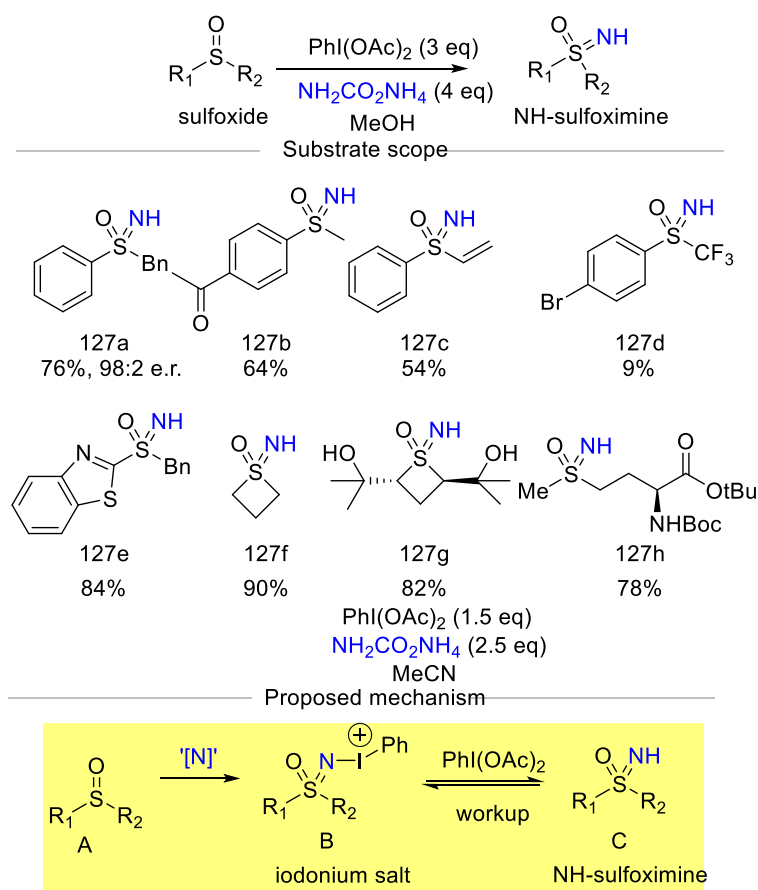
Bull and co-workers disclosed the evidence of iodonitrene and the possible intermediates via mass spectrometry analysis and isotopic labelling using ¹⁵N,⁹⁷ for instance, iminoiodindinane **I** (i.e. PhI=NH) and the unprecedented iodonitrene **II** (i.e. PhI=N⁺) (**Scheme 1.15**, yellow box). However, no evidence of any reactive intermediate was found throughout the NMR studies⁹⁸.



Scheme 1.15 Rhodium catalyzed (Du Bois catalyst) amination reactions involved dirhodium nitrene transfer. **A.** synthesis of *NH*-sulfoximine from sulfoxide (Ge, 2014)⁹⁰, **B.** direct *NH*-aziridine and aniline synthesis from arene and alkene, respectively (Kurti and Falck, 2014 and 2016)^{91, 92} and **C.** direct intramolecular C_{sp3}-H amination with sulfamate (Du Bois, 2004)⁹³. Amination reactions involved iodonitrene as electrophilic aminating reagent. **D.** Direct *NH*-transfer using ammonium carbamate (Luisi and Bull, 2016)⁹⁵; and **E** direct dizairines synthesis from unprotected amino acids (Reboul, 2019)⁹⁶ and the proposed mechanism of iodonitrene formation (yellow box).⁹⁵

1.3.1 Direct *N-H* transfer to sulfoxides and sulfonamides

In 2016, Luisi and Bull and co-workers reported the direct transfer of NH group from iodonitrene to sulfoxide to afford *NH*-sulfoximine.⁹⁵ (Scheme 1.16) Under the standard condition, the iodonitrene generated *in-situ* from reaction between iodophenyldiacetate and ammonium carbamate as source of nitrogen⁹⁹ produced various *NH*-sulfoximine. Aryl-substituted (R_1) sulfoxides proved to be generally excellent substrates for this transformation and the scope with respect to (R_2) was also good including methyl, benzyl, and alkene group. (corresponding products **127a-c** from 54% to 76% yield) However, the presence of electron-withdrawing trifluoromethyl group in R_2 resulted **127d** only 9% yield. On the other hand, benzothiazole-substituted sulfoxide (**127e**) and dialkylated sulfoxides (**127f-h**) demonstrated as good substrate. Mechanistically, electrophilic amination of sulfoxide **A** generates an iodonium salt **B**. The elimination of phenyl iodide from **B** gives *NH*-sulfoximine **C** (Scheme 1.16, yellow box).



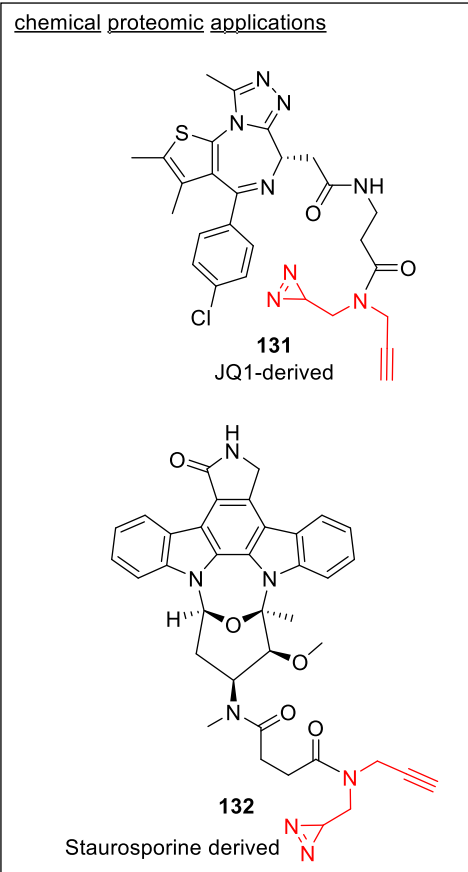
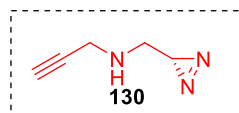
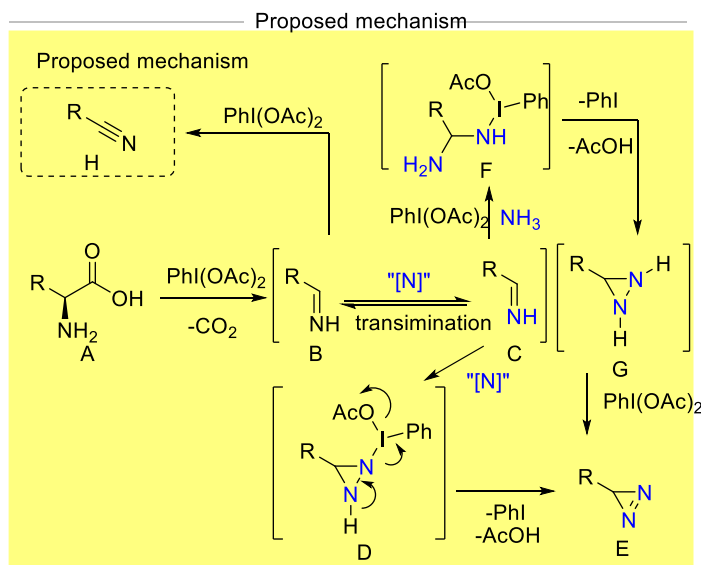
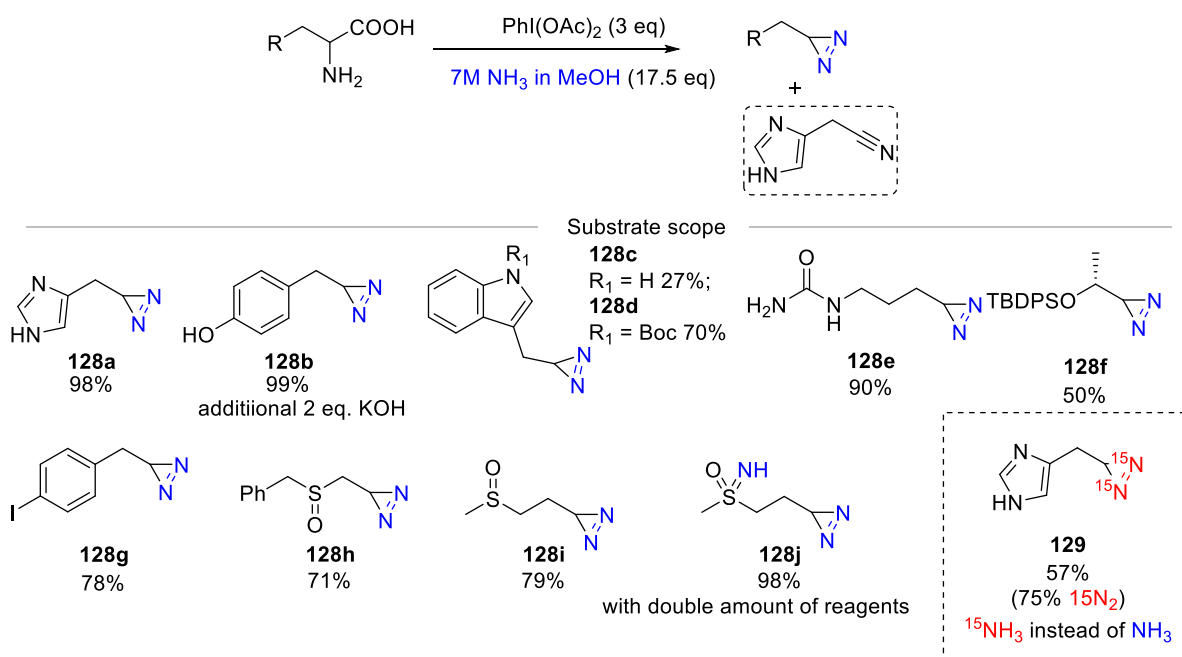
Scheme 1.16 Direct *N-H* transfer to sulfoxides and sulfonamides using iodonitrene chemistry.

1.3.2 Terminal diazirine from amino acid through tandem decarboxylation/iodonitrene transfer

In 2019, Reboul and co-workers disclosed the synthesis of terminal diazirine from amino acid through a tandem decarboxylation/iodonitrene transfer.⁹⁶ (**Scheme 1.17**) Treatment of amino acid with PIDA and 7M ammonia solution, which generated iodonitrene *in-situ*, produced terminal diazirine as major product with small amount of undesired nitrile that resulted from over-oxidation.. Diazirine (**128a-j**) were produced successfully from corresponding unprotected amino acid good yield. Interestingly, addition of double amount of reagent resulted in diazirine formation and sulfoximation from the methionine sulfoxide to give **128j** in 98% yield, in which the standard condition only led to diazirine formation (i.e. **128i**, 79% yield)

Experiments using isotopic ¹⁵N ammonia for diazirine formation was conducted. Treatment of L-histidine with PIDA and ¹⁵N-labeled ammonia afforded ¹⁵N₂-diazirine **129** in 57% yield with 75% label ¹⁵N incorporated. Based on this result, mechanism is proposed (**Scheme 1.17**, yellow box). Unprotected amino acid **A** is subjected to decarboxylation upon treatment with PIDA to give an imine **B**.^{100, 101} Imine formed could be oxidized to a nitrile **H** in the presence of excess oxidant. Transimination¹⁰² of the imine **B** took place with the iodonitrene to give **C**⁹⁵, which reacts with another moiety of iodonitrene via insertion to give the diaziridine intermediate **D**.¹⁰³ Subsequent oxidation, with the release of iodobenzene and acetic acid, affords the expected diazirine **E**.¹⁰⁴ Another possible pathway involves nucleophilic addition of ¹⁵NH₃ to give **F**,¹⁰⁵ followed by cyclization into diaziridine **G**. Oxidation of diaziridine **G** by PIDA afforded diazirine **E**.

Reboul and co-workers provide a convenient, easy-to-handle condition to prepare diazirine for biological application. In 2020, the use of diazirine tag for chemical proteomic applications (inset, JQ1-derived diazirine **131** and staurosporine-derived diazirine **132**) were reported.¹⁰⁶ The diazirine-carrying secondary amine **130** was prepared using Reboul's chemistry. The late-stage incorporation of the secondary amine **130** into the target compounds such as **131** and **132** for further biological investigation.



Scheme 1.17 Synthesis of terminal diazirine from amino acid through tandem decarboxylation /iodonitrene transfer¹⁰⁷ (Yellow box: The proposed mechanism). The use of diazirine tag for chemical proteomic applications (inset, JQ1-derived diazirine **131** and staurosporine-derived diazirine **132**)¹⁰⁶

1.4 Summary

In *Chapter 1.1*, contractive synthesis of carbocycle and its applications in organic synthesis were discussed. Contractive synthesis has played an important role in organic synthesis, forging small carbocycles with highly-condensed functionalities and/or a congested array of stereocentres. It improves the efficiency of synthesis by enabling formation of complex carbocycles, in which otherwise is step-consuming through conventional synthetic approach. Contractive synthesis of carbocycles well-planned out are practical because they encompass one to several concepts of efficient synthesis including step economy, chemoselectivity, protecting-group-free synthesis, atom economy and redox economy. Methods such as semi-pinacol rearrangement demonstrate a late-stage modification of complex structure and open the possibility of late-stage diversification to access diverse structural analogues.

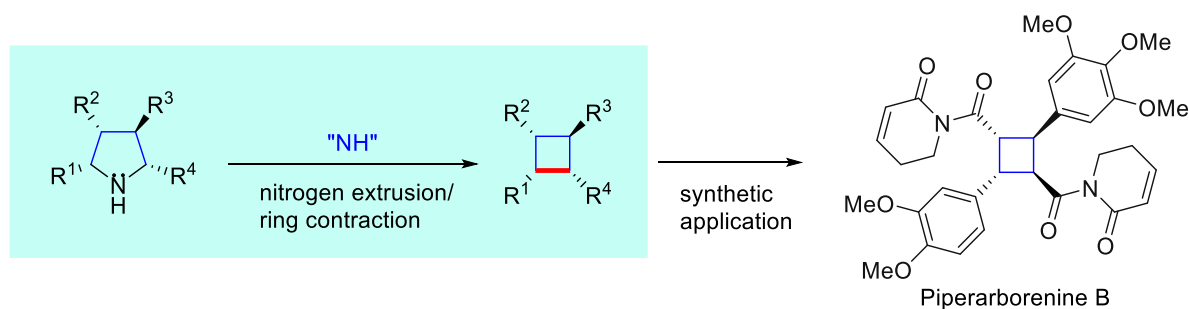
In *Chapter 1.2*, nitrogen extrusion in organic synthesis were introduced using selected examples. Highly strained, small-sized carbocycles could be prepared readily from corresponding 1,1-diazene or 1,2-diazenes, in which biradical intermediates are believed to be involved in the process. The examples we discussed in this chapter, nitrogen extrusion usually takes place under thermal and/or photoirradiation and the use of chemical reagent is not necessary. It is because nitrogen extrusion reaction generally increases in entropy and the formation of new C-C bond in the product may compensate the energy barrier for bond cleavage to take place. Therefore, nitrogen extrusion appears as a useful strategy to construct small sized carbocycles with high strains.

In *Chapter 1.3*, the reported chemical transformations utilizing iodonitrene chemistry were discussed. Iodonitrene, which is *in-situ* generated by the reaction between hypervalent iodine (III) reagent and ammonia in alcoholic solvent, acts as an electrophilic aminating reagent for the synthesis of sulfoxime and diazirine and have demonstrated the practical usefulness in applications. However, the oxidizing power of hypervalent iodine (III) reagent may lead to undesirable side reaction, such as oxidizing the starting materials of the reaction as reported in the diazirine synthesis. As a newly invented source of electrophilic nitrogen, we envisage that new reaction development using iodonitrene to incorporate nitrogen atom into organic molecule will become flourish.

2. Aim of the Thesis

Cyclobutanes are four-membered carbocycles which present a unique structural feature in bioactive natural products.^{88, 108, 109} The congested, sp^3 -enriched small carbocycles possess an array of stereocenters in contiguous fashion which not only confers the potential bioactivities to the cyclobutanes.^{6, 110-112} However, *there are limited synthetic methods directly en route to multi-substituted cyclobutanes* and its synthesis still heavily rely [2+2] cycloaddition and Wolff rearrangement, etc. In particular, *hetero-coupling of two different alkenes to prepare unsymmetrical cyclobutane* in [2+2] cycloaddition is still presenting an intricate task in synthetic chemistry. Therefore, the development of a new synthetic method for the direct stereocontrolled preparation of substituted cyclobutanes is of great importance as it provides an alternative approach for the preparation of small and sterically congested cyclobutanes.

In this thesis, the unprecedented, stereoselective and contractive synthesis of multi-substituted, unsymmetrical cyclobutanes from corresponding pyrrolidines making use of iodonitrene chemistry is discussed (**Scheme 2.1**). The electrophilic amination of *N*-pyrrolidine using iodonitrene and subsequent nitrogen extrusion affords cyclobutane as product, which is highly stereospecific and might involve the 1,4-biradical intermediate. Reaction mechanism is proposed based on experimental evidence. Last but not least, this method was applied to the synthesis of cytotoxic natural product piperarborenine B.



Scheme 2.1 Development of novel, stereoselective synthesis of cyclobutane from pyrrolidine and its application in the synthesis of bioactive natural product.

3. Stereoselective synthesis of cyclobutanes by contraction of pyrrolidines

3.1 Introduction

Cyclobutanes are four-membered carbocycles which present a unique structural feature in bioactive natural products.^{88, 108, 109} (**Figure 3.1**) Structurally, these bioactive natural products such as terpenoids and alkaloids, originating from different natural sources, contain cyclobutanes with various degrees of substitution in a limited amount of space. The congested, sp³-enriched small carbocycles possess an array of stereocenters in contiguous fashion which not only confers the potential bioactivities to the cyclobutanes but also attracts wide interest in the synthetic society for its efficient synthesis.^{6, 110-112}

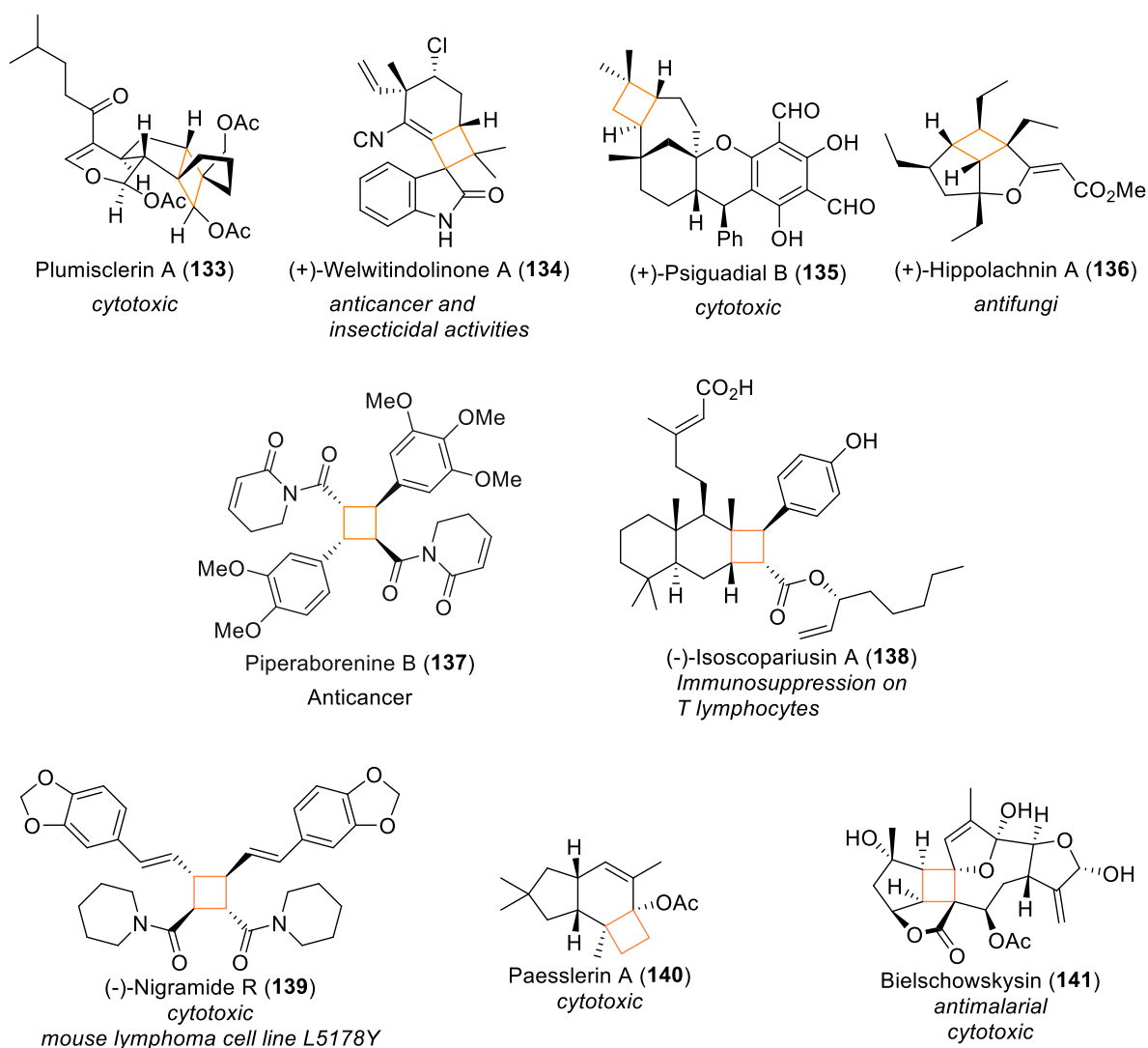
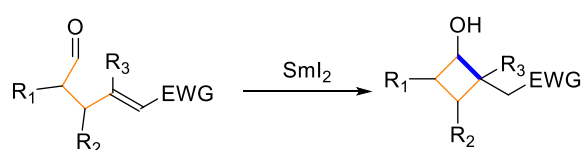


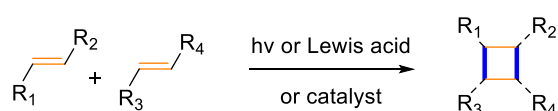
Figure 3.1 Some bioactive natural products contain a cyclobutane core.

Synthetic methods directly *en route* to multi-substituted cyclobutanes, such as [2+2] cycloaddition,¹⁸ radical cyclization^{113, 114} and ring contraction reactions including Wolff rearrangement¹¹⁵⁻¹¹⁷ and oxidative pinacol rearrangement³⁶, are well documented (**Scheme 3.1**). In particular, many recent advances on [2+2] cycloaddition based on photocatalysis, organocatalysis and Lewis acid catalysis have been reported, in which hetero-coupling of two different alkenes is still presenting an intricate task in synthetic chemistry. Therefore, the development of a new synthetic method for the direct stereocontrolled preparation of substituted cyclobutanes is of great importance as it provides an alternative approach for the preparation of small and sterically congested cyclobutanes.

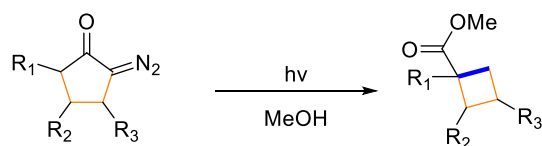
(B) (i) Radical cyclization



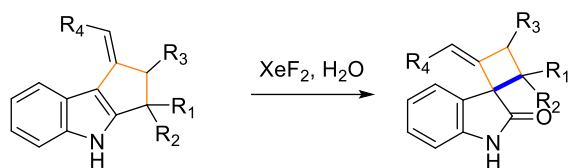
(ii) [2 + 2] cycloaddition



(iii) Wolff rearrangement



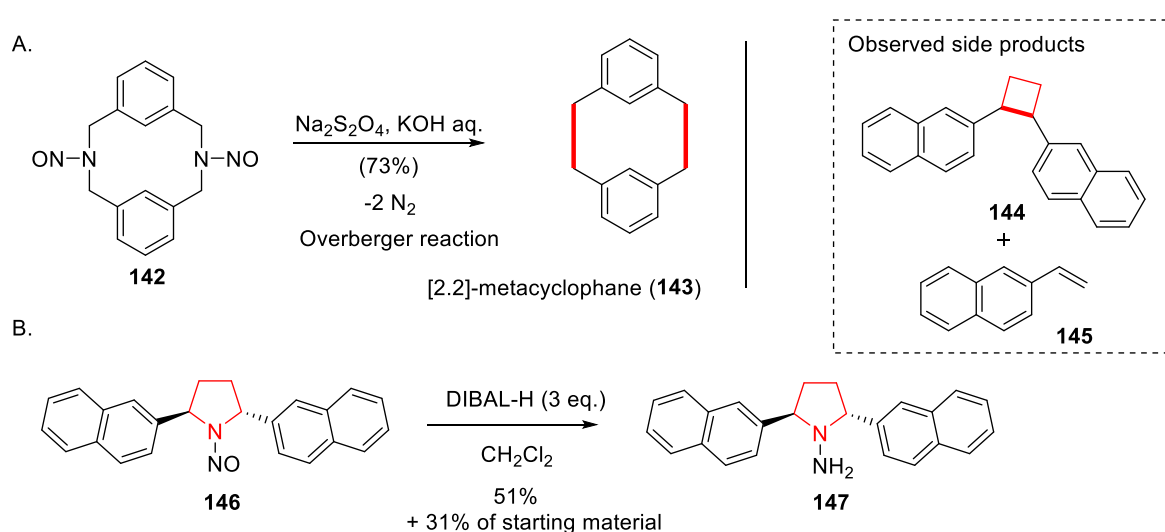
(iv) Oxidative semi-pinacol



Scheme 3.1 Representative synthetic methods *en route* to multi-substituted cyclobutanes.

3.2 Reported synthesis of cyclobutanes *via* nitrogen extrusion

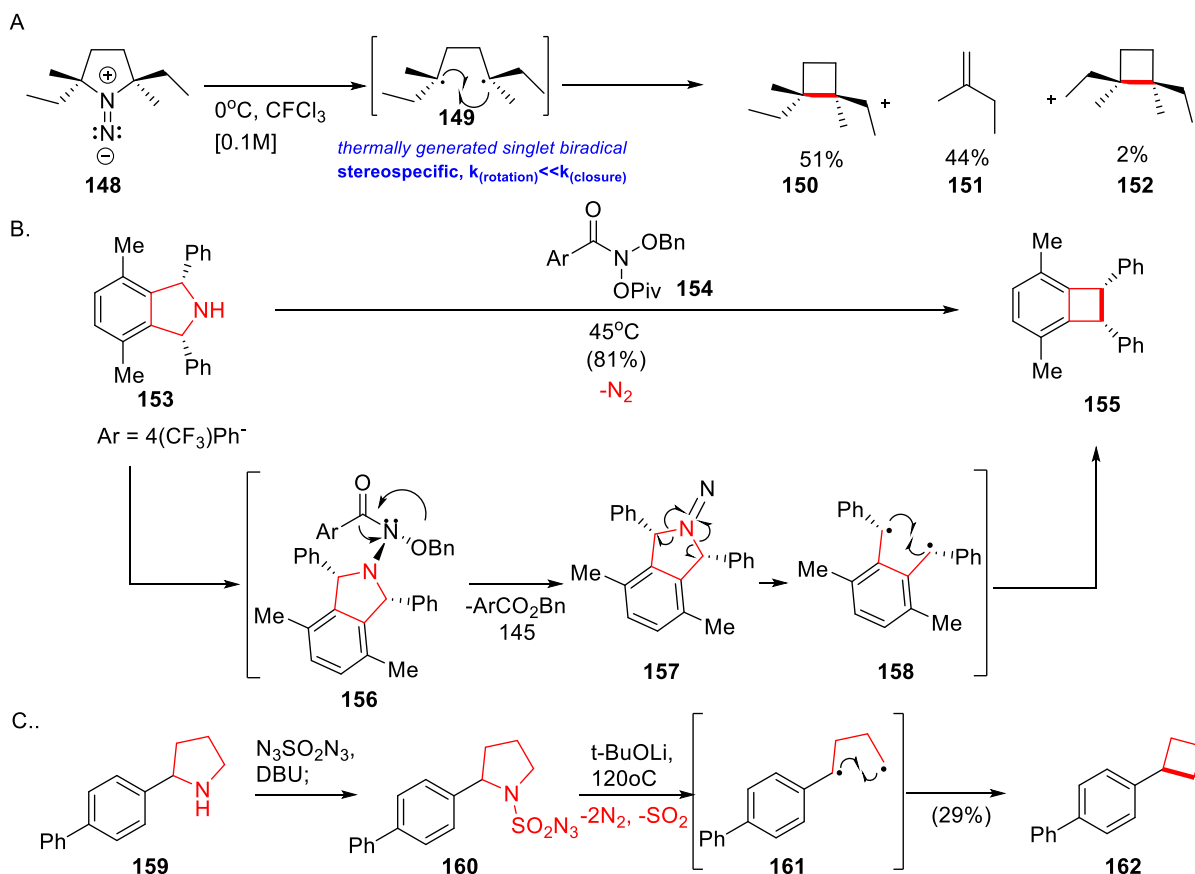
Overberger reaction¹¹⁸, which involved a tandem reduction of *N*-nitroso group of secondary amine/dinitrogen extrusion to give new C-C bond, was used to prepare 10-membered carbocycle [2,2]-metacyclophane (**143**) from *N*-nitrosyl compound **142**¹¹⁹ (Scheme 3.2). As described by Overberger¹¹⁸, this reaction involved an reduction of *N*-nitroso group by sodium dithionite under alkaline condition to generate an 1,1-hydrazine, in which dinitrogen extrusion took place to give a ring-contracted carbocycle. Treatment of *N*-nitroso compound **142** with sodium dithionite in potassium hydroxide afforded [2,2] metacyclophane (**143**) in 73% yield. In 2015, Denmark and co-workers prepared the *N*-aminopyrrolidine **147** via DIBAL-H reduction of *N*-nitrosylpyrrolidine **146**¹²⁰ (Scheme 3.2B). Interestingly, the formation of cyclobutane **144** was observed as a result of Overberger reaction (yield not reported, stereochemistry not verified). Also, olefin **145** was also identified in the reaction mixture.



Scheme 3.2 Reported synthesis of cyclobutanes using Overberger reaction.¹¹⁹ **A.** Overberger reaction enables the synthesis of 10-membered cyclophane **143** *via* tandem reduction of nitrosyl group/C-N bonds cleavages/C-C bond formation. **B.** Unexpected formation of cyclobutane **140** as Overberger reaction product of DIBAL-H reduction of *N*-nitroso compound **138**.¹²⁰

In 1982, Stereospecific synthesis of cyclobutane from 1,1-diazene¹²¹⁻¹²⁴ (isodiazene) derived from pyrrolidine was pioneered by Dervan's group (Scheme 3.3A).¹²⁵⁻¹²⁹ The stereospecificity of the ring contraction is a result of the rapid C-C bond formation from the thermally generated singlet 1,4-biradical via nitrogen extrusion, affording the cyclobutanes stereoretentively. By-products such as the alkene resulting from β -fragmentation and a small quantity of stereoinverted cyclobutane were also identified.

In 2021, nitrogen deletion of secondary amine **153** using *N*-pivaloyloxy-*N*-alkoxyamide **154** leading to C-C bond formation was introduced by Levin and co-workers, and was applied to ring contraction of cyclic secondary amine to carbocycle¹³⁰ (**Scheme 3.3B**). Treatment of pyrrolidine **153** with **154** gave the N-N bond containing compound **156**, which underwent 1,2-rearrangement to give 1,1-diazene **157** by eliminating an ester. Next, dinitrogen extrusion of **157** occurred to afford 1,4-biradical **158** as a possible intermediate. Eventually, intramolecular radical coupling of 1,4-diradical **158** produced **155** in 81% yield. Later in the same year, Lu and co-workers reported another work of nitrogen atom deletion in heterocycle¹³¹ (**Scheme 3.3C**). In Lu's work, a two-step synthesis of cyclobutane **162** from pyrrolidine **159** involved first the preparation of *N*-sulfonyl azide **160**, which was treated with lithium *tert*-butoxide at 120°C to give the cyclobutane **162** in 29% yield. The 1,4-biradical **161** is suggested to be the intermediate.



Scheme 3.3 Reported synthesis of cyclobutanes from pyrrolidines *via* nitrogen extrusion. **A.** Stereospecific synthesis of cyclobutanes from 1,1-diazene through thermally generated 1,4-biradical intermediate.¹²⁵⁻¹²⁹ **B.** Nitrogen deletion of secondary amine **153** using *N*-pivaloyloxy-*N*-alkoxyamide **154** to give cyclobutane **155**.¹³⁰ **C.** Nitrogen-atom deletion of secondary amine **159** using a two-step approach, including *N*-sulfonylazide and then Curtius-type rearrangement to generate cyclobutane **162**.

¹³¹

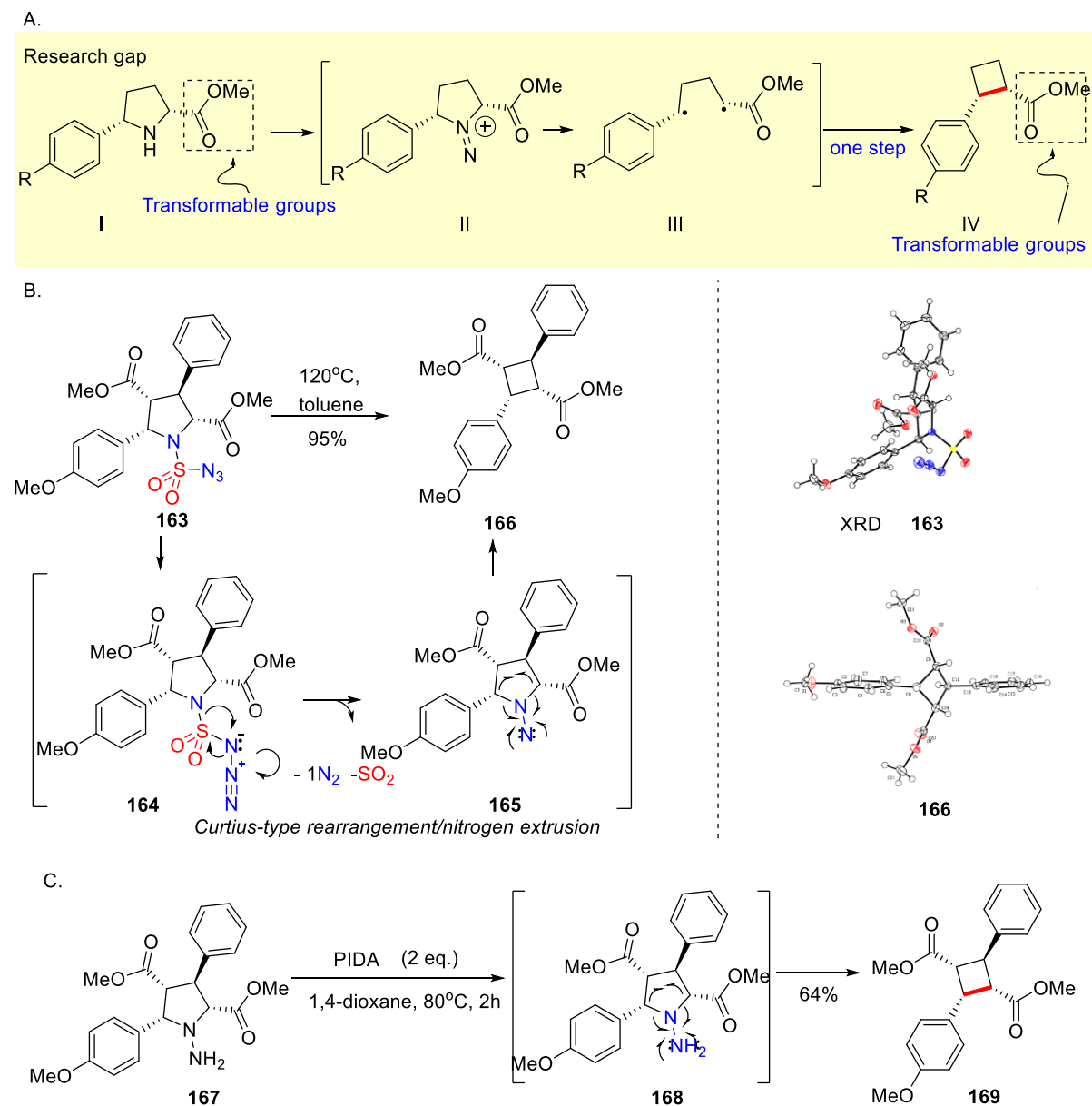
3.3 Preliminary study

Inspired by the serendipitous experimental finding by Denmark and co-workers (*see Scheme 3.2B*), we launched the research project “contractive synthesis of cyclobutanes from pyrrolidines” in 2019. Since the presence of aryl substituents at α -carbon of the nitrogen atom of pyrrolidine is necessary to stabilize the *in-situ* generated C-radical after nitrogen extrusion, we envisage that changing at least one of the aryl groups to stable, transformable functional group (e.g. ester) would be of great interests. However, the requirement of either strong alkaline condition in aqueous medium (**Scheme 3.2A**) or the use of DIBAL-H as reductant (**Scheme 3.2B**) in Overberger reaction led to alkaline hydrolysis of ester or reduction of ester group by DIBAL-H. Identification of reaction condition for nitrogen extrusion that is compatible with ester group is therefore necessary (**Scheme 3.4A**) Formation of 1,1-diazene intermediate **II** from pyrrolidine **I**, that could produce 1,4-diradical species **III**, is proven to be essential for ring contraction process to give cyclobutane **IV**.

Inspired by the seminar work reported by Lu and co-workers,^{132, 133} the *N*-sulfonyl azide of pyrrolidine **163** was prepared (**Scheme 3.4B**). Heating of *N*-sulfonyl azide **163** containing a *para*-methoxy arene as substitute to 120°C in toluene lead to the formation of the cyclobutane **166** in 95% yield, presumably via a Curtius-type rearrangement/nitrogen extrusion process. This excellent yield of this rearrangement type reaction required pre-installation of an auxiliary to the nitrogen atom of pyrrolidine as a synthetic precursor for ring contraction. Noteworthy, the process of ring contraction is stereoselective in which the stereochemistry is conserved and has been confirmed by X-ray structures (i.e. **163**, X-ray structure; **166**, X-ray structure). Lu and others^{132, 133} emphasized the chemical unstable nature of the *N*-sulfonyl azide (e.g. **163**) and may lead to explosion. Therefore, we switch to other approaches which is safe and stable species for ring contraction.

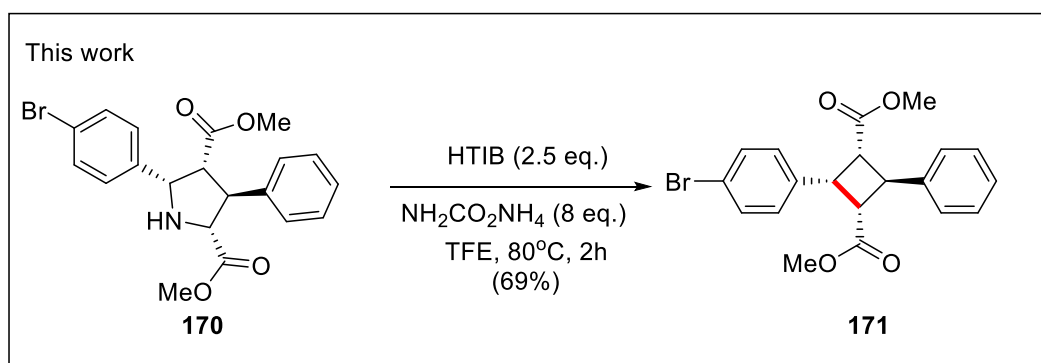
Being reassured by the possible formation of 1,1-diazene intermediate in the Curtius-type rearrangement/nitrogen extrusion process, we envisage that this intermediate may be also formed by oxidation of *N*-aminopyrrolidine (**Scheme 3.4C**). Gratifying, exposure of *N*-aminopyrrolidine **167** to PIDA in 1,4-dioxane at 80°C produced the desired cyclobutane **169** in 64% yield. In this process, oxidation of *N*-aminopyrrolidine **167** using PIDA results in the formation of 1,1-diazene **168**, which facilitates the nitrogen extrusion/biradical formation/C-C bond formation to give the cyclobutane **169**. To develop a one-step synthesis of cyclobutane from corresponding pyrrolidines, it is rational to design a synthetic process as below: (i)

Electrophilic amination of the *N*-atom of pyrrolidine to form 1,1-diaene as intermediate and (ii) Nitrogen extrusion then takes place to generate the biradical that leads to the formation of cyclobutanes.



Scheme 3.4 Preliminary studies of contractive synthesis of multi-substituted cyclobutanes from *N*-activated pyrrolidines. **A.** The current research gap. **B.** Stereoselective ring contraction of *N*-sulfonyl azide **153** gives cyclobutane **154** as exclusive product in high yield **C.** Oxidation of *N*-amino pyrrolidine **157** gives cyclobutane **156**. **D.** One-step, stereoselective synthesis of cyclobutane **160** from corresponding pyrrolidine **159** using iodonitrene chemistry (this work)

After extensive experimentation, treatment of pyrrolidine **170** as standard substrate with 2.5 equivalent of HTIB and 8 equivalent of ammonium carbamate in 2,2,2-trifluoroethanol gave cyclobutane **171** in 69% yield (**Scheme 3.5**).



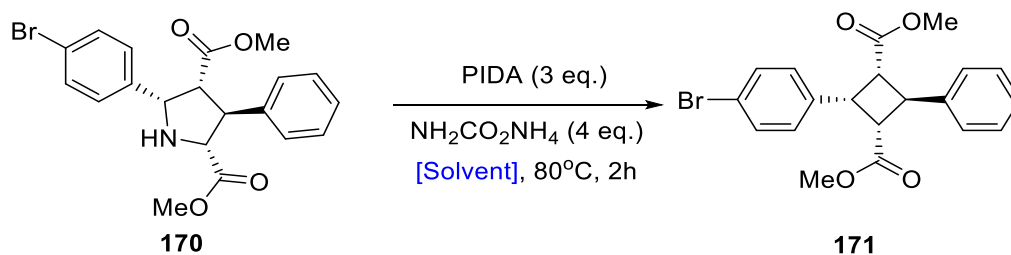
Scheme 3.5 One-step, stereoselective synthesis of cyclobutane **171** from corresponding pyrrolidine **170** using iodoneitrene chemistry (this work)

3.4 Optimization of condition

After the intensive screening of conditions including iodine containing compounds, various sources of nitrogen, solvents and temperatures (**Table 3.1 to Table 3.5**), the optimized conditions were identified based on the screening result.

3.4.1 Screening of solvent

First, the screening of solvent identified that polar, alcoholic solvent gave the best yield among others (**Table 3.1**). Among HFIP, TFE and methanol, TFE gave the highest yield as solvent when PIDA is used as an oxidant. This observation is consistent to the previous report that TFE could increase the rate of reaction that involved iodoneitrene.¹³⁴ Among the fifteen solvents screened, alcoholic solvents such as TFE (**Table 3.1**, entry 1) and methanol (entry 13) gave the highest yield (48-54%). Replacing the alcoholic solvent with non-protonic solvent such as acetonitrile (entry 4), ethylacetate (entry 5) and 1,4-dioxane (entry 12) led to tremendous decrease in yield. Moreover, the use of acetic acid (entry 6), toluene (entry 7) and THF (entry 14) failed to give reaction product. Collectively, the screening results agree with the fact that alcoholic solvent is essential to the formation of iodoneitrene and hence gave the highest yield among the solvents that we screened.



Entry	Variation from standard condition	NMR Yield (%) ^{a,b}
1	2,2,2-trifluoroethanol (TFE)	54
2	<i>i</i> -PrOH	24
3	<i>t</i> -BuOH	21
4	MeCN	36
5	EtOAc	15
6	AcOH	N.D.
7	Toluene	N.D.
8	DMF	3
9	PhCF ₃	15
10	H ₂ O	N.D.
11	1,2-DCE	12
12	1,4-dioxane	15
13	MeOH	48 (44)
14	THF	N.D.
15	HFIP	36

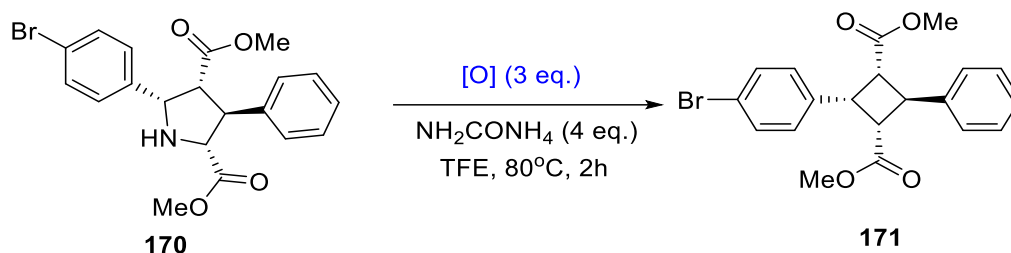
Table 3-1. Screening of solvent

^a0.1 mmol of 1,3,5-trimethylbenzene as internal standard. ^bIsolated yield in parathesis. N.D. represents “not detected”.

3.4.2 Screening of oxidant

Next, the screening of oxidant revealed that hypervalent iodine(III) compounds acts as oxidant that exclusively form iodonitrene as reactive species in the presence of ammonia surrogate (**Figure 3-2**). Among the hypervalent iodine(III) reagents we tested, HTIB (also known as Koser’s reagent or HTIB) performed well and gave the highest yield (**Table 3.2**). Interestingly, hypervalent iodine(III) compound with less vacant sites such as diphenyliodonium bromide and iodosolactone failed to give any reaction product (entry 6). Moreover, hypervalent iodine (III) compounds carrying intramolecular lactone(s) failed to give reaction product (entries 14 and 19). These observations agree with the suggested mechanism of iodonitrene formation, in which λ^3 iodane (e.g. PIDA, HTIB or PhI=O, etc.) is necessary to react with ammonia surrogate to form the reactive species iodonitrene. Furthermore, other iodine containing compounds, such as IBX (entry 7), iodine (entry 9) and N iodosuccinimide (entry 10) do not give the desired

product. Collectively, these results suggest that the formation of iodonitrene from λ^3 iodane are essential for ring contraction of pyrrolidine to corresponding cyclobutanes.



Entry	Variation from standard condition	NMR Yield (%) a,b
1	PIDA (S1)	54
2	PIFA (S2)	6 (37)
3	[bis-(Trifluoroacetoxy)iodo]pentafluorobenzene (S3)	33
4	Bis(tert-butylcarbonyloxy)iodobenzene (S4)	51
5	Iodosobenzene (S5)	51 (51)
6	Diphenyliodonium bromide (S6)	N.D. (0)
7	IBX (S7)	N.D.
8	HTIB (S8)	63 (69)
9	Iodine (S9)	N.D.
10	<i>N</i> -Iodosuccinimide (S10)	N.D.
11	1-Acetoxy-1,2-benziodoxol-3-(1 <i>H</i>)-one (S11)	N.D.
12	(4-chlorophenyl)(hydroxy)- λ^3 -iodaneyl 4-methylbenzenesulfonate (S12)	59
13	PhI=NTs (S13); without NH_2CONH_4	N.D.
14	1-hydroxy-1 λ^3 -benzo[d][1,2]iodaoxol-3(1 <i>H</i>)-one (S14)	N.D.
15	(4-(<i>tert</i> -butyl)phenyl)(hydroxy)- λ^3 -iodaneyl 4-methylbenzenesulfonate (S15)	48
16	(2-(methoxymethyl)phenyl)- λ^3 -iodanediyl diacetate (S16)	37
17	PhI (20 mol%), <i>m</i> -CPBA (3 eq)	N.D.
18	[Hydroxy(methanesulfonyloxy)iodo]benzene (S17)	63 (63)
19	Iodosodilactone (S18)	N.D.

Table 3-2. Screening of oxidant.

^a0.1 mmol of 1,3,5-trimethylbenzene as internal standard. ^bIsolated yield in parathesis. N.D. represents “not detected”.

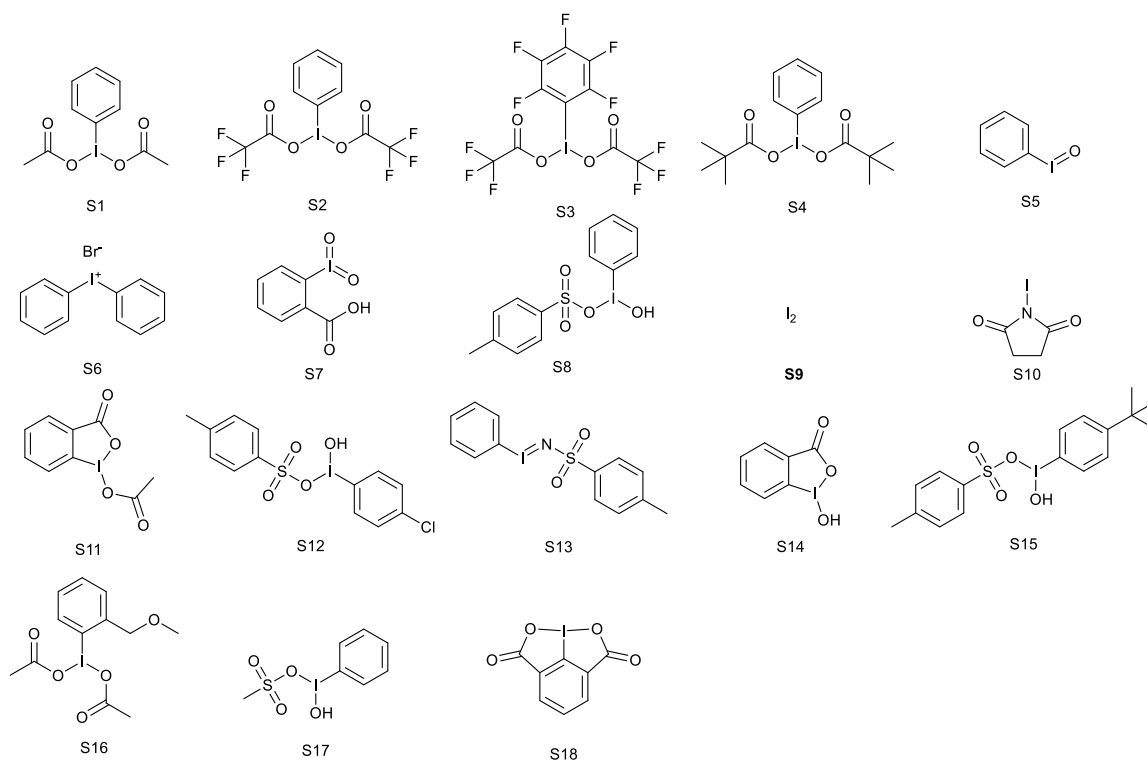
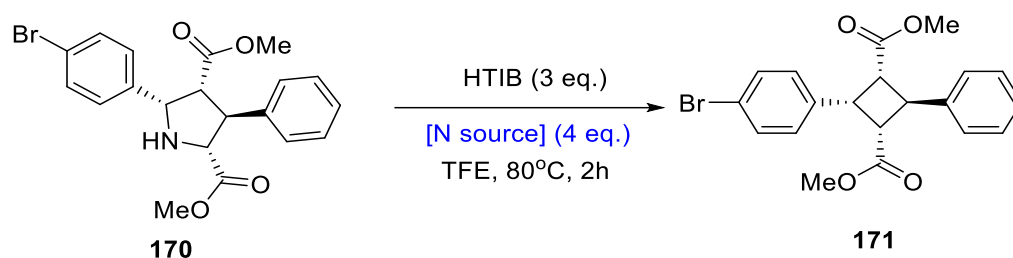


Figure 3-2. Chemical structure of iodine containing oxidants

3.4.3 Screening of nitrogen source

Then the source of nitrogen for iodonitrene formation is investigated (**Table 3.3**). Among the possible tested source of nitrogen, only ammonia in aqueous solution, ammonium carbamate and ammonia in methanol (7M) are eligible as effective nitrogen source for iodonitrene formation with HTIB. Ammonium carbamate not only give the highest yield among the others but also have the advantages such as easy to handle, chemically stable and commercially accessible. Other nitrogen sources such as ammonium salt (entries 4-6, 9 and 16) and amine containing compounds (entries 11-15 and 17) did not give cyclobutane, which implies that ammonia or its surrogate is necessary for the formation of iodonitrene as reactive species.



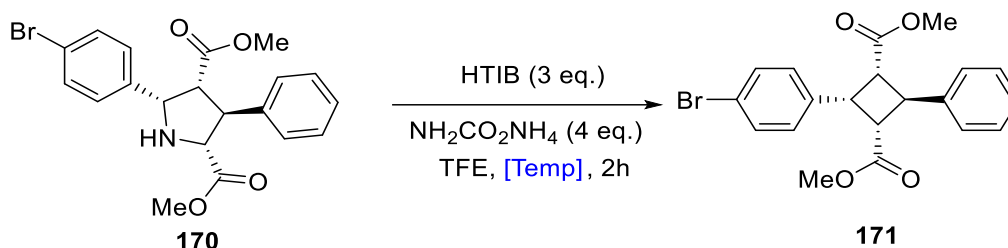
Entry	Variation from standard condition	NMR Yield (%) ^{a,b}
1	$\text{NH}_2\text{CO}_2\text{NH}_4$	63 (69)
2	O-(2,4-dinitrophenyl)hydroxylamine (DPH); PIDA 3eq instead of HTIB 3eq.	N.D.
3	PhI=NTs (S13) ; without HTIB	N.D.
4	NH_4Cl	N.D.
5	NH_4OAc	N.D.
6	NH_4PF_6	N.D.
7	NH_4OH (25% aq ammonia)	54
8	Hydrazine monohydrate ($\text{H}_2\text{NNH}_2\cdot\text{H}_2\text{O}$)	N.D.
9	NH_4HCO_2	N.D.
10	$\text{NH}_2\text{-OH}$ (50% wt aq. solution)	N.D.
11	Hydroxylamine- <i>O</i> -sulfonic acid	N.D.
12	$(\text{NH}_2)_2\text{C=S}$	N.D.
13	NH_3 (7M in MeOH)	55
14	<i>tert</i> -butyl carbamate	N.D.
15	Boc- ONH_2	N.D.
16	NH_4HCO_3	N.D.
17	<i>N</i> -aminophthalimide	N.D.

Table 3.3 Screening of nitrogen source

^a0.1 mmol of 1,3,5-trimethylbenzene as internal standard. ^bIsolated yield in parathesis. N.D. represents “not detected”.

3.4.4 Screening of reaction temperature

After studying the reaction temperature, 80°C is the optimal reaction temperature for reaction to take place (**Table 3.4**). The yield of the reaction reduced significantly at lower temperature but reaction could take place at lower temperature (e.g. 20°C). Since the iodonitrene could be formed in room temperature and nitrogen extrusion from the 1,1-diazene occurs at 0°C, ring contraction of pyrrolidine take place at lower temperature align with the prior research findings.^{96, 135} We were puzzled about the necessity of heating the reaction. It should be noted that pyrrolidine is sparingly soluble in methanol and dissolves completely upon short heating (ca. 1 min) at 80°C. However, the pyrrolidine crystallized after standing at room temperature. We therefore suggest that the optimized reaction temperature compromises for the solubility of starting material, iodonitrene formation, nitrene transfer and nitrogen extrusion.



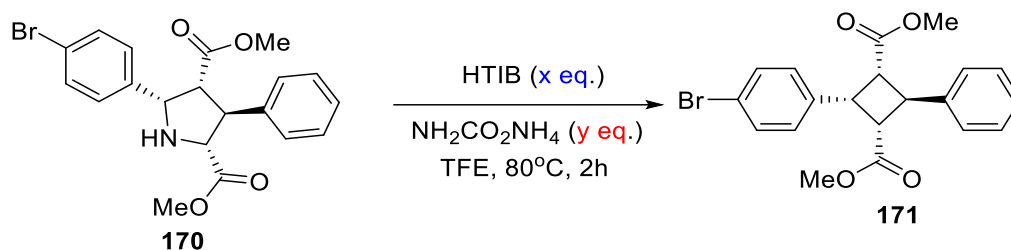
Entry	Variation from standard condition	NMR Yield (%) ^{a,b}
1	80°C	63 (69)
2	20°C	15
3	40°C	29
4	60°C	62
5	100°C	42
6	120°C	63
7	80°C; In seal tube instead of reaction vial	(65)

Table 3-4. Screening of reaction temperature

^a0.1 mmol of 1,3,5-trimethylbenzene as internal standard. ^bIsolated yield in parathesis. N.D. represents “not detected”.

3.4.5 Screening of equivalence of reagents

Finally, the last parameter needs to be optimized is the equivalent of reagents (**Table 3.5**). Initially, 2.5 eq. of HTIB and 4 eq. of ammonium carbamate was found to be the optimal for ring contraction. However, the yield of reaction varies (i.e. yield decreased and side product was observed). After careful investigation, the addition of 8 eq. of ammonium carbamate gave the best yield and the formation of side product is suppressed.



Entry	Variation from standard condition	NMR Yield (%) ^{a,b}
1	HTIB (3 eq), NH ₂ CO ₂ NH ₄ (4 eq.)	63 (69) ^c
2	2 eq of HTIB instead of 3 eq	56
3	2.5 eq of HTIB instead of 3 eq	62 (54)
4	3.5 eq of HTIB instead of 3 eq	22
5	4 eq of HTIB instead of 3 eq	35
6	6 eq of HTIB instead of 3 eq	13
7	8 eq of HTIB instead of 3 eq	5
8	2 eq of NH ₂ CO ₂ NH ₄	N.D.
9	3 eq of NH ₂ CO ₂ NH ₄	15
10	6 eq of NH ₂ CO ₂ NH ₄	50
11	8 eq of NH ₂ CO ₂ NH ₄	58
12	HTIB (2.5 eq), NH ₂ CO ₂ NH ₄ (8 eq.)	(69)

Table 3-5. Screening of equivalence of reagents

^a0.1 mmol of 1,3,5-trimethylbenzene as internal standard. ^bIsolated yield in parathesis. N.D. represents “not detected”. ^c Oxidation of pyrrolidine was observed when 4 eq. of ammonium carbamate was used. (see Scheme S3)

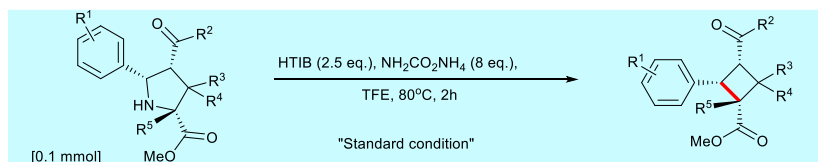
3.5 Study of the substrate scope

With the optimized conditions in hand, we investigated the substrate scope (**Scheme 3.6**). First, all substrates with *para*-substituent on the 2-phenyl ring of pyrrolidine gave a yield of 51-69% (i.e. **171** - **176**). Substrates with *meta*-substituent (i.e. *meta*-methoxy **177**) and *ortho*-substituents (i.e. **178** - **180**) showed also good yields. It is noteworthy that **179** with *ortho*-chloro group gave the best yield among all substrates. Besides the substituted 2-phenyl group, other groups such as naphthalene **181**, thiophene **182** and pentafluorophenyl group **183** were compatible to the optimized conditions for ring contraction. Pyrrolidines with electron-rich α -aryl substituents gave cyclobutanes (**177**, **178**) in lower yield compared to those with electron-deficient groups (**174**, **179**). This is due to the known over-oxidation of electron rich arenes by hypervalent iodine reagents.¹³⁶ In general, the position of substituents on the α -aryl ring did not pose prominent effect on the yield. Interestingly, our optimized condition was applied successfully to prepare heterocycle-substituted cyclobutane, which is previously inaccessible but is pharmaceutically important.

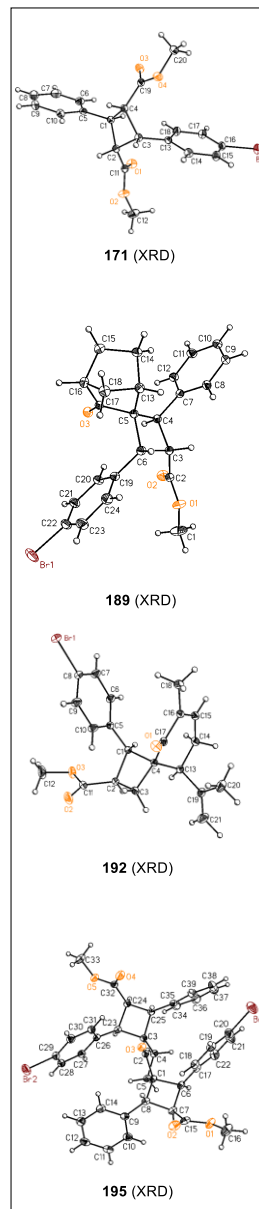
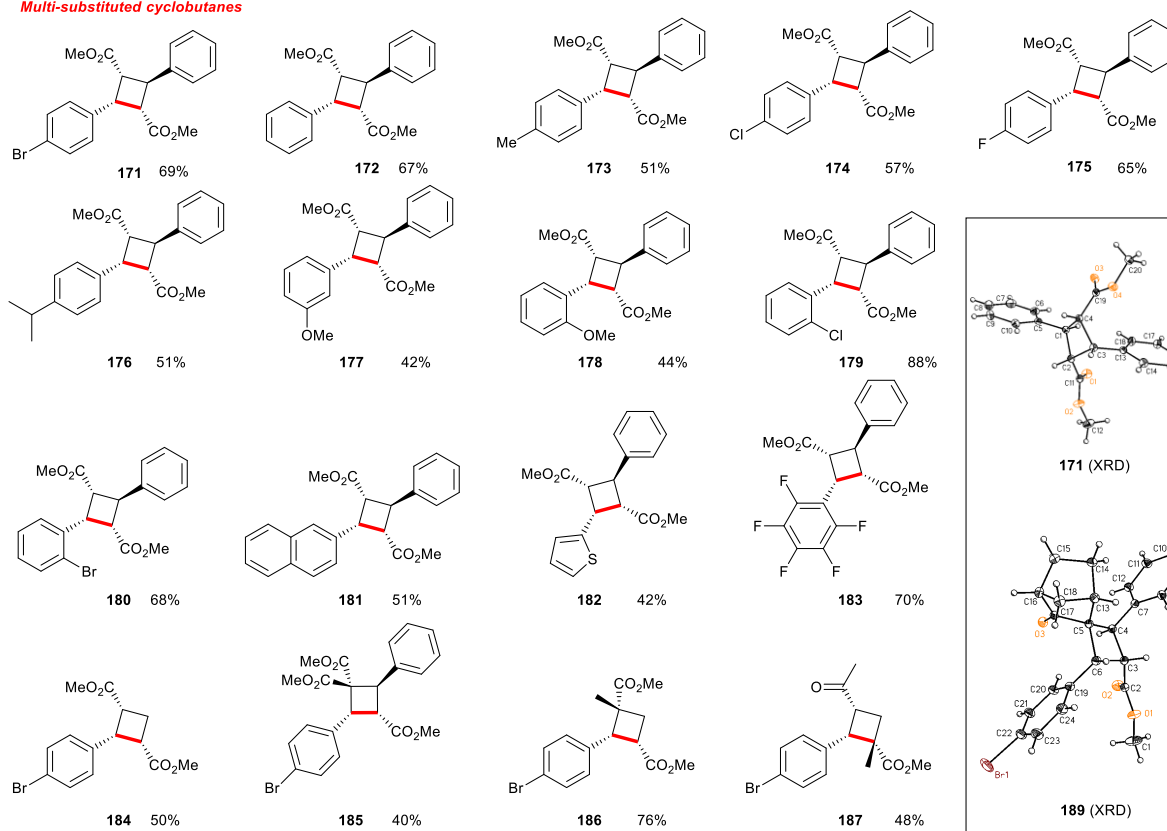
Next, we aimed to test our conditions with pyrrolidines with different structural characteristics. Changing the 4-phenyl group of pyrrolidine of **171** to a methylene group gave cyclobutane **184** in 50% yield. Ring contraction of corresponding pyrrolidines bearing quaternary carbon centers gave the corresponding cyclobutanes **185** and **186** in 40% yield and 76% yield, respectively. Importantly, **187** is the first example where ring contraction took place on a pyrrolidine containing a quaternary carbon contiguous to the nitrogen atom and a quaternary carbon atom in the ring contraction process is generated. The β -quaternary carbon on pyrrolidine may positively guide the formation of a strained C-C bond *via* Thorpe-Ingold effect.¹³⁷ Further, **97** showed that the reactive ketone group is compatible to ring contraction without any need of protection.

Excited by the possibility of ring contraction on pyrrolidines bearing quaternary carbon centers (e.g. **185** and **186**), we anticipated that more structurally intriguing pyrrolidines could be converted to the corresponding cyclobutanes, which present a synthetic hurdle in organic and medicinal chemistry. We expanded the substrate scope by preparing challenging spirocyclobutanes.¹³⁸ Spirocyclobutanes including **188**, carbonyl-carrying **189** and **190**, and **191** were synthesized under our optimized conditions. Natural-product-derived pyrrolidines, such as **192** and **193** which were prepared from carvone and (+)-sclareolide (structures not depicted) respectively, gave spiro-cyclobutanes in modest yield. Importantly, our method allows the synthesis of complex scaffolds, connecting bioactive structures with a cyclobutane to form spirocycles, to explore bio-chemical space.¹³⁹

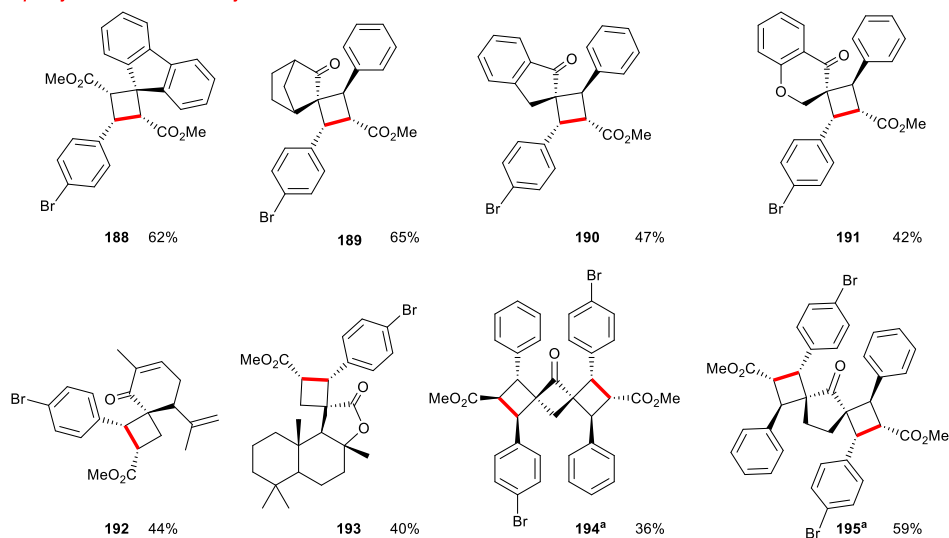
After the successful preparation of multi-substituted cyclobutanes and spiro-cyclobutanes, we wondered about the possibility to carry out simultaneous ring contraction of two pyrrolidines on the same compound. When the amount of HTIB was increased to 5 equivalents, double ring contraction of pyrrolidines occurred and gave the corresponding cyclobutanes **194** and **195**. These molecular architectures, which were not reported before, may inspire the design of new functionalized materials.



Multi-substituted cyclobutanes



Spirocyclic multi-substituted cyclobutanes

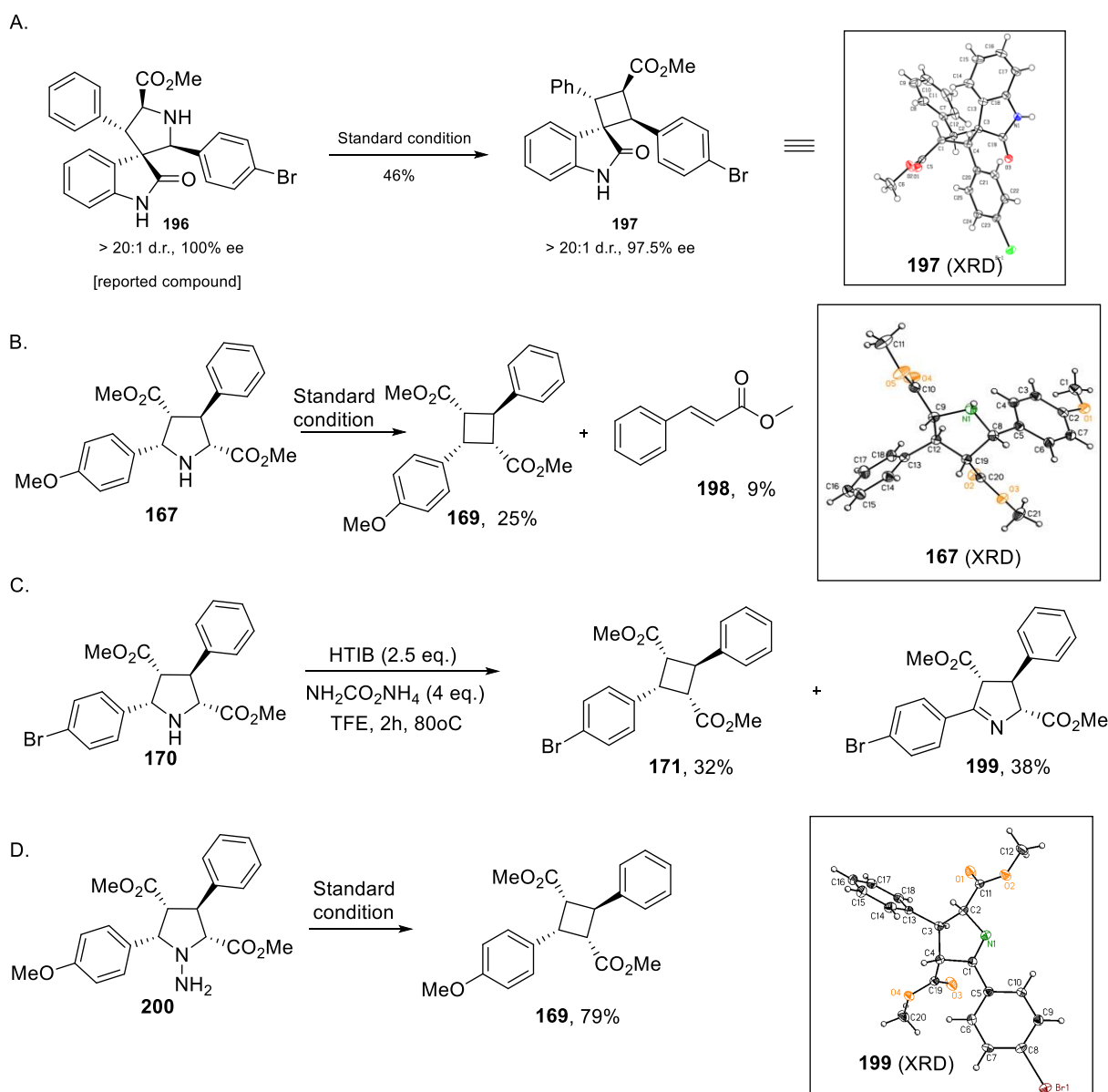


^a. 5 eq. of HTIB and reaction for 12h is required.

Scheme 3.6 Scope of contractive synthesis of multi-substituted cyclobutane from pyrrolidine.

3.6 Investigation of reaction mechanism

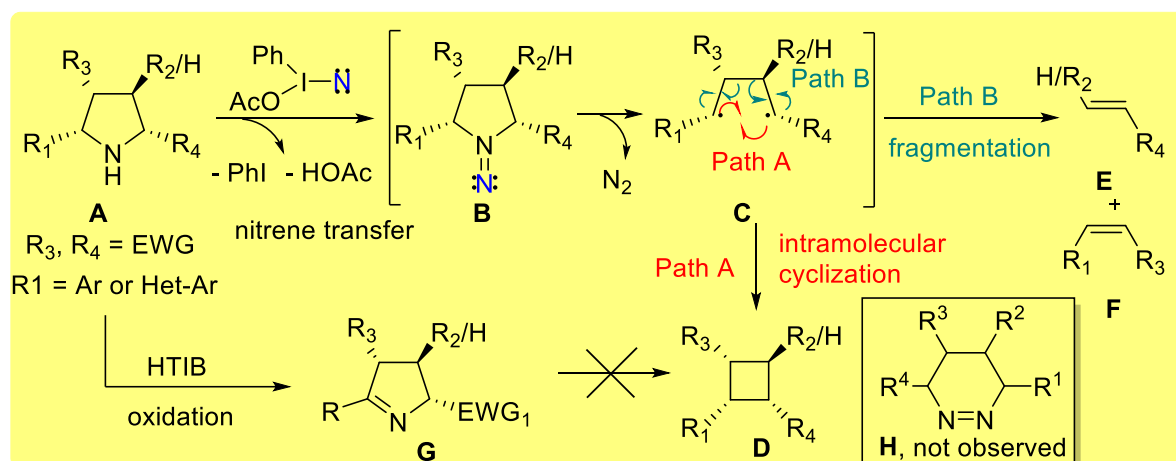
After demonstrating the substrate scope, further investigation was conducted to understand the possible reaction mechanism (**Scheme 3.7**). Exposure of the enantioenriched spiro-oxindole pyrrolidine **196**¹⁴⁰ (60% *ee*) to the standard conditions gave spirooxindole cyclobutane **197** (60% *ee*) in 44% yield (**Scheme 3.7A**). Conservation of enantioselectivity proved that the stereochemistry is retained throughout the ring contraction process. Next, we wanted to identify the possible side products of our reaction, aiming to suppress any possible side reaction(s) (**Scheme 3.7B**). Under the optimized conditions, cyclobutane **169** was formed and was isolated in 25% yield. Furthermore, *trans*-methyl cinnamate **198** was isolated in 9% yield. We postulated that *trans*-methyl cinnamate was formed during the nitrogen extrusion process. Moreover, oxidation of pyrrolidine **167** took place to give the imine **199** when 4 equivalents of ammonium carbamate were used (**Scheme 3.7C**); X-ray structure of **167**, inset). Since oxidation of pyrrolidine by hypervalent iodine(III) reagent to the corresponding imine is known,¹⁴¹⁻¹⁴³ the formation imine **199** implies the presence of excess HTIB as oxidant or oxidation of pyrrolidine by HTIB takes place in prior to *in-situ* formation of iodonitrene with ammonium carbamate. To suppress the imine oxidation by HTIB, an excessive amount of ammonium carbamate was added. To verify our initial proposal that contraction synthesis of cyclobutane from pyrrolidine involves electrophilic amination of pyrrolidines, a *N*-aminated pyrrolidine **200** was prepared and was exposed to the standard conditions. Gratifyingly, cyclobutane **169** was formed in 79% yield, which is a significant improvement to the direct ring contraction from pyrrolidine (i.e. 25% yield). (**Scheme 3.7D**)



Scheme 3.7 Further investigation of contractive synthesis of cyclobutanes from pyrrolidines. **A.** Ring contraction using enantioenriched pyrrolidine. **B.** Observation of olefinic side products using pyrrolidine with electron-rich arene substituents. **C.** Oxidation of pyrrolidine to corresponding imine **167** when less equivalent of ammonium carbamate was added. **D.** *N*-aminopyrrolidine **157** gave cyclobutane **156** in good yield under the standard condition.

Based on the results we discussed above, the proposed reaction mechanism is illustrated (**Scheme 3.8**). A high degree of stereo retention was observed in the cyclobutane product and the formation of olefinic side product suggests that the contractive synthesis of cyclobutane may involve the formation of 1,4-biradical species. Treatment of pyrrolidine **A** with the *in-situ* generated iodonitrene species leads to electrophilic amination affording 1,1-diazene **B** as reactive intermediate. This reactive 1,1-diazene **B** proceeds further to give 1,4-biradical **C**,

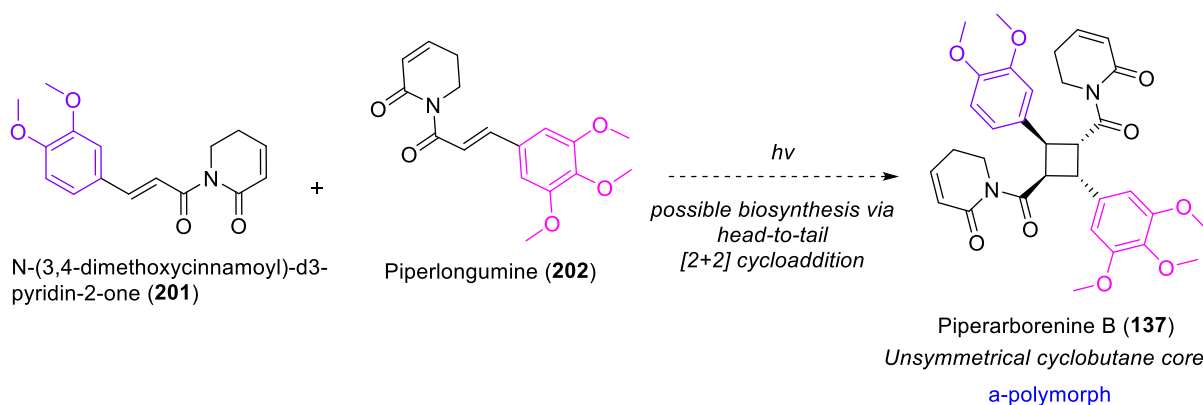
presumably *via* nitrogen extrusion. Since two C–N bonds must be cleaved in order to extrude the dinitrogen from 1,1-diazene **B**, external energy such as heating is necessary for this process to take place. The intramolecular cyclization of the 1,4-biradical **C** results in a C–C bond formation to give cyclobutane **D** (path A). We do not have any information on whether C–N bond breaking is occurring simultaneously or stepwise while 1,2-diazene **B** arranged from 1,1-diazene **H** was not observed. The stereospecificity of the cyclobutane **D** from **B** reflects simultaneous two C–N bond cleavages with formation 1,4-biradical **C** which rapidly undergoes to cyclization. Meanwhile, olefinic side products formed as an outcome of fragmentation of 1,4-biradical **C** through homolytic C–C bond cleavage (path B). On the other hand, the presence of free and/or excess HTIB could oxidize the pyrrolidine **A** to the corresponding imine **G**,¹⁴¹⁻¹⁴³ which is inconvertible to the cyclobutane.



Scheme 3.8 The proposed mechanism based on the experimental evidences.

3.7 Cytotoxic cyclobutane natural product Piperarborenine B

Piperarborenine B (**137**) is a cytotoxic natural product isolated from *Piper arborescens*.¹⁴⁴ Biologically, piperarborenine B (**137**) exhibited *in vitro* cytotoxicity against P-388, HT-29, and A549 cancer cell lines ($IC_{50} < 4 \mu\text{g/mL}$). Structurally, piperarborenine B (**137**) possesses an unsymmetrical truxillate core, which is highly likely to be a result from a head-to-tail [2+2] cycloaddition via biosynthetic synthesis (**Scheme 3.9**).¹⁴⁵⁻¹⁴⁷ Despite there is a tremendous advancements in the hetero-[2+2] cycloaddition reaction and its application, the direct synthesis of piperarborenine B (**137**) using an intermolecular [2+2] cycloaddition of N-(3,4-dimethoxycinnamoyl)-d3-pyridine-2-one **201** and piperlongumine (**202**) is yet to be reported.



Scheme 3.9 Possible biosynthesis of piperaroborenine B (**137**) via head-to-tail [2+2] cycloaddition

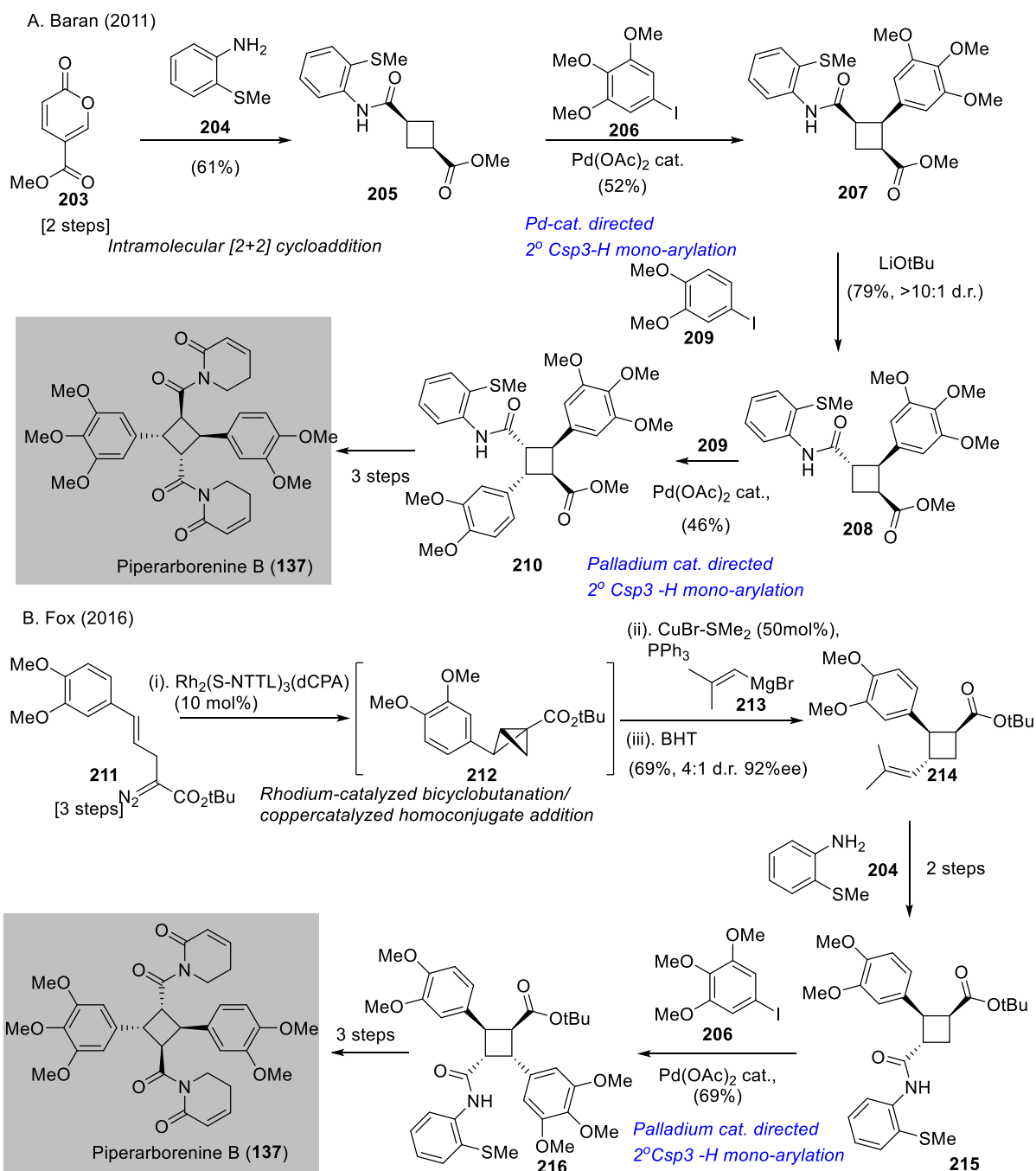
3.8 Reported synthesis of cytotoxic natural product Piperaroborenine B

The total synthesis of piperaroborenine B (**137**) was reported firstly by Baran and co-workers in 2011.¹⁴⁸ In 2016, Fox and co-workers reported the enantioselective synthesis of piperaroborenine B (**137**).¹⁴⁹ Later in the same year, Tang and Xie reported the enantioselective synthesis of (+)-piperaroborenine B.¹⁵⁰ The general strategy of the reported total syntheses involved construction of the cyclobutane core followed by transition-metal catalyzed, directed β -C_{sp³}-H bond arylation to access the multi-substituted cyclobutane core.

Baran's synthesis of piperaroborenine B (**137**) began with a sequence of reaction on **203** including intramolecular [2+2] cycloaddition/lactone's hydrolysis/amidation with aniline **204** to give cyclobutane **205** in 61% yield (**Scheme 3.10A**). A directed, palladium catalyzed β C_{sp³}-H arylation of **205** with aryl iodide **206** gave **207** in 52% yield, which was treated with lithium *tert*-butoxide that led to inversion of stereochemistry of the amide group to give **208** in 79% yield with >10:1 d.r.. Another directed, palladium catalyzed β C_{sp³}-H arylation of **208** with aryl iodide **209** gave the fully-functionalized cyclobutane precursor **210** in 46% yield. The synthesis of piperaroborenine B (**137**) was completed in steps. In this work, Baran and co-workers elegantly used one directing group to facilitate two separated β C_{sp³}-H arylation and is one of the pioneer application of palladium catalyzed C_{sp³}-H activation in natural product synthesis.

Fox's reported the first enantioselective synthesis of piperaroborenine B (**137**) making use of their rhodium catalysis chemistry (**Scheme 3.10B**). A tandem rhodium-catalyzed bicyclobutanation/copper catalyzed conjugated addition of **211** with **213** produced **214** in 69%

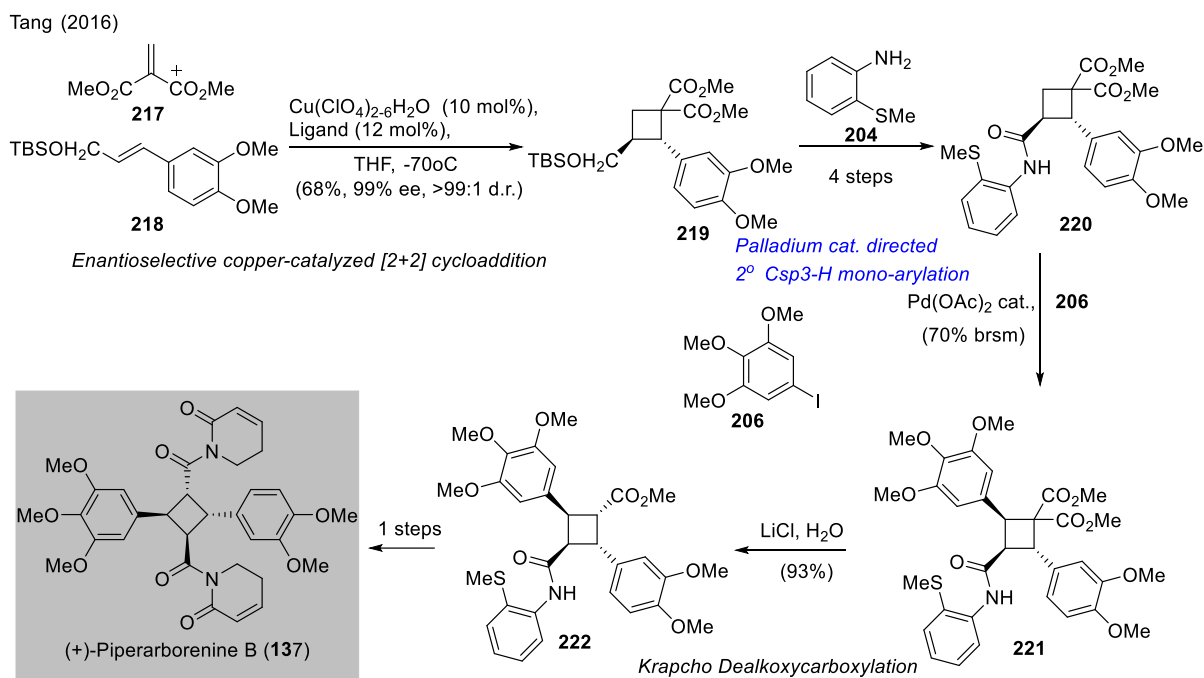
yield with a 4:1 d.r. in 92% *ee*. The freshly prepared enantioenriched cyclobutane **214** was converted into amide **215** in two steps, in which a directed, palladium catalyzed β C_{sp3}-H arylation of **215** with aryl iodide **206** gave **216** in 69% yield. This newly formed cyclobutane precursor **216** was converted into piperarborenine B (**137**) in three steps.



Scheme 3.10 Reported total synthesis of piperarborenin B (**137**). (A) Baran (2011) and (B) Fox (2016).

Xie and Tang disclosed another enantioselective synthesis of (+)-piperarborenine B (**137**) shortly after Fox's report (**Scheme 3.11**). The synthesis commenced with an enantioselective copper-catalyzed unsymmetrical intermolecular [2+2] cycloaddition between **217** and **218** to give **219** in 68% yield with >99% ee. After a four-step synthesis to install the amide directing group, **220** formed was subjected to directed, palladium catalyzed β C_{sp3}-H arylation with aryl iodide **206** to give **221** in 70% yield (by recovering starting material). Krapcho decarboxylation of **221** gave functionalized cyclobutane **222**, which was transformed to piperarborenine B (**137**) in one step.

Enlightened by these perceptive synthetic designs, we postulated that our method can be applied to synthesize the functionalized cyclobutane core of piperarborenine B (**137**) and eschews the need of directing group manipulations in catalytic C_{sp3}-H activation reactions.

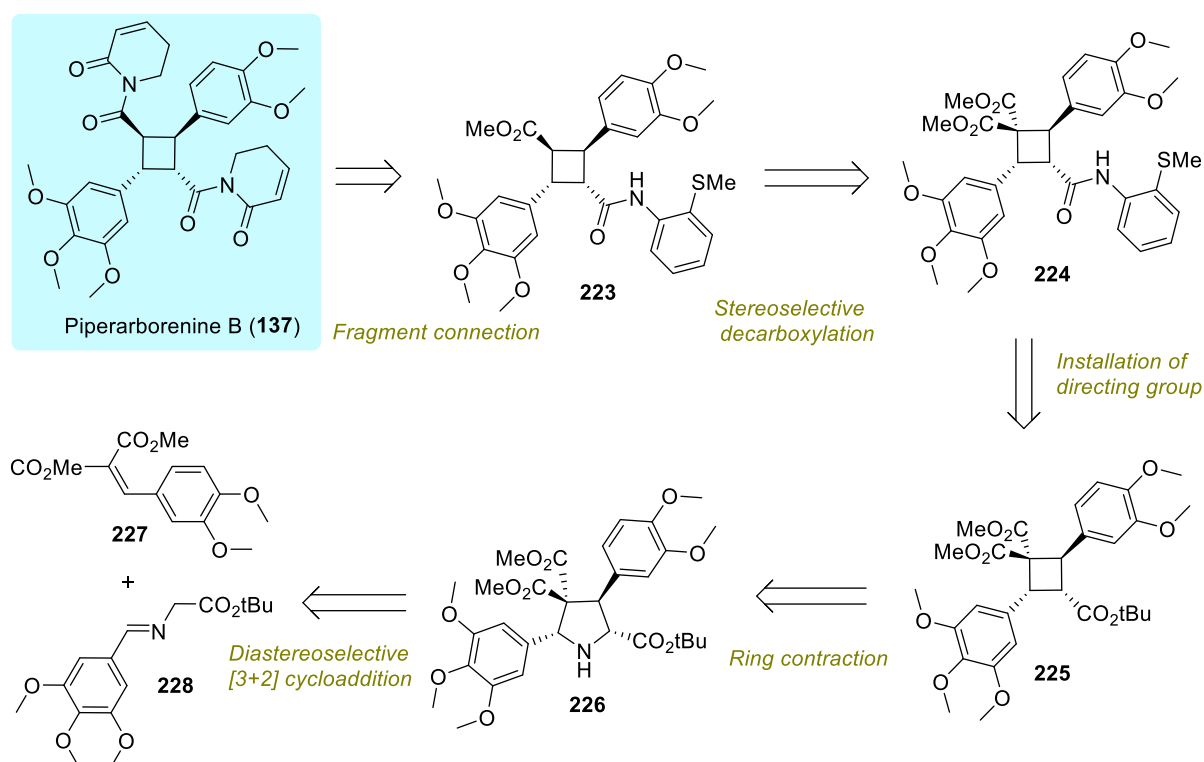


Scheme 3.11 Reported total synthesis of piperarborenin B (**137**) by Tang and Xie in 2016.

3.9 Retrosynthetic analysis of piperarborenine B

After the discussion of the reported synthetic protocol of piperarborenine B (**137**), we envision that our method could improve the overall synthetic efficiency by enabling the direct accomplishment of multi-substituted, unsymmetrical cyclobutane core of piperarborenine B (**137**). Retrosynthetic analysis of piperarborenine B (**137**) is shown (**Scheme 3.12**) The

stereoselective decarboxylation of **224** was assisted by the 2-thiomethylaniline using Krapcho dealkoxycarbonylation to give natural product precursor **223**. Cyclobutane **225**, which could be prepared by our ring contraction method, is subjected to selective saponification of *tert*-butyl ester group followed by amidation to give the anilide **224**. Finally, pyrrolidine **226** could be synthesized readily from the alkene **227** and imine **228** via silver/PPh₃ catalyzed diastereoselective [3+2] cycloaddition.

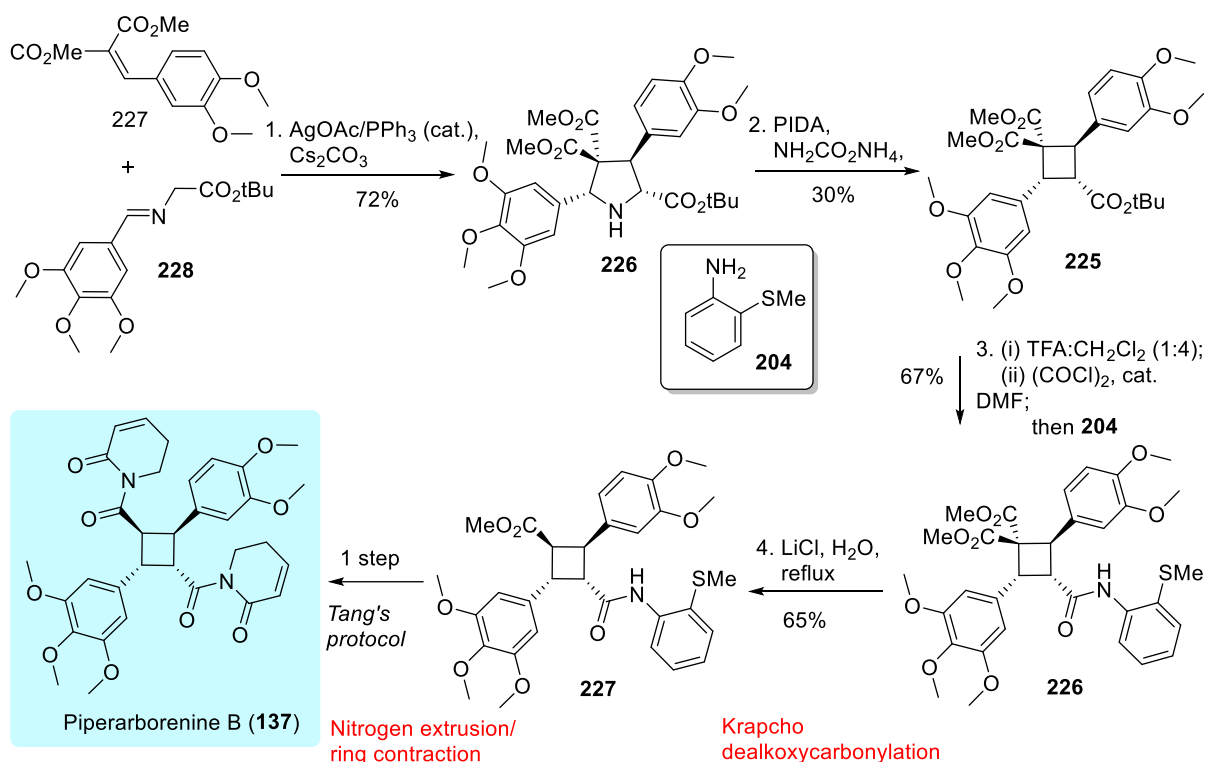


Scheme 3.12 Retrosynthetic analysis of piperarborenine B (**137**)

3.9 Formal synthesis of piperarborenine B using ring contraction approach

Our synthesis of piperarborenine B (**3**) commenced with silver-catalyzed [3+2] cycloaddition¹⁵¹ to give pyrrolidine **226** in 72% yield (**Scheme 3.13**). Nitrogen extrusion/ring contraction of pyrrolidine **226** gave cyclobutane **225** in 30% yield. Treatment of cyclobutane **225** with TFA in dichloromethane led to the hydrolysis of the *tert*-butyl ester, in which the resultant carboxylic acid was converted to the corresponding acyl chloride followed by acylation with aniline **204** to give **226** in 67% yield in one-pot. The freshly prepared cyclobutane **226** was subjected to Krapcho dealkoxycarbonylation to give substituted cyclobutane precursor **227**. Precursor **227** was transformed into piperarborenine B (**137**) using

Tang's procedure.¹⁴⁷ Our approach enables the direct access to multi-substituted cyclobutanes from pyrrolidine, and hence shows an alternative path to the synthesis of biologically important cyclobutanes containing natural products, especially to those containing an unsymmetrical cyclobutane core.



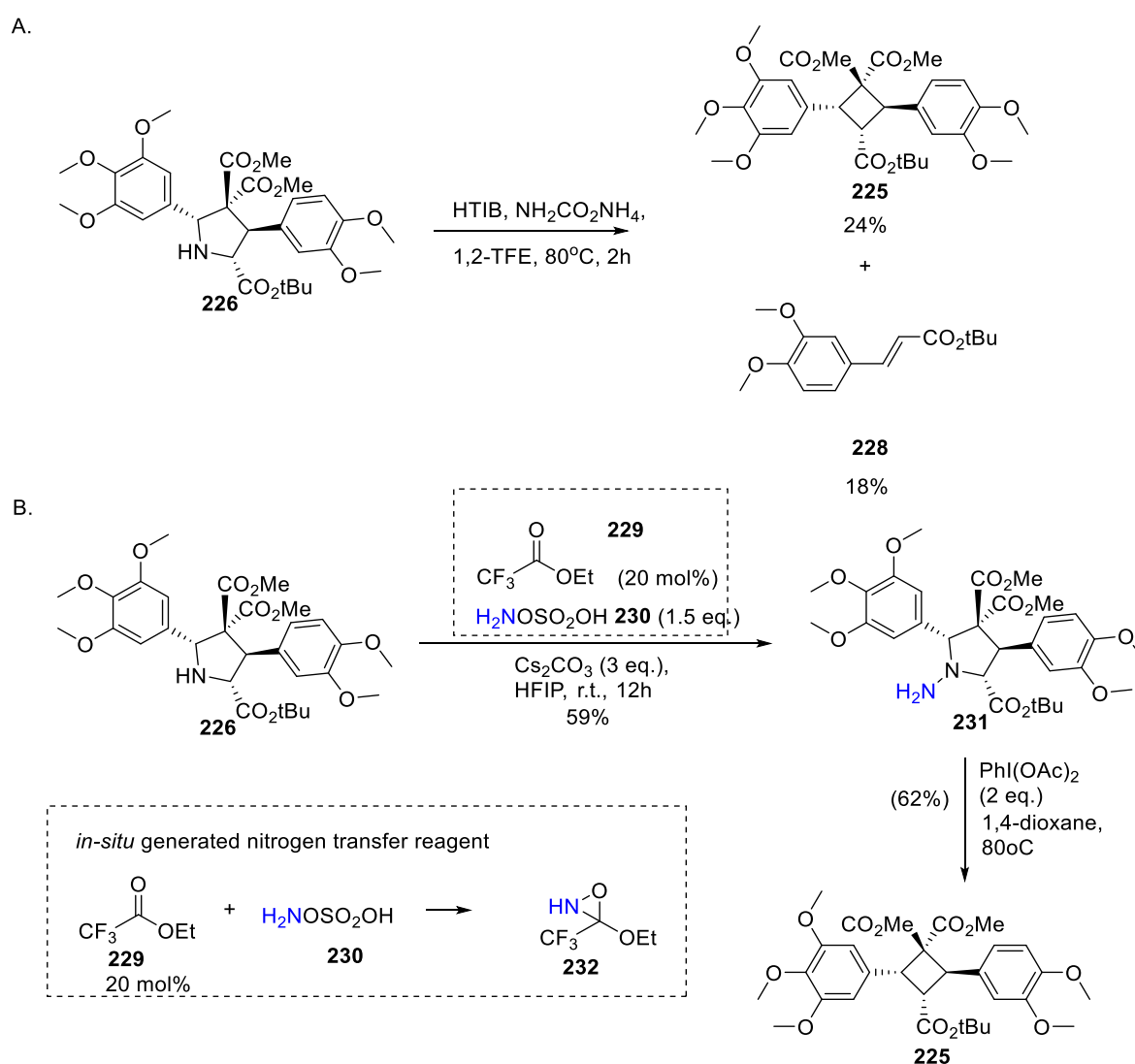
Scheme 3.13 Formal stereoselective synthesis of piperarborenine B (**137**) features contractive synthesis of cyclobutane as key step.

3.10 Improvement of ring contraction step of piperarborenine B's synthesis

In the formal synthesis of piperarborenine B (**137**) (Scheme 3.14), PIDA instead of HTIB was used as hypervalent iodine (III) reagent for contractive synthesis of cyclobutane **225**. Under the standard condition, pyrrolidine was converted to cyclobutane **225** in 24% yield and olefin **228** was isolated in 18% yield (Scheme 3.14A). In the presence of electron-rich aryl group on pyrrolidine at α carbon of nitrogen atom, PIDA (i.e.30%) performs better than HTIB (i.e. 24%) to give cyclobutane in higher yield.

Since the yield of contractive synthesis of cyclobutane **225** is not satisfactory, we envisage that a two-step approach including *N*-amination of pyrrolidine followed by nitrogen extrusion/ring contraction might solve the problem of low synthetic yield of one-step approach (Scheme

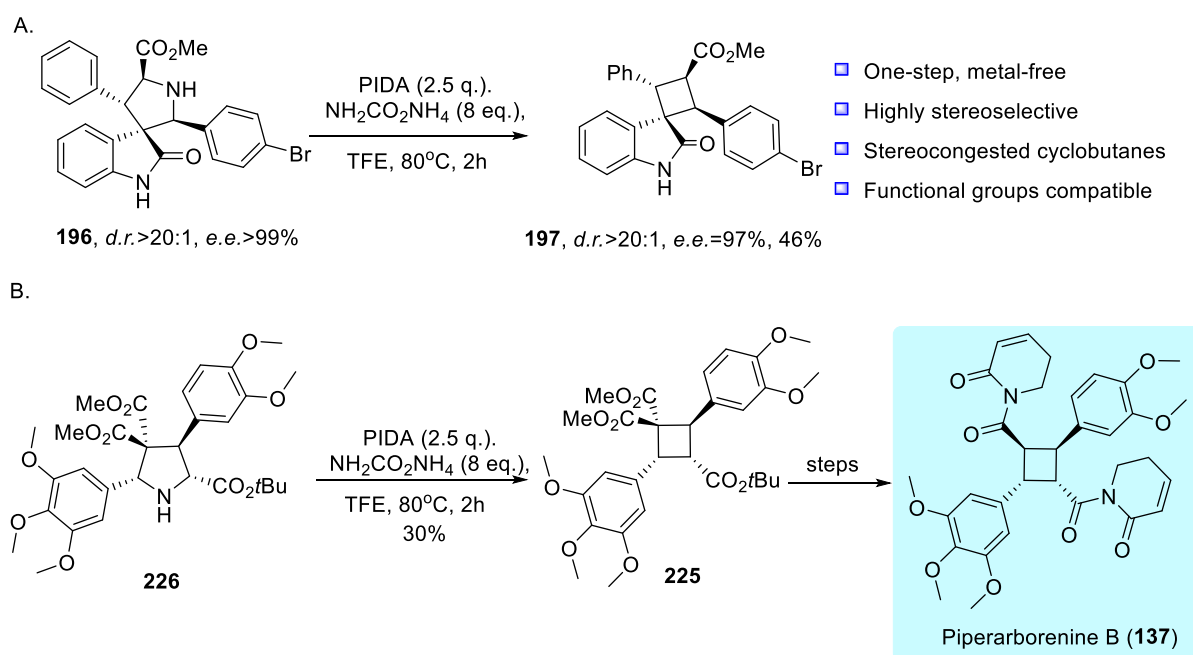
3.14B). Initially, a routine *N*-amination of secondary amine (i.e. *N*-nitrosylation of pyrrolidine followed by zinc reduction) was adopted to afford the desired *N*-aminopyrrolidine **231**. However, over-reduction of *N*-nitrosyl group back to the starting material pyrrolidine **226** was observed. To overcome this over-reduction, a new approach was identified. Treatment of pyrrolidine **226** with catalytic amount of ethyl trifluoroacetate **229**, hydroxylamine-*O*-sulfonic acid (HOSA) and cesium carbonate as base in HFIP afforded the desired *N*-aminopyrrolidine **231** in 59% yield. Oxidation of the freshly prepared *N*-aminopyrrolidine **231** with PIDA at 80°C afforded the desired cyclobutane **225** in 62% yield. (36% yield, 2 steps form **226**).



Scheme 3.14 A. Olefinic side product observed when standard condition using HTIB was applied. B. A two-step ring contraction of pyrrolidine **191** gives the desired cyclobutane precursor **192**.

4 Summary of the thesis

In summary, we developed a novel contractive synthesis of substituted cyclobutanes from easily accessible pyrrolidines using iodonitrene chemistry (**Scheme 3.15**). The developed method shows a good functional group compatibility and many unprecedented spirocyclobutane compounds were prepared successfully in one step from their corresponding substrates. This provides an opportunity to create combined scaffolds, for instance, connecting bioactive structures and/or fragments with a cyclobutane structure in form of spirocycles to explore wider bio-chemical space and eventually identify new lead compounds for drug development.¹³⁹ Studies on the reaction mechanism suggested formation of 1,4-diradical as a possible intermediate. The developed method was applied to concise formal synthesis of piperarborenine B (**137**).



Scheme 3.15 Summary of the contractive synthesis of cyclobutanes from pyrrolidines.

5. Experimental section

5.1 General Information

Unless otherwise noted, all commercially available compounds were used as provided without further purifications. Dry solvents (THF, toluene, DCM) were used as commercially available. Solvents for chromatography were technical grade. Oxygen and/or moisture sensitive solutions were transferred using syringes and cannulas.

Analytical thin-layer chromatography (TLC) was performed on *Merck silica gel aluminium plates* with F-254 indicator. Compounds were visualized by irradiation with UV light or potassium permanganate staining. Column chromatography was performed using *silica gel Merck 60* (particle size 0.040-0.063 mm). Solvent mixtures are understood as volume/volume.

^1H -NMR and ^{13}C -NMR were recorded on a *Bruker DRX400* (400 MHz), *Bruker DRX500* (500 MHz) and *INOVA500* (500 MHz) using CDCl_3 or CD_2Cl_2 as solvent. Data are reported in the following order: chemical shift (δ) values are reported in ppm with the solvent resonance as internal standard (CDCl_3 : $\delta = 7.26$ ppm for ^1H , $\delta = 77.16$ ppm for ^{13}C ; CD_2Cl_2 : $\delta = 5.32$ ppm for ^1H , $\delta = 53.8$ ppm for ^{13}C); multiplicities are indicated br s (broadened singlet), s (singlet), d (doublet), t (triplet), q (quartet) m (multiplet); coupling constants (J) are given in Hertz (Hz).

Low resolution mass spectra (MS-ESI) were collected using a *Waters Corp. LC-MS system* (column: LC revers phase CC Nucleodur C4 Gravity, 5 μm from Macherey-Nagel) equipped with an *UV-Waters 2487 Dual Absorbance Detector* and *Waters Micromass ZQ 2000 ESCI+ Multi-Mode-Ionisation MS-Detector*.

High resolution mass spectra were recorded on a *LTQ Orbitrap* mass spectrometer coupled to an *Acceka HPLC-System* (HPLC column: *Hypersyl GOLD*, 50 mm x 1 mm, particle size 1.9 μm , ionization method: electron spray ionization). Fourier transform infrared spectroscopy (FT-IR) spectra were obtained with a *Bruker Tensor 27* spectrometer (ATR, neat) and are reported in terms of frequency of absorption (cm^{-1}). Optical rotations were measured in a *Schmidt + Haensch Polartronic HH8* polarimeter.

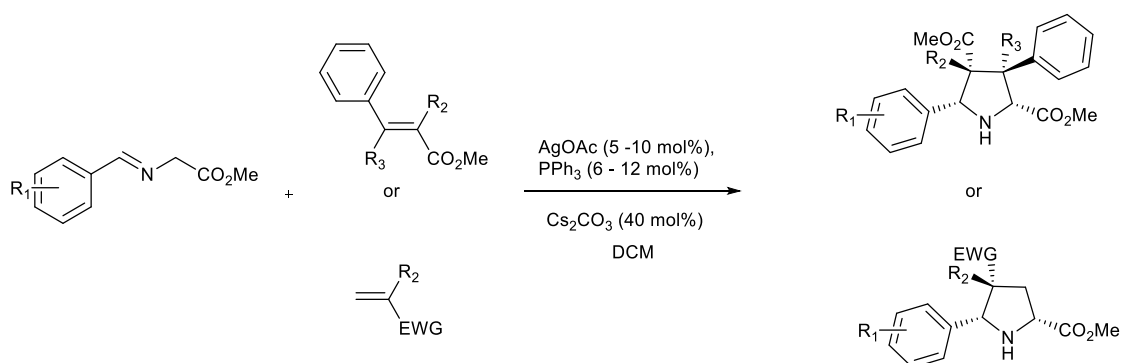
Fourier transform infrared spectroscopy (FT-IR) spectra were obtained with a *Bruker Tensor 27* spectrometer (ATR, neat) and are reported in terms of frequency of absorption (cm^{-1}).

The enantiomeric excesses were determined by HPCL analysis using a chiral stationary phase column (column: CHIRALCEL IC, eluent: (*iso*-hexane/ *iso*-propanol). The chiral HPLC methods were calibrated with the corresponding racemic mixtures. The ratio of diastereomers was determined by ¹H-NMR analysis via integration of characteristic signals of methyl esters. Chemical yields refer to pure isolated substances. Yields and enantiomeric excesses, diastereoselectivity are given in the tables. The chemicals and solvents were purchased from the companies Sigma-Aldrich, Acros Organic, ABCR and Alfa Aesar. (*Rp*)-2-(*tert*-Butylthio)-1-(diphenyl-phosphino)ferrocene (purity: 98%), were purchased from Sigma-Aldrich.

5.2 General Procedure for the preparation of pyrrolidines

General Procedure A

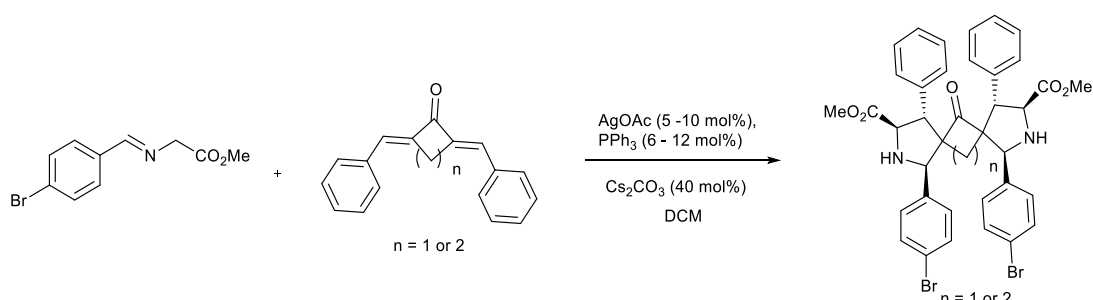
The preparation of pyrrolidines as reaction substrate



Under argon atmosphere, PPh₃ (6 - 12 mol%) and AgOAc (5 – 6 mol%) were dissolved in 20 mL DCM in a 50 ml round bottom flask, and stirred at room temperature for 1 hour. Then, imine substrate (1 mmol, 1 eq.), Cs₂CO₃ (40 mol%) and enone (1.1 mmol, 1.1 eq.) were added sequentially. Once starting material was consumed (monitored by TLC), the mixture was filtered through celite and the filtrate was concentrated to dryness. The crude product was purified by column chromatography (petroleum ether:acetone = 10:1) to give the corresponding cycloaddition product. The iminoesters used for 1,3-dipolar cycloaddition were prepared according to the reported procedure.¹⁵²

General Procedure B

The preparation of pyrrolidines as reaction substrate with double [3+2] cycloaddition



Under argon atmosphere, PPh₃ (0.24 mmol, 15 mol%) and AgOAc (0.16 mmol, 10 mol%) were dissolved in 2 mL DCM, and stirred at room temperature for about 1h. Then, imine substrate (4.84 mmol, 3 eq.), Cs₂CO₃ (0.65 mmol, 40 mol%) and dienone or bis- α,β -unsaturated ester (1.61 mmol, 1 eq.) were added sequentially. Once starting material was consumed (monitored by TLC), the mixture was filtered through celite and the filtrate was concentrated to dryness. The crude product was purified by column chromatography (petroleum ether:acetone = 5:1) to

give the corresponding cycloaddition product. The dienone were prepared according to the reported procedure.¹⁵³ The iminoesters used for 1,3-dipolar cycloaddition were prepared according to reference 1.

5.3 General Procedure for the synthesis of cylcobutanes from pyrrolidines.

General procedure C

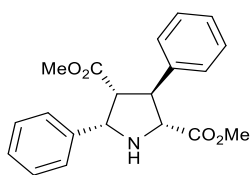
Under ambient atmosphere, HTIB (98 mg, 0.25 mmol, 2.5 eq.), ammonium carbamate (62 mg, 0.8 mmol, 8 eq.) and pyrrolidine (0.1 mmol, 1 eq.) were dissolved in 1 mL 2,2,2-trifluoroethanol and stirred at 80°C for two hours. The reaction vial was cooled down to room temperature and the vial cap was opened slowly. The reaction mixture was filtered through a cotton wool and the filtrate was concentrated under vacuum. The crude mixture was directly charged onto silica gel and the product was isolated using petroleum ether / acetone as eluent.

General procedure D

Similar procedure to general procedure 1 except 5 eq. of HTIB is used instead of 2.5 eq. The reaction time is extended from 2h to 12h.

5.5 Characterization data for pyrrolidines

rac-Dimethyl (2*R*,3*S*,4*R*,5*S*)-3,5-diphenylpyrrolidine-2,4-dicarboxylate (Compound **A1**)



Compound **A1** is prepared using procedure A.

Isolated yield: 44% (silica gel, 1:10 = acetone:petroleum ether, R_F = 0.25)

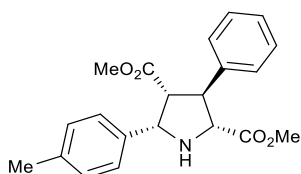
$^1\text{H NMR}$ (500 MHz, CDCl_3) δ 7.54 – 7.37 (m, 2H), 7.37 – 7.31 (m, 6H), 7.31 – 7.27 (m, 2H), 4.88 (d, J = 8.7, 1H), 4.14 – 4.08 (m, 1H), 3.91 (dd, J = 8.4, 8.4 Hz, 1H), 3.73 (s, 3H), 3.55 (dd, J = 8.4, 8.4 Hz, 1H), 3.16 ppm (s, 3H).

$^{13}\text{C NMR}$ (126 MHz, CDCl_3) δ 172.95, 171.89, 140.01, 139.13, 128.86, 128.36, 127.93, 127.72, 127.34, 127.05, 67.72, 65.36, 58.88, 52.40, 52.27, 51.46 ppm.

HR-MS calculated for $\text{C}_{20}\text{H}_{22}\text{NO}_4$: m/z (%): 340.1543 $[\text{M}+\text{H}]^+$, found: 340.1550

IR ν_{max} (cm^{-1}) 1732, 1603, 1495, 1454, 1434, 1376, 1264, 1215, 1166, 1029.

rac-Dimethyl (2*R*,3*S*,4*R*,5*S*)-3-phenyl-5-(*p*-tolyl)pyrrolidine-2,4-dicarboxylate (Compound **A2**)



Compound **A2** is prepared using procedure A.

Isolated yield: 48% (silica gel, 1:10 = acetone:petroleum ether, R_F = 0.25)

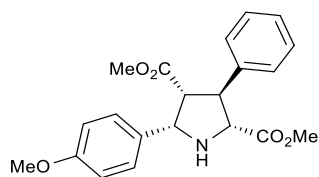
$^1\text{H NMR}$ (500 MHz, CDCl_3) δ 7.43 – 7.33 (m, 4H), 7.33 – 7.23 (m, 3H), 7.16 (d, J = 7.9 Hz, 2H), 4.89 (d, J = 8.7 Hz, 1H), 4.14 (d, J = 8.9 Hz, 1H), 3.91 (dd, J = 8.4, 8.4 Hz, 1H), 3.74 (s, 3H), 3.56 (dd, J = 8.4, 8.4 Hz, 1H), 3.22 (s, 3H), 2.34 ppm (s, 3H).

$^{13}\text{C NMR}$ (126 MHz, CDCl_3) δ 172.82, 171.84, 139.90, 137.70, 135.72, 129.10, 128.87, 127.72, 127.37, 126.90, 67.54, 65.15, 58.77, 52.49, 52.26, 51.52, 21.16 ppm.

HR-MS calculated for $\text{C}_{21}\text{H}_{24}\text{NO}_4$: m/z (%): 354.1700 $[\text{M}+\text{H}]^+$, found: 354.1700

IR ν_{max} (cm^{-1}) 1733, 1515, 1497, 1435, 1378, 1264, 1211, 1167, 1031, 822.

rac-Dimethyl (2*R*,3*S*,4*R*,5*S*)-5-(4-methoxyphenyl)-3-phenylpyrrolidine-2,4-dicarboxylate
(Compound **167**)



Compound **167** is prepared using procedure A.

Isolated yield: 67% (silica gel, 1:10 = acetone:petroleum ether R_F = 0.2)

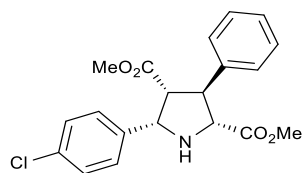
$^1\text{H NMR}$ (500 MHz, CDCl_3) δ 7.39 – 7.30 (m, 6H), 7.29 – 7.22 (m, 2H), 6.87 (d, J = 8.7 Hz, 2H), 4.82 (d, J = 8.7 Hz, 1H), 4.05 (d, J = 9.0 Hz, 1H), 3.88 (t, J = 8.6 Hz, 1H), 3.79 (s, 3H), 3.71 (s, 3H), 3.58 – 3.47 (m, 1H), 3.20 ppm (s, 3H).

$^{13}\text{C NMR}$ (126 MHz, CDCl_3) δ 173.14, 172.01, 159.15, 140.09, 131.49, 128.81, 128.24, 127.73, 127.27, 113.64, 67.71, 64.89, 58.89, 55.25, 52.32, 52.28, 51.50 ppm.

HR-MS calculated for $\text{C}_{21}\text{H}_{24}\text{NO}_5$: m/z (%): $[\text{M}+\text{H}]^+$, 370.1649, found: 370.1650.

IR ν_{max} (cm^{-1}) 1732, 1611, 1513, 1435, 1246, 1214, 1167, 1032, 835.

rac-Dimethyl (2*R*,3*R*,4*R*,5*S*)-5-(4-chlorophenyl)-3-phenylpyrrolidine-2,4-dicarboxylate
(Compound **A3**)



Compound **A3** is prepared using procedure A.

Isolated yield: 45% (silica gel, 1:10 = acetone:petroleum ether, R_F = 0.25)

$^1\text{H NMR}$ (500 MHz, CDCl_3) δ 7.33 (m, 8H), 7.28 (d, J = 6.8 Hz, 1H), 4.92 – 4.81 (m, 1H), 4.17 – 4.07 (m, 1H), 3.90 (dd, J = 10.2, 6.7 Hz, 1H), 3.72 (s, 3H), 3.59 – 3.51 (m, 1H), 3.22 ppm (s, 3H).

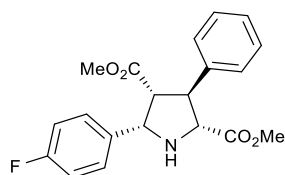
$^{13}\text{C NMR}$ (126 MHz, CDCl_3) δ 171.67, 129.02, 128.95, 128.67, 128.64, 127.91, 127.82, 127.58, 127.57, 67.47, 64.51, 58.55, 52.60, 51.95, 51.75 ppm.

HR-MS calculated for $\text{C}_{20}\text{H}_{21}^{35}\text{ClNO}_4$: m/z (%): 374.1154 $[\text{M}+\text{H}]^+$, found: 374.1166;

calculated for $\text{C}_{20}\text{H}_{21}^{37}\text{ClNO}_4$: m/z (%): 376.1124 $[\text{M}+\text{H}]^+$, found: 376.1137;

IR ν_{max} (cm^{-1}) 1729, 1491, 1435, 1373, 1265, 1214, 1168, 1090, 1014, 836.

rac-Dimethyl (2*R*,3*S*,4*R*,5*S*)-5-(4-fluorophenyl)-3-phenylpyrrolidine-2,4-dicarboxylate
(Compound **A4**)



Compound **A4** is prepared using procedure A.

Isolated yield: 41% (silica gel, 1:10 = acetone:petroleum ether, R_F = 0.25)

^1H NMR (500 MHz, CDCl_3) δ 7.40 – 7.31 (m, 2H), 7.31 – 7.24 (m, 3H), 7.24 – 7.18 (m, 2H), 6.97 (t, J = 8.7 Hz, 2H), 4.80 (d, J = 8.8 Hz, 1H), 4.02 (d, J = 9.0 Hz, 1H), 3.84 (dd, J = 8.6, 8.6 Hz, 1H), 3.66 (s, 3H), 3.47 (t, J = 8.6, 8.6 Hz, 1H), 3.14 ppm (s, 3H).

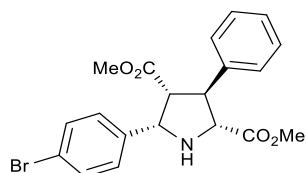
^{13}C NMR (126 MHz, CDCl_3) δ 173.06, 171.75, 162.31 (d, $J_{\text{C-F}}$ = 246.3 Hz), 139.84, 135.44 (d, $J_{\text{C-F}}$ = 3.1 Hz), 128.85, 128.79, 127.72, 127.36, 115.16 (d, $J_{\text{C-F}}$ = 21.4 Hz), 67.57, 64.45, 58.68, 52.35, 51.93, 51.51 ppm.

^{19}F NMR (470 MHz, CDCl_3) δ -114.50.

HR-MS calculated for $\text{C}_{20}\text{H}_{21}\text{FNO}_4$: m/z (%): 358.1449 $[\text{M}+\text{H}]^+$, found: 358.1456.

IR ν_{max} (cm^{-1}) 1736, 1604, 1509, 1435, 1261, 1222, 1166, 841.

rac-Dimethyl (2*R*,3*S*,4*R*,5*S*)-5-(4-bromophenyl)-3-phenylpyrrolidine-2,4-dicarboxylate
(Compound **166**)



Compound **166** is prepared using procedure A.

Isolated yield: 74% (silica gel, 1:10 = acetone:petroleum ether, R_F = 0.25)

^1H NMR (500 MHz, CDCl_3) δ 7.53 – 7.43 (m, 2H), 7.38 – 7.30 (m, 4H), 7.31 – 7.26 (m, 3H), 4.89 (d, J = 8.7 Hz, 1H), 4.18 (d, J = 8.9 Hz, 1H), 3.91 (t, J = 8.5 Hz, 1H), 3.73 (s, 3H), 3.58 – 3.54 (m, 1H), 3.24 ppm (s, 3H).

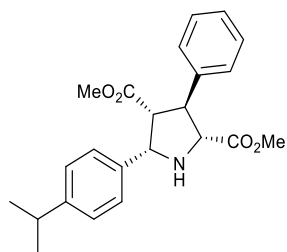
^{13}C NMR (126 MHz, CDCl_3) δ 172.63, 171.50, 139.46, 137.87, 131.68, 129.08, 128.95, 127.81, 127.68, 122.21, 67.24, 64.46, 58.37, 52.76, 51.84, 51.83 ppm.

HR-MS calculated for $\text{C}_{20}\text{H}_{21}^{79}\text{BrNO}_4$: m/z (%): 418.0649 $[\text{M}+\text{H}]^+$, found: 418.0653;

calculated for $\text{C}_{20}\text{H}_{21}^{81}\text{BrNO}_4$: m/z (%): 420.0628 $[\text{M}+\text{H}]^+$, found: 420.0628.

IR ν_{\max} (cm⁻¹) 1744, 1725, 1486, 1434, 1408, 1266, 1213, 1167, 1124, 1103, 1071, 1010, 969, 836.

rac-Dimethyl (2*R*,3*S*,4*R*,5*S*)-5-(4-isopropylphenyl)-3-phenylpyrrolidine-2,4-dicarboxylate (Compound **A5**)



Compound **A5** is prepared using procedure A.

Isolated yield: 58% (silica gel, 1:10 = acetone:petroleum ether, R_F = 0.25)

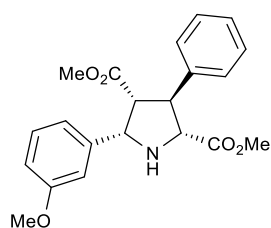
¹H NMR (500 MHz, CDCl₃) δ 7.40 – 7.24 (m, 7H), 7.20 (d, J = 8.2 Hz, 2H), 4.86 (d, J = 8.7 Hz, 1H), 4.08 (d, J = 9.0 Hz, 1H), 3.98 – 3.87 (m, 1H), 3.72 (s, 3H), 3.60 – 3.46 (m, 1H), 3.14 (s, 3H), 2.90 (tt, J = 13.9, 6.9 Hz, 1H), 1.24 (s, 3H), 1.22 ppm (s, 3H).

¹³C NMR (126 MHz, CDCl₃) δ 172.12, 171.40, 149.23, 129.03, 129.00, 127.74, 127.62, 126.99, 126.71, 126.66, 66.88, 64.90, 58.42, 52.87, 51.78, 51.69, 51.64, 33.80, 23.93 ppm.

HR-MS calculated C₂₃H₂₈NO₄: m/z (%):382.20123 [M+H]⁺, found: 382.2022.

IR ν_{\max} (cm⁻¹) 1735, 1436, 1265, 1216, 1168, 905, 835.

rac-Dimethyl (2*R*,3*S*,4*R*,5*S*)-5-(3-methoxyphenyl)-3-phenylpyrrolidine-2,4-dicarboxylate (Compound **A6**)



Compound **A6** is prepared using procedure A.

Isolated yield: 32% (silica gel, 1:10 = acetone:petroleum ether, R_F = 0.15)

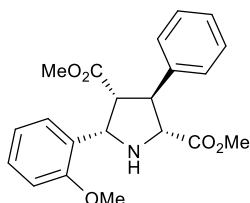
¹H NMR (500 MHz, CDCl₃) δ 7.41 – 7.34 (m, 4H), 7.32 – 7.27 (m, 2H), 7.03 – 6.96 (m, 2H), 6.88 – 6.81 (m, 1H), 4.89 (d, J = 8.6 Hz, 1H), 4.13 (d, J = 8.9 Hz, 1H), 3.92 (t, J = 8.5 Hz, 1H), 3.84 (s, 3H), 3.75 (s, 3H), 3.63 – 3.56 (m, 1H), 3.25 ppm (s, 3H).

¹³C NMR (126 MHz, CDCl₃) δ 173.05, 171.88, 159.71, 140.95, 140.02, 129.49, 128.96, 127.83, 127.47, 119.33, 113.65, 112.75, 67.71, 65.33, 58.82, 55.41, 52.53, 52.19, 51.66 ppm.

HR-MS calculated C₂₁H₂₄NO₅: m/z (%):370.1649 [M+H]⁺, found: 370.1657.

IR ν_{\max} (cm⁻¹) 1736, 1613, 1513, 1434, 1248, 1168, 1031, 834.

rac-Dimethyl (2*R*,3*S*,4*R*,5*S*)-5-(2-methoxyphenyl)-3-phenylpyrrolidine-2,4-dicarboxylate
(Compound **A7**)



Compound **A7** is prepared using procedure A.

Isolated yield: 38% (silica gel, 1:10 = acetone:petroleum ether, R_F= 0.15)

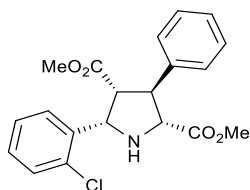
¹H NMR (500 MHz, CDCl₃) δ 7.50 – 7.33 (m, 5H), 7.33 – 7.22 (m, 2H), 6.99 (td, *J* = 7.5, 1.1 Hz, 1H), 6.88 (dd, *J* = 8.2, 1.1 Hz, 1H), 5.08 (d, *J* = 8.1 Hz, 1H), 4.02 (d, *J* = 8.5 Hz, 1H), 3.91 – 3.87 (m, 1H), 3.87 (s, 3H), 3.76 (s, 3H), 3.64 (dd, *J* = 8.1, 5.7 Hz, 1H), 3.14 ppm (s, 3H).

¹³C NMR (126 MHz, CDCl₃) δ 173.23, 172.78, 156.75, 141.52, 128.88, 128.68, 127.69, 127.14, 126.56, 126.47, 120.46, 110.00, 68.50, 61.16, 57.57, 55.46, 53.75, 52.29, 51.32 ppm.

HR-MS calculated C₂₁H₂₄NO₅: m/z (%):370.1649 [M+H]⁺, found: 370.1657.

IR ν_{\max} (cm⁻¹) 1736, 1603, 1495, 1436, 1381, 1247, 1203, 1165, 1028, 912.

rac-Dimethyl (2*R*,3*S*,4*R*,5*S*)-5-(2-chlorophenyl)-3-phenylpyrrolidine-2,4-dicarboxylate
(Compound **A8**)



Compound **A8** is prepared using procedure A.

Isolated yield: 50% (silica gel, 1:10 = acetone:petroleum ether, R_F= 0.25)

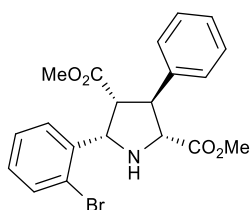
¹H NMR (400 MHz, CDCl₃) δ 7.58 (dd, *J* = 7.8, 1.7 Hz, 1H), 7.46 – 7.31 (m, 5H), 7.29 (dd, *J* = 7.2, 1.5 Hz, 2H), 7.22 (td, *J* = 7.6, 1.7 Hz, 1H), 5.20 (d, *J* = 8.2 Hz, 1H), 4.04 (d, *J* = 8.3 Hz, 1H), 3.95 (dd, *J* = 8.3, 5.7 Hz, 1H), 3.76 (s, 3H), 3.69 (dd, *J* = 8.3, 5.7 Hz, 1H), 3.13 ppm (s, 3H).

^{13}C NMR (101 MHz, CDCl_3) δ 172.53, 140.98, 136.17, 133.41, 129.17, 128.92, 128.81, 127.64, 127.55, 127.28, 126.83, 67.91, 62.24, 56.46, 52.56, 52.32, 51.40 ppm.

HR-MS calculated $\text{C}_{20}\text{H}_{21}^{35}\text{ClNO}_4$: m/z (%): 374.1154 $[\text{M}+\text{H}]^+$, found: 374.1158; calculated $\text{C}_{20}\text{H}_{21}^{37}\text{ClNO}_4$: m/z (%): 376.1124 $[\text{M}+\text{H}]^+$, found: 376.1126.

IR ν_{max} (cm^{-1}) 1737, 1650, 1438, 1264, 1203, 1175, 1035, 905.

rac-Dimethyl (2*R*,3*S*,4*R*,5*S*)-5-(2-bromophenyl)-3-phenylpyrrolidine-2,4-dicarboxylate
(Compound **A9**)



Compound **A9** is prepared using procedure A.

Isolated yield: 67% (silica gel, 1:10 = acetone:petroleum ether, R_F = 0.25)

^1H NMR (500 MHz, CDCl_3) δ 7.56 (d, J = 7.9 Hz, 2H), 7.41 – 7.32 (m, 5H), 7.31 – 7.26 (m, 1H), 7.16 (td, J = 7.6, 1.7 Hz, 1H), 5.20 (d, J = 8.2 Hz, 1H), 4.07 (d, J = 8.2 Hz, 1H), 3.97 (dd, J = 8.2, 5.7 Hz, 1H), 3.76 (s, 3H), 3.73 (dd, J = 8.2, 5.7 Hz, 1H), 3.14 ppm (s, 3H).

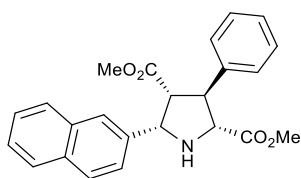
^{13}C NMR (126 MHz, CDCl_3) δ 172.43, 172.40, 140.89, 137.43, 132.57, 129.25, 128.97, 127.79, 127.67, 127.47, 127.34, 123.94, 67.78, 64.58, 56.20, 52.44, 52.31, 51.47 ppm.

HR-MS calculated $\text{C}_{20}\text{H}_{21}^{79}\text{BrNO}_4$: m/z (%): 418.0649 $[\text{M}+\text{H}]^+$, found: 418.0653;

HR-MS calculated $\text{C}_{20}\text{H}_{21}^{81}\text{BrNO}_4$: m/z (%): 420.0628 $[\text{M}+\text{H}]^+$, found: 420.0629.

IR ν_{max} (cm^{-1}) 1736, 1496, 1435, 1379, 1205, 1168, 1121, 1026, 908,

rac-Dimethyl (2*R*,3*S*,4*R*,5*S*)-5-(2-bromophenyl)-3-phenylpyrrolidine-2,4-dicarboxylate
(Compound **A10**)



Compound **A10** is prepared using procedure A.

Isolate yield: 65% (silica gel, 1:10 = acetone:petroleum ether, R_F = 0.25)

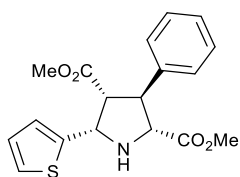
^1H NMR (500 MHz, CDCl_3) δ 7.90 – 7.84 (m, 2H), 7.82 (d, J = 8.7 Hz, 2H), 7.53 – 7.45 (m, 3H), 7.37 (d, J = 4.5 Hz, 4H), 7.32 – 7.27 (m, 1H), 5.06 (d, J = 7.9 Hz, 1H), 4.18 (d, J = 7.9 Hz, 1H), 3.99 (t, J = 8.2 Hz, 1H), 3.76 (s, 3H), 3.64 (t, J = 8.1 Hz, 1H), 3.08 ppm (s, 3H).

^{13}C NMR (126 MHz, CDCl_3) δ 172.84, 171.92, 140.08, 140.04, 133.14, 132.98, 128.91, 128.11, 128.04, 127.74, 127.65, 127.41, 126.26, 126.12, 125.91, 125.05, 67.69, 65.47, 58.74, 52.51, 52.36, 51.52 ppm.

HR-MS calculated $\text{C}_{24}\text{H}_{24}\text{NO}_4$: m/z (%): 390.1700 $[\text{M}+\text{H}]^+$, found: 390.1704.

IR ν_{max} (cm^{-1}) 1736, 1601, 1497, 1434, 1376, 1270, 1221 1166, 859, 823.

rac-Dimethyl (2*R*,3*S*,4*R*,5*S*)-3-phenyl-5-(thiophen-2-yl)pyrrolidine-2,4-dicarboxylate
(Compound A11)



Compound A11 is prepared using procedure A.

Isolated yield: 37% (silica gel, 1:10 = acetone:petroleum ether, R_F = 0.15)

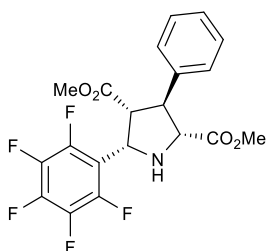
^1H NMR (500 MHz, CDCl_3) δ 7.34 (dd, J = 6.0, 2.9 Hz, 4H), 7.30 – 7.27 (m, 1H), 7.23 (d, J = 5.2 Hz, 1H), 7.06 (d, J = 3.7 Hz, 1H), 6.98 (m, 1H), 5.11 (d, J = 8.1 Hz, 1H), 4.07 (d, J = 7.8 Hz, 1H), 3.93 (t, J = 8.8 Hz, 1H), 3.71 (s, 3H), 3.60 (t, J = 4.3 Hz, 1H), 3.36 ppm (s, 3H).

^{13}C NMR (126 MHz, CDCl_3) δ 171.11, 128.82, 128.02, 127.83, 127.38, 126.89, 126.87, 125.09, 124.96, 67.23, 60.65, 58.53, 52.43, 51.75, 51.10 ppm.

HR-MS calculated $\text{C}_{18}\text{H}_{20}\text{NO}_4\text{S}$: m/z (%): 346.1108 $[\text{M}+\text{H}]^+$, found: 346.1117.

IR ν_{max} (cm^{-1}) 1735, 1603, 1497, 1435, 1376, 1348, 1273, 1213, 1167, 1094, 1030, 925, 850.

rac-Dimethyl (2*R*,3*S*,4*R*,5*S*)-5-(perfluorophenyl)-3-phenylpyrrolidine-2,4-dicarboxylate
(Compound A12)



Compound A12 is prepared using procedure A.

Isolate yield: 41% (silica gel, 1:10 = acetone:petroleum ether, R_F = 0.25)

^1H NMR (400 MHz, CDCl_3) δ 7.49 – 7.11 (m, 5H), 5.08 (d, J = 9.0 Hz, 1H), 4.04 – 3.79 (m, 2H), 3.64 (s, 3H), 3.53 (dd, J = 9.0, 7.4 Hz, 1H), 3.34 ppm (s, 3H).

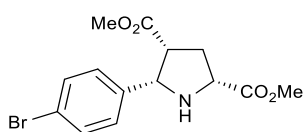
^{13}C NMR (101 MHz, CDCl_3) δ 172.07, 171.51, 146.56, 144.09 (d, $J = 2.9$ Hz), 142.03, 139.77, 139.49, 138.86, 138.73, 136.47, 129.07, 127.71, 127.63, 112.91, 112.80, 112.65, 68.23, 57.93, 56.58, 52.70, 52.53, 52.14 ppm.

^{19}F NMR (377 MHz, CDCl_3) δ -140.73, -140.75, -140.79, -140.80, -153.77, -153.83, -153.89, -161.50, -161.52, -161.56, -161.57, -161.61, -161.63 ppm.

HR-MS calculated $\text{C}_{20}\text{H}_{17}\text{F}_5\text{NO}_4$: m/z (%): 430.1072 $[\text{M}+\text{H}]^+$, found: 430.1078.

IR ν_{max} (cm^{-1}) 1739, 1653, 1524, 1502, 1437, 1223, 1169, 1131, 1000, 970, 912.

rac-Dimethyl (2*R*,4*R*,5*S*)-5-(4-bromophenyl)pyrrolidine-2,4-dicarboxylate (Compound **A13**)



Compound **A13** is prepared using procedure A.

Isolated yield: 64% (silica gel, 1:10 = acetone:petroleum ether, $R_F = 0.3$)

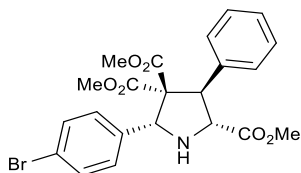
^1H NMR (500 MHz, CDCl_3) δ 7.43 (d, $J = 8.5$ Hz, 2H), 7.24 – 7.19 (m, 2H), 4.50 (d, $J = 7.8$ Hz, 1H), 3.98 (t, $J = 8.2$ Hz, 1H), 3.82 (s, 3H), 3.31 (td, $J = 7.5, 6.6$ Hz, 1H), 3.27 (s, 3H), 2.41 ppm (ddd, $J = 8.1, 7.0, 2.0$ Hz, 2H).

^{13}C NMR (126 MHz, CDCl_3) δ 173.71, 172.77, 138.35, 131.32, 128.61, 121.53, 65.05, 59.79, 52.41, 51.48, 49.46, 33.09 ppm.

HR-MS calculated $\text{C}_{14}\text{H}_{17}^{79}\text{BrNO}_4$: m/z (%): 342.0336 $[\text{M}+\text{H}]^+$, found: 342.0345; calculated $\text{C}_{14}\text{H}_{17}^{81}\text{BrNO}_4$: m/z (%): 344.0315 $[\text{M}+\text{H}]^+$, found: 344.0322.

IR ν_{max} (cm^{-1}) 1734, 1653, 1559, 1436, 1203, 1010.

rac-Trimethyl (2*R*,3*R*,5*R*)-5-(4-bromophenyl)-3-phenylpyrrolidine-2,4,4-tricarboxylate (Compound **A14**)



Compound **A14** is prepared using procedure A.

Isolated yield: 78% (silica gel, 1:5 = acetone:petroleum ether, $R_F = 0.1$)

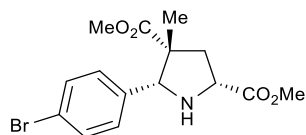
¹H NMR (500 MHz, CDCl₃) δ 7.46 (d, *J* = 8.5 Hz, 2H), 7.37 (d, *J* = 8.4 Hz, 2H), 7.34 – 7.29 (m, 5H), 5.29 (s, 1H), 4.41 (d, *J* = 6.6 Hz, 1H), 4.23 (d, *J* = 6.6 Hz, 1H), 3.78 (s, 3H), 3.20 (s, 3H), 3.17 ppm (s, 3H).

¹³C NMR (126 MHz, CDCl₃) δ 173.22, 169.73, 169.14, 138.52, 137.46, 131.47, 129.39, 128.90, 128.59, 127.90, 122.25, 71.02, 67.51, 66.12, 55.96, 52.70, 52.43, 52.12 ppm.

HR-MS calculated C₂₂H₂₃⁷⁹BrNO₆: *m/z* (%): 476.0703 [M+H]⁺, found: 476.0706; calculated C₂₂H₂₃⁸¹BrNO₆: *m/z* (%): 478.0682 [M+H]⁺, found: 478.0682.

IR ν_{max} (cm⁻¹) 1729, 1434, 1275, 1267, 1211, 1009.

rac-Dimethyl (2*R*,4*R*,5*R*)-5-(4-bromophenyl)-4-methylpyrrolidine-2,4-dicarboxylate (Compound **A15**)



Compound **A15** is prepared using procedure A.

Isolated yield: 55% (silica gel, 1:10 = acetone:petroleum ether, R_F= 0.25)

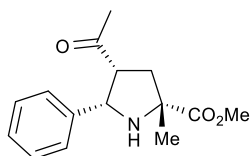
¹H NMR (500 MHz, CDCl₃) δ 7.45 (d, *J* = 8.5 Hz, 2H), 7.20 (d, *J* = 8.3 Hz, 2H), 4.13 – 4.01 (m, 3H), 3.85 (s, 3H), 3.30 (s, 3H), 2.74 (dd, *J* = 13.3, 7.0 Hz, 1H), 2.13 (dd, *J* = 13.3, 9.0 Hz, 1H), 1.42 ppm (s, 3H).

¹³C NMR (126 MHz, CDCl₃) δ 174.50, 174.20, 137.92, 131.30, 128.50, 121.80, 73.14, 58.82, 54.55, 52.36, 51.57, 41.12, 22.57 ppm.

HR-MS calculated C₁₅H₁₉⁷⁹BrNO₄: *m/z* (%): 356.0492 [M+H]⁺, found: 356.0502; calculated C₁₅H₁₉⁸¹BrNO₄: *m/z* (%): 358.0472 [M+H]⁺, found: 358.0477.

IR ν_{max} (cm⁻¹) 1729, 1487, 1433, 1210, 1141, 1109, 1009, 826.

rac-Methyl (2*R*,4*R*,5*S*)-4-acetyl-2-methyl-5-phenylpyrrolidine-2-carboxylate (Compound **A16**)



Compound **A16** is prepared using procedure A.

Isolated yield: 51% (silica gel, 1:10 = acetone:petroleum ether, R_F= 0.25)

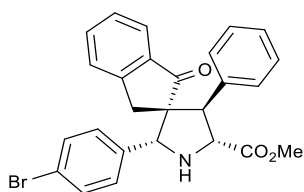
¹H NMR (500 MHz, CDCl₃) δ 7.49 – 7.42 (m, 2H), 7.40 – 7.27 (m, 3H), 4.41 (d, *J* = 8.3 Hz, 1H), 3.76 (s, 3H), 3.12 (ddd, *J* = 9.9, 8.3, 6.8 Hz, 1H), 2.63 (dd, *J* = 13.3, 6.9 Hz, 1H), 2.13 (dd, *J* = 13.2, 9.9 Hz, 1H), 1.98 (s, 3H), 1.50 ppm (s, 3H).

¹³C NMR (126 MHz, CDCl₃) δ 207.87, 177.39, 128.89, 128.55, 127.70, 127.13, 65.23, 64.15, 59.45, 52.59, 38.75, 30.19, 26.86 ppm.

HR-MS calculated C₁₅H₂₀NO₃: *m/z* (%): 262.1438 [M+H]⁺, found: 262.1442.

IR ν_{max} (cm⁻¹) 1729, 1605, 1493, 1455, 1360, 1265, 1174, 1105, 1028, 982, 913, 818.

rac-Methyl (2*R*,2'*R*,4'*R*,5'*R*)-2'-(4-bromophenyl)-1-oxo-4'-phenyl-1,3-dihydrospiro[indene-2,3'-pyrrolidine]-5'-carboxylate (Compound **A17**)



Compound A17 is prepared using procedure A.

Isolated yield: 53% (silica gel, 1:10 = acetone:petroleum ether, R_F= 0.2)

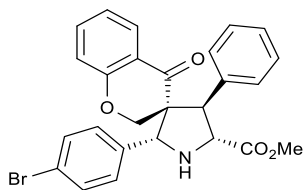
¹H NMR (500 MHz, CDCl₃) δ 7.44 – 7.34 (m, 3H), 7.34 – 7.30 (m, 2H), 7.30 – 7.27 (m, 2H), 7.19 (d, *J* = 8.4 Hz, 2H), 7.16 – 7.10 (m, 2H), 7.04 (d, *J* = 8.5 Hz, 2H), 4.52 (s, 1H), 4.36 (d, *J* = 6.0 Hz, 1H), 3.98 (d, *J* = 6.1 Hz, 1H), 3.84 (s, 3H), 2.89 (d, *J* = 17.5 Hz, 1H), 2.77 ppm (d, *J* = 17.6 Hz, 1H).

¹³C NMR (126 MHz, CDCl₃) δ 207.57, 173.18, 151.74, 140.91, 135.89, 135.59, 134.80, 131.17, 128.98, 128.78, 128.49, 127.46, 127.42, 125.56, 123.48, 121.86, 73.44, 67.38, 65.62, 55.89, 52.55, 35.58 ppm.

HR-MS calculated C₂₆H₂₃⁷⁹BrNO₃: *m/z* (%): 476.0856 [M+H]⁺, found: 476.0858; calculated C₂₆H₂₃⁸¹BrNO₃: *m/z* (%): 478.0835 [M+H]⁺, found: 478.0833.

IR ν_{max} (cm⁻¹) 1734, 1700, 1653, 1616, 1559, 1436, 1275, 1261.

rac-Methyl (2*R*,3*R*,4'*R*,5'*R*)-2'-(4-bromophenyl)-4-oxo-4'-phenylspiro[chromane-3,3'-pyrrolidine]-5'-carboxylate (Compound **A18**)



Compound A18 is prepared using procedure A.

Isolated yield: 46% (silica gel, 1:5 = acetone:petroleum ether, $R_F=0.1$)

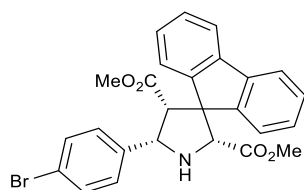
$^1\text{H NMR}$ (500 MHz, CDCl_3) δ 7.49 (dd, $J = 7.9, 1.7$ Hz, 1H), 7.35 (d, $J = 4.3$ Hz, 4H), 7.32 – 7.27 (m, 2H), 7.15 (d, $J = 8.5$ Hz, 2H), 7.03 (d, $J = 8.5$ Hz, 2H), 6.81 (ddd, $J = 8.1, 7.2, 1.1$ Hz, 1H), 6.67 (dd, $J = 8.4, 1.0$ Hz, 1H), 4.88 (s, 1H), 4.52 (d, $J = 8.2$ Hz, 1H), 4.47 (d, $J = 8.1$ Hz, 1H), 4.17 (dd, $J = 12.0, 12.0$ Hz, 1H), 3.84 (dd, $J = 12.0, 12.0$ Hz, 1H), 3.80 ppm (s, 3H).

$^{13}\text{C NMR}$ (126 MHz, CDCl_3) δ 192.36, 172.81, 160.34, 136.28, 135.95, 135.88, 131.00, 129.54, 128.91, 128.61, 127.91, 127.31, 122.16, 121.45, 120.97, 117.15, 72.77, 69.43, 64.08, 59.36, 52.87, 51.77 ppm.

HR-MS calculated $\text{C}_{26}\text{H}_{23}^{79}\text{BrNO}_4$: m/z (%): 492.0805 (M+H⁺), found: 492.0808; calculated $\text{C}_{26}\text{H}_{23}^{81}\text{BrNO}_4$: m/z (%): 494.0785 (M+H⁺), found: 494.0785.

IR ν_{max} (cm^{-1}) 1737, 1686, 1605, 1478, 1295, 1213, 1010, 913.

rac-Dimethyl (2'*R*,4'*R*,5'*S*)-5'-(4-bromophenyl)spiro[fluorene-9,3'-pyrrolidine]-2',4'-dicarboxylate (Compound A19)



Compound A19 is prepared using procedure A.

Isolated yield: 67% (silica gel, 1:10 = acetone:petroleum ether, $R_F=0.2$)

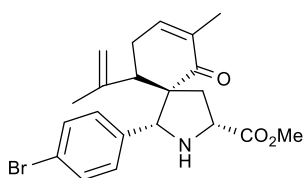
$^1\text{H NMR}$ (500 MHz, CDCl_3) δ 7.63 – 7.55 (m, 2H), 7.53 – 7.49 (m, 1H), 7.46 – 7.41 (m, 1H), 7.35 (dtd, $J = 19.8, 7.4, 1.3$ Hz, 2H), 7.21 – 7.13 (m, 2H), 7.01 – 6.92 (m, 2H), 6.73 – 6.55 (m, 2H), 4.91 (d, $J = 8.0$ Hz, 1H), 4.85 (s, 1H), 3.86 (s, 3H), 3.78 (d, $J = 8.0$ Hz, 1H), 3.27 ppm (s, 3H).

$^{13}\text{C NMR}$ (126 MHz, CDCl_3) δ 171.88, 141.63, 130.26, 128.31, 128.06, 127.62, 127.40, 127.12, 125.45, 124.15, 119.95, 119.39, 70.84, 62.57, 61.01, 56.23, 52.59, 51.80 ppm.

HR-MS calculated $\text{C}_{26}\text{H}_{23}^{79}\text{BrNO}_4$: m/z (%): 492.0805 [M+H]⁺, found: 492.0807; calculated $\text{C}_{26}\text{H}_{23}^{81}\text{BrNO}_4$: m/z (%): 494.0785 [M+H]⁺, found: 494.0784.

IR ν_{max} (cm^{-1}) 1733, 1487, 1449, 1436, 1207, 1176, 1010, 825.

rac-Methyl (1*R*,3*R*,5*S*,10*S*)-1-(4-bromophenyl)-7-methyl-6-oxo-10-(prop-1-en-2-yl)-2-azaspiro[4.5]dec-7-ene-3-carboxylate (Compound A20)



Compound A20 is prepared using procedure A.

Isolated yield: 41% (silica gel, 1:5 = acetone:petroleum ether, $R_F=0.2$)

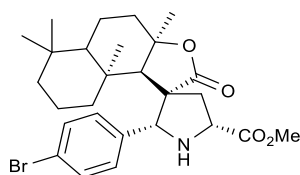
$^1\text{H NMR}$ (500 MHz, CDCl_3) δ 7.35 (d, $J = 8.5$ Hz, 2H), 7.08 (d, $J = 8.5$ Hz, 2H), 6.20 (ddt, $J = 5.5, 2.7, 1.3$ Hz, 1H), 4.75 (t, $J = 1.7$ Hz, 1H), 4.71 (d, $J = 1.8$ Hz, 1H), 4.33 (s, 1H), 3.94 (dd, $J = 8.7, 7.5$ Hz, 1H), 3.85 (s, 3H), 2.98 (d, $J = 6.9$ Hz, 1H), 2.74 – 2.62 (m, 1H), 2.17 (dd, $J = 20.2, 5.6$ Hz, 1H), 2.10 (dd, $J = 13.5, 8.6$ Hz, 1H), 1.53 (s, 3H), 1.52 – 1.40 ppm (m, 3H).

$^{13}\text{C NMR}$ (126 MHz, CDCl_3) δ 199.64, 174.69, 146.84, 140.96, 138.88, 136.32, 131.67, 131.09, 129.49, 128.81, 122.00, 114.38, 72.47, 60.08, 58.62, 52.46, 51.15, 36.66, 28.93, 21.40, 16.23 ppm.

HR-MS calculated $\text{C}_{21}\text{H}_{25}^{79}\text{BrNO}_3$: m/z (%): 418.1012 $[\text{M}+\text{H}]^+$, found: 418.1015; calculated $\text{C}_{21}\text{H}_{25}^{81}\text{BrNO}_3$: m/z (%): 420.0992 $[\text{M}+\text{H}]^+$, found: 420.0993.

IR ν_{max} (cm^{-1}) 1737, 1665, 1488, 1434, 1376, 1261, 1206, 1073, 1009, 901, 816.

rac-Methyl (2'*R*,3*aR*,5'*R*,9*aS*,9*bR*)-2'-(4-bromophenyl)-3*a*,6,6,9*a*-tetramethyl-2-oxodecahydro-2*H*-spiro[naphtho[2,1-*b*]furan-1,3'-pyrrolidine]-5'-carboxylate (Compound **A21**)



Compound A21 is prepared using procedure A.

Isolated yield: 70% (silica gel, 1:5 = acetone:petroleum ether, $R_F=0.2$)

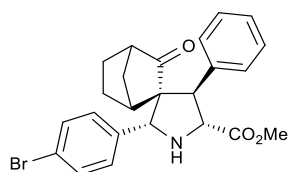
$^1\text{H NMR}$ (500 MHz, CDCl_3) δ 7.48 (d, $J = 8.5$ Hz, 2H), 7.30 (d, $J = 8.5$ Hz, 2H), 4.39 (s, 1H), 4.08 (dd, $J = 10.0, 4.2$ Hz, 1H), 3.81 (s, 3H), 2.84 (dd, $J = 13.6, 10.1$ Hz, 1H), 2.53 (dd, $J = 13.5, 4.4$ Hz, 1H), 2.16 (s, 1H), 1.92 (s, 2H), 1.86 – 1.76 (m, 2H), 1.76 – 1.67 (m, 1H), 1.57 (dt, $J = 14.1, 3.5$ Hz, 1H), 1.53 – 1.42 (m, 1H), 1.40 (s, 3H), 1.39 – 1.32 (m, 2H), 1.30 – 1.19 (m, 1H), 1.15 (s, 3H), 1.01 – 0.92 (m, 1H), 0.87 (s, 3H), 0.84 ppm (s, 3H).

¹³C NMR (126 MHz, CDCl₃) δ 178.99, 172.76, 134.54, 131.84, 130.62, 122.80, 85.13, 70.94, 59.19, 58.24, 56.95, 52.70, 42.07, 40.73, 39.13, 38.91, 35.51, 33.61, 33.45, 31.08, 25.95, 21.22, 20.63, 18.22, 17.68 ppm.

HR-MS calculated C₂₇H₃₆⁷⁹BrNO₄: m/z (%): 518.1901 [M+H]⁺, found: 518.1914; calculated C₂₇H₃₆⁸¹BrNO₄: m/z (%): 520.1880 [M+H]⁺, found: 520.1891.

IR ν_{max} (cm⁻¹) 1753, 1435, 1391, 1315, 1282, 1203, 1174, 1124, 1078, 1041, 1022, 1010, 942, 912, 819.

rac-Methyl (1*R*,2*R*,2'*R*,4'*R*,5'*R*)-2'-(4-bromophenyl)-3-oxo-4'-phenylspiro[bicyclo[2.2.1]heptane-2,3'-pyrrolidine]-5'-carboxylate (Compound **A22**)



Compound **A22** is prepared using procedure **A**.

Isolated yield: 73% (silica gel, 1:10 = acetone:petroleum ether, R_F= 0.25)

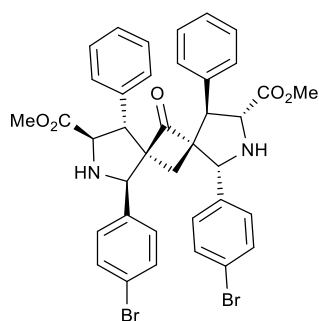
¹H NMR (500 MHz, CDCl₃) δ 7.85 – 7.44 (m, 2H), 7.44 – 7.34 (m, 4H), 7.29 (dd, *J* = 8.5, 6.7 Hz, 3H), 4.62 (s, 1H), 3.93 (d, *J* = 3.8 Hz, 1H), 3.85 (s, 3H), 3.64 (d, *J* = 3.8 Hz, 1H), 2.38 (d, *J* = 2.4 Hz, 1H), 2.33 – 2.21 (m, 1H), 1.78 – 1.59 (m, 1H), 1.53 – 1.40 (m, 2H), 1.33 – 1.16 (m, 2H), 1.02 ppm (ddd, *J* = 10.7, 1.8, 0.9 Hz, 1H).

¹³C NMR (126 MHz, CDCl₃) δ 173.33, 173.32, 142.44, 138.89, 131.99, 130.38, 128.87, 128.75, 127.19, 122.47, 71.87, 68.40, 67.39, 56.64, 52.58, 50.36, 43.07, 34.51, 26.54, 24.94 ppm.

HR-MS calculated C₂₄H₂₅⁷⁹BrNO₃: m/z (%): 454.1012 [M+H]⁺, found: 454.1014; calculated C₂₄H₂₅⁸¹BrNO₃: m/z (%): 456.0992 [M+H]⁺, found: 456.0990;

IR ν_{max} (cm⁻¹) 1733, 1489, 1434, 1216, 1134, 1073, 1010, 912, 825.

rac-Dimethyl (1*R*,3*R*,4*R*,5*R*,7*R*,8*R*,10*R*,11*R*)-1,8-bis(4-bromophenyl)-6-oxo-4,11-diphenyl-2,9-diazadispiro[4.1.47.15]dodecane-3,10-dicarboxylate (Compound **A23**)



Compound A23 is prepared using procedure B.

Isolated Yield: 40% (silica gel, 1:5 = acetone:petroleum ether, $R_F=0.1$)

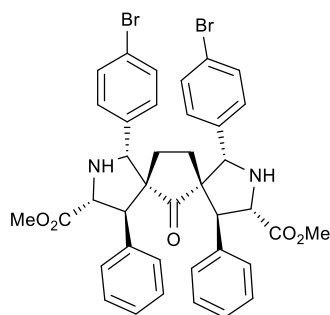
$^1\text{H NMR}$ (500 MHz, CDCl_3) δ 7.56 (d, $J = 8.4$ Hz, 4H), 7.28 (d, $J = 8.5$ Hz, 6H), 7.25 – 7.21 (m, 4H), 6.81 – 6.77 (m, 4H), 4.25 (s, 2H), 3.93 (s, 1H), 3.83 (s, 6H), 3.22 (s, 1H), 2.57 (d, $J = 2.7$ Hz, 2H), 1.58 ppm (s, 2H).

$^{13}\text{C NMR}$ (126 MHz, CDCl_3) δ 212.27, 172.53, 138.81, 132.09, 130.95, 128.71, 128.57, 127.72, 127.41, 123.00, 71.95, 69.64, 66.45, 52.66, 52.18, 22.42 ppm.

HR-MS calculated $\text{C}_{38}\text{H}_{35}^{79}\text{Br}^{81}\text{BrN}_2\text{O}_5$: m/z (%): 759.0887 $[\text{M}+\text{H}]^+$, found: : 759.0902; calculated $\text{C}_{38}\text{H}_{35}^{81}\text{Br}^{81}\text{BrN}_2\text{O}_5$: m/z (%): 761.0866 $[\text{M}+\text{H}]^+$, found : 761.0886.

IR ν_{max} (cm^{-1}) 1739, 1493, 1434, 1222, 1011, 914.

rac-Dimethyl (1*R*,3*R*,4*R*,5*R*,7*S*,8*S*,10*S*,11*S*)-1,8-bis(4-bromophenyl)-6-oxo-4,11-diphenyl-2,9-diazadispiro[4.1.47.25]tridecane-3,10-dicarboxylate (Compound **A24**)



Compound A24 is prepared using procedure B.

Isolated yield: 57% (silica gel, 1:5 = acetone:petroleum ether, $R_F=0.1$)

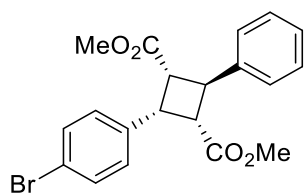
$^1\text{H NMR}$ (700 MHz, CD_2Cl_2) δ 7.59 (d, $J = 8.5$ Hz, 4H), 7.40 – 7.20 (m, 9H), 7.20 – 7.11 (m, 2H), 6.56 (s, 3H), 4.18 (s, 2H), 3.89 (s, 6H), 3.85 (d, $J = 3.4$ Hz, 2H), 2.75 (d, $J = 3.4$ Hz, 2H), 1.16 – 0.97 ppm (m, 4H).

$^{13}\text{C NMR}$ (176 MHz, CD_2Cl_2) δ 221.29, 174.02, 141.19, 138.07, 132.60, 130.94, 129.11, 128.89, 127.48, 123.28, 73.78, 67.85, 65.60, 56.27, 52.75, 29.07 ppm.

HR-MS calculated $C_{39}H_{37}^{79}Br^{79}BrN_2O_5$: m/z (%): 771.1064 $[M+H]^+$, found: 771.1085;
calculated $C_{39}H_{37}^{79}Br^{81}BrN_2O_5$: m/z (%): 773.1043 $[M+H]^+$, found: 773.1066; calculated
 $C_{39}H_{37}^{81}Br^{81}BrN_2O_5$: m/z (%): 775.1023 $[M+H]^+$, found: 775.1023.
IR ν_{max} (cm^{-1}) 1733, 1491, 1454, 1434, 1219, 1145, 1075, 1009, 953, 901, 814.

5.6 Characterization data for cyclobutanes

Dimethyl (1*R*,2*s*,3*S*,4*s*)-2-(4-bromophenyl)-4-phenylcyclobutane-1,3-dicarboxylate (Compound **171**)



Compound 171 is prepared using procedure C.

Isolated yield: 69% (silica gel, 1:50 = acetone:petroleum ether, R_F = 0.2)

$^1\text{H NMR}$ (500 MHz, CDCl_3) δ 7.42 (d, J = 8.5 Hz, 2H), 7.38 – 7.30 (m, 4H), 7.28 – 7.23 (m, 1H), 7.16 (d, J = 8.5 Hz, 2H), 4.74 (dd, J = 10.7, 10.7 Hz, 1H), 4.16 (dd, J = 10.1, 10.1 Hz, 1H), 3.70 (dd, J = 10.4, 10.4 Hz, 2H), 3.40 ppm (s, 6H).

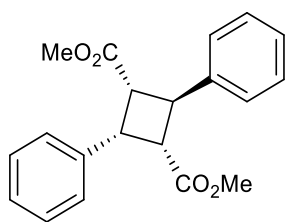
$^{13}\text{C NMR}$ (126 MHz, CDCl_3) δ 171.47, 141.46, 136.57, 131.46, 129.91, 128.65, 126.97, 126.41, 121.31, 51.75, 46.23, 43.86, 41.74 ppm.

HR-MS calculated for $\text{C}_{20}\text{H}_{20}^{79}\text{BrO}_4$: m/z (%): 403.0540 $[\text{M}+\text{H}]^+$, found: 403.0542;

calculated for $\text{C}_{20}\text{H}_{20}^{81}\text{BrO}_4$: m/z (%): 405.0519 $[\text{M}+\text{H}]^+$, found: 405.0520;

IR ν_{max} (cm^{-1}) 1739, 1723, 1490, 1433, 1337, 1225, 1204, 1180, 1161, 1107, 1075, 1045, 1008, 942, 837.

Dimethyl (1*R*,2*r*,3*S*,4*s*)-2,4-diphenylcyclobutane-1,3-dicarboxylate (Compound **172**)



Compound 172 is prepared using procedure C.

Isolated yield: 67% (silica gel, 1:20 = acetone:petroleum ether, R_F = 0.4)

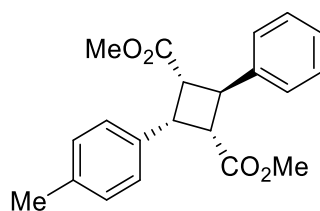
$^1\text{H NMR}$ (500 MHz, CDCl_3) δ 7.35 (d, J = 5.7 Hz, 4H), 7.31 – 7.26 (m, 4H), 7.26 – 7.20 (m, 2H), 4.79 (dd, J = 10.7, 10.7, 1H), 4.20 (m, 1H), 3.69 (dd, J = 10.4, 10.4 Hz, 2H), 3.36 ppm (s, 6H).

$^{13}\text{C NMR}$ (126 MHz, CDCl_3) δ 171.75, 141.80, 137.46, 128.61, 128.33, 128.12, 127.26, 126.84, 126.45, 51.59, 46.43, 44.45, 41.76 ppm.

HR-MS calculated for $\text{C}_{20}\text{H}_{21}\text{O}_4$: m/z (%): 325.1434 $[\text{M}+\text{H}]^+$, found: 325.1440.

IR ν_{\max} (cm⁻¹) 1732, 1496, 1435, 1327, 1265, 1204.

Dimethyl (1*R*,2*s*,3*S*,4*s*)-2-phenyl-4-(*p*-tolyl)cyclobutane-1,3-dicarboxylate (Compound **173**)



Compound 173 is prepared using procedure C.

Isolated yield: 51% (silica gel, 5% acetone in petroleum ether, $R_F=0.2$)

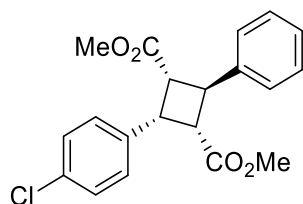
¹H NMR (500 MHz, CDCl₃) δ 7.34 (d, $J = 6.0$ Hz, 4H), 7.25 – 7.23 (m, 1H), 7.16 (d, $J = 8.2$ Hz, 2H), 7.08 (d, $J = 8.1$ Hz, 2H), 4.78 (dd, $J = 10.7, 10.7$ Hz, 1H), 4.17 (dd, $J = 10.1, 10.1$ Hz, 1H), 3.67 (dd, $J = 10.4, 10.4$ Hz, 2H), 3.38 (s, 6H), 2.30 ppm (s, 3H).

¹³C NMR (126 MHz, CDCl₃) δ 171.81, 141.86, 136.76, 134.25, 129.02, 128.59, 127.99, 126.81, 126.46, 51.60, 46.47, 44.16, 41.70, 21.11 ppm.

HR-MS calculated for C₂₁H₂₃O₄: m/z (%): 339.1591 [M+H]⁺, found: 339.1596.

IR ν_{\max} (cm⁻¹) 1730, 1484, 1429, 1410, 1369, 1335, 1279, 1233, 1205, 1180, 1121, 1009, 938, 839.

Dimethyl (1*R*,2*s*,3*S*,4*s*)-2-(4-chlorophenyl)-4-phenylcyclobutane-1,3-dicarboxylate (Compound **174**)



Compound 174 is prepared using procedure C.

Isolated yield: 51% (silica gel, 1:50 = acetone:petroleum ether, $R_F=0.2$)

¹H NMR (500 MHz, CDCl₃) δ 7.35 – 7.23 (m, 4H), 7.22 – 7.12 (m, 5H), 4.68 (dd, $J = 10.7, 10.7$ Hz, 1H), 4.11 (dd, $J = 10.1, 10.1$ Hz, 1H), 3.64 (dd, $J = 10.4, 10.4$ Hz, 2H), 3.32 ppm (s, 6H).

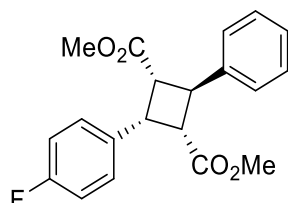
¹³C NMR (126 MHz, CDCl₃) δ 171.60, 141.58, 136.16, 133.24, 129.67, 128.76, 128.61, 127.06, 126.51, 60.73, 51.83, 46.40, 43.89, 41.83 ppm.

HR-MS calculated for $C_{20}H_{20}^{35}ClO_4$: m/z (%): 359.1044 $[M+H]^+$, found: 359.1052;

calculated for $C_{20}H_{20}^{37}ClO_4$: m/z (%): 361.1015 $[M+H]^+$, found: 361.1023;

IR ν_{max} (cm^{-1}) 1731, 1495, 1435, 1329, 1205, 1094, 1045, 1013, 838.

Dimethyl (1*R*,2*S*,3*S*,4*S*)-2-(4-fluorophenyl)-4-phenylcyclobutane-1,3-dicarboxylate
(Compound **175**)



Compound 175 is prepared using procedure C.

Isolated yield: 65% (silica gel, 1:50 = acetone:petroleum ether, R_F = 0.2)

1H NMR (500 MHz, $CDCl_3$) δ 7.35 – 7.23 (m, 4H), 7.22 – 7.15 (m, 3H), 6.92 (m, 2H), 4.69 (dd, J = 10.7, 10.7 Hz, 1H), 4.13 (dd, J = 10.1, 10.1 Hz, 1H), 3.61 (dd, J = 10.4, 10.4 Hz, 2H), 3.32 ppm (s, 6H).

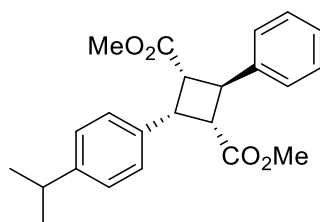
^{13}C NMR (126 MHz, $CDCl_3$) δ 171.59, 162.96, 161.00, 141.55, 133.29, 133.26, 129.85, 129.79, 128.64, 126.93, 126.42, 115.31, 115.14, 51.68, 46.42, 43.67, 41.65 ppm.

^{19}F NMR (470 MHz, $CDCl_3$) δ -115.18.

HR-MS calculated for $C_{20}H_{20}FO_4$: m/z (%): 343.1340 $[M+H]^+$, found: 343.1346.

IR ν_{max} (cm^{-1}) 1732, 1606, 1512, 1436, 1333, 1204, 1163, 1101, 1045, 940, 842.

Dimethyl (1*R*,2*S*,3*S*,4*S*)-2-(4-isopropylphenyl)-4-phenylcyclobutane-1,3-dicarboxylate
(Compound **176**)



Compound 176 is prepared using procedure C.

Isolated yield: 51% (silica gel, 1:50 = acetone:petroleum ether, R_F = 0.2)

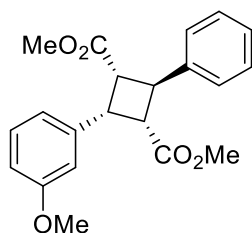
1H NMR (500 MHz, $CDCl_3$) δ 7.39 – 7.31 (m, 4H), 7.26 – 7.22 (m, 1H), 7.18 (d, J = 8.3 Hz, 2H), 7.13 (d, J = 8.3 Hz, 2H), 4.78 (dd, J = 10.7, 10.7 Hz, 1H), 4.18 (dd, J = 10.1, 10.1 Hz, 1H), 3.66 (dd, J = 10.4, 10.4 Hz, 2H), 3.35 (s, 6H), 2.86 (p, J = 6.9 Hz, 1H), 1.22 (s, 3H), 1.20 ppm (s, 3H).

^{13}C NMR (126 MHz, CDCl_3) δ 171.85, 147.73, 141.88, 134.58, 128.59, 128.02, 126.79, 126.46, 126.29, 51.55, 46.49, 44.16, 41.64, 33.66, 23.93 ppm.

HR-MS calculated for $\text{C}_{23}\text{H}_{27}\text{O}_4$: m/z (%): 367.1904 $[\text{M}+\text{H}]^+$, found: 367.1908.

IR ν_{max} (cm^{-1}) 1735, 1436, 1271, 1205, 835.

Dimethyl (1*R*,2*s*,3*S*,4*s*)-2-(3-methoxyphenyl)-4-phenylcyclobutane-1,3-dicarboxylate
(Compound **177**)



Compound **177** is prepared using procedure C.

Isolated yield: 42% (silica gel, 1:50 = acetone:petroleum ether to 1:20 = acetone:petroleum ether, $R_F = 0.1$)

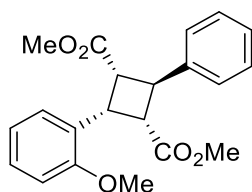
^1H NMR (500 MHz, CDCl_3) δ 7.38 – 7.30 (m, 4H), 7.26 (s, 1H), 7.20 (t, $J = 7.9$ Hz, 1H), 6.90 – 6.73 (m, 3H), 4.79 (dd, $J = 10.7, 10.7$ Hz, 1H), 4.17 (dd, $J = 10.2, 10.2$ Hz, 1H), 3.80 (s, 3H), 3.68 (dd, $J = 10.4, 10.4$ Hz, 2H), 3.39 ppm (s, 6H).

^{13}C NMR (126 MHz, CDCl_3) δ 171.87, 159.53, 141.90, 139.13, 129.44, 128.73, 126.97, 126.55, 120.43, 113.79, 113.18, 55.30, 51.79, 46.51, 44.64, 41.89 ppm.

HR-MS calculated for $\text{C}_{21}\text{H}_{23}\text{O}_5$: m/z (%): 355.1540 $[\text{M}+\text{H}]^+$, found: 355.1544.

IR ν_{max} (cm^{-1}) 1729, 1602, 1584, 1489, 1454, 1394, 1328, 1269, 1254, 1203, 1182, 1089, 1041, 874.

Dimethyl (1*R*,2*s*,3*S*,4*s*)-2-(2-methoxyphenyl)-4-phenylcyclobutane-1,3-dicarboxylate
(Compound **178**)



Compound **178** is prepared using procedure C.

Isolated yield: 44% (silica gel, 1:50 = acetone:petroleum ether to 1:20 = acetone:petroleum ether, $R_F = 0.1$)

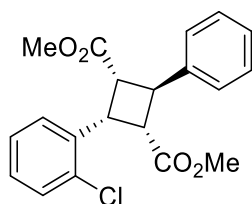
¹H NMR (500 MHz, CDCl₃) δ 7.34 – 7.23 (m, 4H), 7.20 – 7.13 (m, 2H), 7.10 (ddd, *J* = 8.2, 7.4, 1.7 Hz, 1H), 6.80 (td, *J* = 7.5, 1.2 Hz, 1H), 6.74 (dd, *J* = 8.2, 1.1 Hz, 1H), 4.68 (dd, *J* = 10.3, 10.3 Hz, 1H), 4.59 (dd, *J* = 10.6, 10.6 Hz, 1H), 3.70 (s, 3H), 3.57 (dd, *J* = 10.4, 10.4 Hz, 2H), 3.29 ppm (s, 6H).

¹³C NMR (126 MHz, CDCl₃) δ 172.27, 157.37, 142.43, 128.43 (d, *J* = 32.9 Hz), 126.67, 126.51, 126.04, 120.46, 110.40, 55.30, 51.47, 45.87, 42.06 ppm.

HR-MS calculated for C₂₁H₂₃O₅: *m/z* (%): 355.1540 [M+H]⁺, found: 355.1544.

IR ν_{max} (cm⁻¹) 1728, 1601, 1494, 1457, 1435, 1329, 1294, 1244, 1203, 1115, 1029.

Dimethyl (1*R*,2*s*,3*S*,4*s*)-2-(2-chlorophenyl)-4-phenylcyclobutane-1,3-dicarboxylate
(Compound **179**)



Compound 179 is prepared using procedure C.

Isolated yield: 88% (silica gel, 1:50 = acetone:petroleum ether, R_F= 0.2)

¹H NMR (500 MHz, CDCl₃) δ 7.43 (dd, *J* = 7.9, 1.6 Hz, 1H), 7.38 (dd, *J* = 7.9, 1.4 Hz, 1H), 7.35 (d, *J* = 5.2 Hz, 4H), 7.27 (d, *J* = 3.1 Hz, 1H), 7.25 – 7.20 (m, 1H), 7.17 (td, *J* = 7.7, 1.7 Hz, 1H), 4.91 (dd, *J* = 10.3, 10.3 Hz, 1H), 4.75 (dd, *J* = 10.8, 10.8 Hz, 1H), 3.75 (dd, *J* = 10.5, 10.5 Hz, 2H), 3.39 ppm (s, 6H).

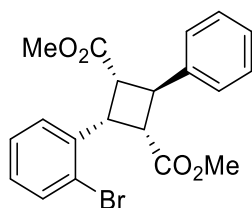
¹³C NMR (126 MHz, CDCl₃) δ 171.70, 135.18, 134.93, 129.74, 128.66, 128.32, 127.50, 126.97, 126.74, 126.49, 51.67, 45.80, 41.90, 39.28 ppm.

HR-MS calculated for C₂₀H₂₀³⁵ClO₄: *m/z* (%): 359.1045 [M+H]⁺, found: 359.1052;

calculated for C₂₀H₂₀³⁷ClO₄: *m/z* (%): 361.1015 [M+H]⁺, found: 361.1022.

IR ν_{max} (cm⁻¹) 1730, 1497, 1478, 1436, 1328, 1202, 1091, 1062, 1040.

Dimethyl (1*R*,2*s*,3*S*,4*s*)-2-(2-bromophenyl)-4-phenylcyclobutane-1,3-dicarboxylate
(Compound **180**)



Compound 180 is prepared using procedure C.

Isolated yield: 68% (silica gel, 1:50 = acetone:petroleum ether, $R_F=0.2$)

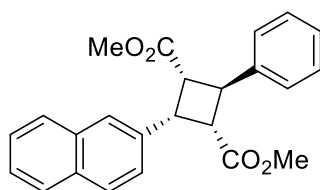
$^1\text{H NMR}$ (500 MHz, CDCl_3) δ 7.49 (dd, $J = 8.0, 1.4$ Hz, 1H), 7.34 (dd, $J = 7.9, 1.7$ Hz, 1H), 7.27 (d, $J = 2.1$ Hz, 1H), 7.22 – 7.15 (m, 4H), 7.00 (ddd, $J = 8.0, 7.3, 1.6$ Hz, 2H), 4.80 (td, $J = 10.3, 10.27, 1.1$ Hz, 1H), 4.66 (dd, $J = 10.7, 10.7$ Hz, 1H), 3.66 (dd, $J = 10.5, 10.5$ Hz, 2H), 3.31 ppm (s, 6H).

$^{13}\text{C NMR}$ (126 MHz, CDCl_3) δ 171.67, 141.47, 136.81, 133.14, 128.66, 128.61, 127.50, 127.39, 126.97, 126.49, 125.93, 51.66, 45.86, 42.35, 41.82 ppm.

HR-MS calculated for $\text{C}_{20}\text{H}_{20}^{79}\text{BrO}_4$: m/z (%): 403.0540 $[\text{M}+\text{H}]^+$, found: 403.0542;
calculated for $\text{C}_{20}\text{H}_{20}^{81}\text{BrO}_4$: m/z (%): 405.0519 $[\text{M}+\text{H}]^+$, found: 405.0519.

IR ν_{max} (cm^{-1}) 1729, 1497, 1474, 1434, 1329, 1203, 1042, 1021, 940.

Dimethyl (1*R*,2*s*,3*S*,4*s*)-2-(naphthalen-2-yl)-4-phenylcyclobutane-1,3-dicarboxylate
(Compound **181**)



Compound 181 is prepared using procedure C.

Isolated yield: 51% (silica gel, 1:50 = acetone:petroleum ether, $R_F=0.2$)

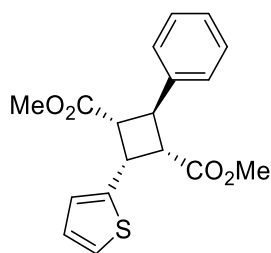
$^1\text{H NMR}$ (500 MHz, CDCl_3) δ 7.84 – 7.75 (m, 4H), 7.49 – 7.45 (m, 2H), 7.44 (dd, $J = 8.4, 2.0$ Hz, 1H), 7.41 – 7.35 (m, 4H), 7.30 – 7.26 (m, 1H), 4.93 (dd, $J = 10.7, 10.7$ Hz, 1H), 4.40 (dd, $J = 10.1, 10.1$ Hz, 1H), 3.77 (dd, $J = 10.4, 10.4$ Hz, 2H), 3.30 ppm (s, 6H).

$^{13}\text{C NMR}$ (126 MHz, CDCl_3) δ 171.77, 141.80, 135.06, 133.30, 132.55, 128.65, 127.98, 127.95, 127.58, 127.46, 126.90, 126.49, 126.06, 125.92, 125.85, 51.67, 46.53, 44.64, 41.92 ppm.

HR-MS calculated for $\text{C}_{24}\text{H}_{23}\text{O}_4$: m/z (%): 375.1591 $[\text{M}+\text{H}]^+$, found: 375.1595.

IR ν_{max} (cm^{-1}) 1733, 1601, 1497, 1435, 1331, 1204, 1047, 860, 824.

Dimethyl (1*R*,2*s*,3*S*,4*s*)-2-phenyl-4-(thiophen-2-yl)cyclobutane-1,3-dicarboxylate
(Compound **182**)



Compound 182 is prepared using procedure C.

Isolated yield: 42% (silica gel, 1:20 = acetone:petroleum ether to 1:10 = acetone:petroleum ether, $R_F = 0.1$)

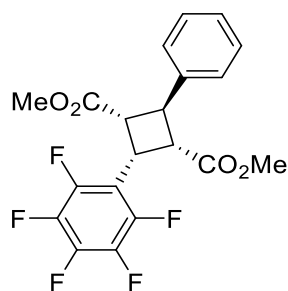
^1H NMR (500 MHz, CDCl_3) δ 7.27 (d, $J = 6.3$ Hz, 4H), 7.18 (d, $J = 4.9$ Hz, 1H), 7.08 (dd, $J = 5.2, 1.1$ Hz, 1H), 6.93 (dd, $J = 3.6, 1.2$ Hz, 1H), 6.88 (dd, $J = 5.1, 3.6$ Hz, 1H), 4.69 (dd, $J = 10.9, 10.9$ Hz, 1H), 4.38 (dd, $J = 9.8, 9.8$ Hz, 1H), 3.59 (dd, $J = 10.9, 9.6$ Hz, 2H), 3.40 ppm (s, 6H).

^{13}C NMR (126 MHz, CDCl_3) δ 171.21, 141.17, 139.19, 128.62, 127.20, 126.96, 126.50, 125.48, 124.15, 51.78, 47.13, 41.46, 39.29 ppm.

HR-MS calculated for $\text{C}_{18}\text{H}_{19}\text{O}_4\text{S}$: m/z (%): 331.0999 $[\text{M}+\text{H}]^+$, found: 331.1004; calculated for $\text{C}_{18}\text{H}_{18}\text{O}_4\text{SNa}$: m/z (%): 353.0818 $[\text{M}+\text{Na}]^+$, found: 353.0818.

IR ν_{max} (cm^{-1}) 1730, 1497, 1435, 1331, 1204, 1041, 850.

Dimethyl (1*R*,2*S*,3*S*,4*S*)-2-(perfluorophenyl)-4-phenylcyclobutane-1,3-dicarboxylate (Compound **183**)



Compound 183 is prepared using procedure C.

Isolated yield: 70% (silica gel, 1:50 = acetone:petroleum ether, $R_F = 0.2$)

^1H NMR (500 MHz, CDCl_3) δ 7.42 – 7.36 (m, 4H), 7.32 – 7.27 (m, 1H), 4.69 (dd, $J = 10.2, 10.2$ Hz, 1H), 4.62 (dd, $J = 10.8, 10.8$ Hz, 1H), 3.76 (dd, $J = 10.5, 10.5$ Hz, 2H), 3.57 ppm (s, 6H).

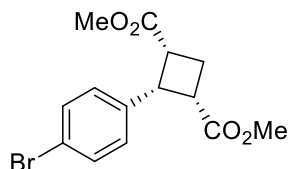
^{13}C NMR (126 MHz, CDCl_3) δ 171.37, 141.41, 128.72, 127.17, 126.52, 52.06, 44.54, 43.24, 31.69 ppm.

^{19}F NMR (470 MHz, CDCl_3) δ -139.20 (d, $J = 16.0$ Hz), -154.89, -162.36 ppm (d, $J = 6.8$ Hz).

HR-MS calculated for C₂₀H₁₆F₅O₄: m/z (%): 415.0963 [M+H]⁺, found: 415.0965.

IR ν_{\max} (cm⁻¹) 1733, 1523, 1498, 1437, 1323, 1210, 1149, 1063, 1016, 982, 939, 867.

Dimethyl (1*R*,2*s*,3*S*)-2-(4-bromophenyl)cyclobutane-1,3-dicarboxylate (Compound **184**)



Compound 184 is prepared using procedure C.

Isolated yield: 50% yield (silica gel, 1:50 = acetone:petroleum ether, R_F= 0.3)

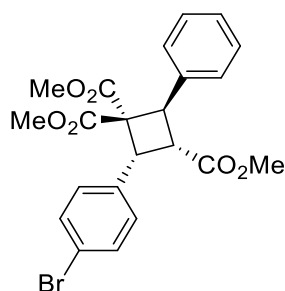
¹H NMR (500 MHz, CDCl₃) δ 7.37 (d, *J* = 8.5 Hz, 2H), 7.06 (d, *J* = 8.5 Hz, 2H), 4.18 – 4.08 (m, 1H), 3.73 – 3.54 (m, 2H), 3.34 (s, 6H), 3.21 (tdd, *J* = 12.4, 11.3, 10.6, 1.0 Hz, 1H), 2.39 ppm (dtd, *J* = 12.7, 8.8, 8.8, 2.4 Hz, 1H).

¹³C NMR (126 MHz, CDCl₃) δ 172.09, 137.10, 131.41, 129.75, 121.24, 53.58, 51.66, 47.29, 39.49, 24.51 ppm.

HR-MS calculated for C₁₄H₁₆⁷⁹BrO₄: m/z (%): 327.0227 [M+H]⁺, found: 327.0232; calculated for C₁₄H₁₆⁸¹BrO₄: m/z (%): 329.0206 [M+H]⁺, found: 329.0210.

IR ν_{\max} (cm⁻¹) 1731, 1489, 1435, 1410, 1335, 1243, 1199, 1179, 1075, 1031, 1010, 836.

rac-Trimethyl (2*R*,3*S*,4*R*)-2-(4-bromophenyl)-4-phenylcyclobutane-1,1,3-tricarboxylate (Compound **185**)



Compound 185 is prepared using procedure C.

Isolated yield: 40% (silica gel, 1:20 = acetone:petroleum ether to 1:10 = acetone:petroleum ether, R_F= 0.15)

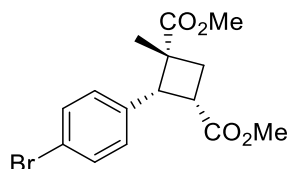
¹H NMR (500 MHz, CDCl₃) δ 7.42 (d, *J* = 8.5 Hz, 2H), 7.32 (d, *J* = 4.3 Hz, 4H), 7.25 – 7.23 (m, 1H), 7.16 (d, *J* = 8.5 Hz, 2H), 5.11 (d, *J* = 11.6, 1H), 4.52 (d, *J* = 10.5, 1H), 4.21 (dd, *J* = 11.6, 10.5 Hz, 1H), 3.40 (s, 3H), 3.32 (s, 3H), 3.24 ppm (s, 3H).

^{13}C NMR (126 MHz, CDCl_3) δ 171.27, 169.19, 136.74, 135.77, 131.66, 130.19, 128.43, 127.73, 127.48, 121.80, 62.37, 52.62, 52.45, 51.96, 46.55, 45.49, 41.63 ppm.

HR-MS calculated for $\text{C}_{22}\text{H}_{22}^{79}\text{BrO}_6$: m/z (%): 461.0594 $[\text{M}+\text{H}]^+$, found: 461.0594; calculated for $\text{C}_{22}\text{H}_{22}^{81}\text{BrO}_6$: m/z (%): 463.0574 $[\text{M}+\text{H}]^+$, found: 463.0573.

IR ν_{max} (cm^{-1}) 1728, 1490, 1434, 1248, 1211, 1173, 1143, 1106, 1075, 1047, 1010, 942, 838.

rac-(1*R*,2*R*,3*S*)-2-(4-bromophenyl)-1-methylcyclobutane-1,3-dicarboxylate (Compound **186**)



Compound 186 is prepared using procedure C.

Isolated yield: 76% yield (silica gel, 1:50 = acetone:petroleum ether to 1:20 = acetone:petroleum ether, $R_F=0.2$)

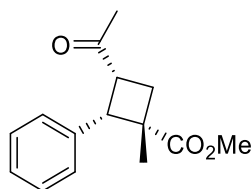
^1H NMR (500 MHz, CDCl_3) δ 7.38 (d, $J = 8.5$ Hz, 2H), 7.03 (d, $J = 8.5$ Hz, 2H), 3.68 (td, $J = 10.3, 8.7$ Hz, 1H), 3.60 (dd, $J = 10.0, 2.8$ Hz, 1H), 3.38 (dd, $J = 12.6, 10.5$ Hz, 1H), 3.35 (s, 3H), 3.30 (s, 3H), 2.07 (ddd, $J = 12.6, 8.7, 2.8$ Hz, 1H), 1.65 ppm (s, 3H).

^{13}C NMR (126 MHz, CDCl_3) δ 174.63, 172.56, 137.65, 131.20, 129.45, 120.90, 54.62, 51.56, 51.54, 45.97, 37.09, 30.71, 25.77 ppm.

HR-MS calculated for $\text{C}_{15}\text{H}_{18}^{79}\text{BrO}_4$: m/z (%): 341.0383 $[\text{M}+\text{H}]^+$, found: 341.0392; calculated for $\text{C}_{15}\text{H}_{18}^{81}\text{BrO}_4$: m/z (%): 343.0363 $[\text{M}+\text{H}]^+$, found: 343.0368.

IR ν_{max} (cm^{-1}) 1730, 1489, 1434, 1358, 1305, 1291, 1246, 1196, 1160, 1138, 1074, 1043, 1010, 960, 835.

rac-Methyl (1*S*,2*S*,3*R*)-3-acetyl-1-methyl-2-phenylcyclobutane-1-carboxylate (Compound **187**)



Compound 187 is prepared using procedure C.

Isolated yield: 48% yield (silica gel, 1:50 = acetone:petroleum ether to 1:20 = acetone:petroleum ether, $R_F=0.2$)

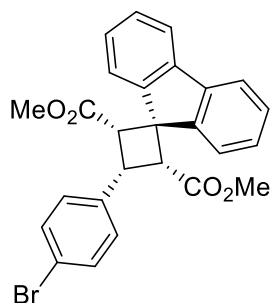
¹H NMR (500 MHz, CDCl₃) δ 7.37 – 7.32 (m, 3H), 7.28 – 7.21 (m, 2H), 4.10 (d, *J* = 10.3 Hz, 1H), 3.75 (s, 3H), 3.55 (q, *J* = 9.6 Hz, 1H), 2.66 (dd, *J* = 11.4, 9.6 Hz, 1H), 2.12 (s, 3H), 1.99 (ddd, *J* = 11.3, 8.9, 0.8 Hz, 1H), 1.05 ppm (s, 3H).

¹³C NMR (126 MHz, CDCl₃) δ 208.40, 177.00, 137.74, 128.49, 127.87, 127.09, 52.29, 47.89, 43.73, 43.50, 31.38, 28.28, 19.16 ppm.

HR-MS calculated for C₁₅H₁₉O₃: *m/z* (%): 247.1329 [M+H]⁺, found: 247.1331.

IR ν_{max} (cm⁻¹) 1726, 1709, 1604, 1498, 1452, 1356, 1312, 1224, 1202, 1161, 1105, 1033, 992, 881

Dimethyl (2*R*,3*r*,4*S*)-3-(4-bromophenyl)spiro[cyclobutane-1,9'-fluorene]-2,4-dicarboxylate (Compound **188**)



Compound 188 is prepared using procedure C.

Isolated yield: 62% yield (silica gel, 1:20 = acetone:petroleum ether, R_F= 0.2)

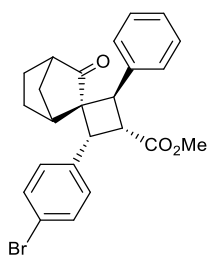
¹H NMR (500 MHz, CDCl₃) δ 8.04 (dt, *J* = 7.8, 0.9 Hz, 1H), 7.82 – 7.73 (m, 2H), 7.70 – 7.63 (m, 1H), 7.48 – 7.37 (m, 2H), 7.33 (td, *J* = 7.5, 1.1 Hz, 1H), 7.15 (td, *J* = 7.6, 1.2 Hz, 1H), 7.12 – 7.08 (m, 2H), 6.34 – 6.29 (m, 2H), 4.72 (d, *J* = 10.0 Hz, 1H), 4.28 (t, *J* = 10.2 Hz, 1H), 4.20 (d, *J* = 10.4 Hz, 1H), 3.83 (s, 3H), 3.18 ppm (s, 3H).

¹³C NMR (126 MHz, CDCl₃) δ 172.13, 169.34, 150.53, 142.80, 140.87, 139.99, 135.99, 130.72, 128.78, 128.49, 128.32, 127.88, 127.40, 122.12, 120.03, 119.92, 119.61, 58.14, 53.59, 52.17, 51.51, 47.01, 46.12, 41.03 ppm.

HR-MS calculated for C₂₆H₂₁⁷⁹BrO₄: *m/z* (%): 477.0696 [M+H]⁺, found: 477.0696; calculated for C₂₆H₂₁⁸¹BrO₄: *m/z* (%): 479.0676 [M+H]⁺, found: 479.0675.

IR ν_{max} (cm⁻¹) 1736, 1688, 1586, 1489, 1450, 1437, 1398, 1377, 1197, 1171, 1100, 1072, 1011, 838.

rac-Methyl (1*R*,2*R*,2'*R*,3'*S*,4'*R*)-2'-(4-bromophenyl)-3-oxo-4'-phenylspiro[bicyclo[2.2.1]heptane-2,1'-cyclobutane]-3'-carboxylate (Compound **189**)



Compound 189 is prepared using procedure C.

Isolated yield: 65% (silica gel, 1:20 = acetone:petroleum ether to 1:10 = acetone:petroleum ether, $R_F = 0.2$)

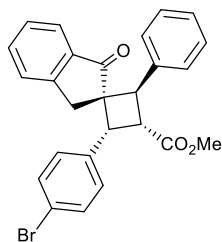
$^1\text{H NMR}$ (500 MHz, CDCl_3) δ 7.35 – 7.30 (m, 2H), 7.28 – 7.22 (m, 4H), 7.19 (s, 1H), 7.16 – 7.10 (m, 2H), 4.65 (d, $J = 11.3$ Hz, 1H), 3.95 (t, $J = 11.2$ Hz, 1H), 3.71 (d, $J = 11.0$ Hz, 1H), 3.32 (s, 3H), 2.73 (dd, $J = 4.5, 2.0$ Hz, 1H), 2.35 – 2.25 (m, 1H), 1.70 (dt, $J = 10.5, 1.8$ Hz, 1H), 1.58 – 1.46 (m, 1H), 1.38 (ddd, $J = 10.5, 2.1, 1.0$ Hz, 1H), 1.12 (dddd, $J = 13.0, 9.0, 4.7, 2.0$ Hz, 1H), 1.03 (ddt, $J = 13.3, 12.4, 4.6$ Hz, 1H), 0.39 ppm (dddd, $J = 13.6, 9.1, 4.9, 2.2$ Hz, 1H).

$^{13}\text{C NMR}$ (126 MHz, CDCl_3) δ 214.85, 171.60, 138.37, 136.10, 131.24, 130.63, 128.79, 127.96, 127.38, 121.40, 62.12, 53.22, 51.68, 49.67, 46.43, 42.86, 41.72, 34.28, 27.39, 21.59 ppm.

HR-MS calculated for $\text{C}_{24}\text{H}_{24}^{79}\text{BrO}_3$: m/z (%): 439.0903 $[\text{M}+\text{H}]^+$, found: 439.0907;
 calculated for $\text{C}_{24}\text{H}_{24}^{81}\text{BrO}_3$: m/z (%): 441.0883 $[\text{M}+\text{H}]^+$, found: 441.0885;

IR ν_{max} (cm^{-1}) 1733, 1489, 1435, 1198, 1179, 1076, 1010, 834.

rac-Methyl (1*R*,2*R*,3*S*,4*R*)-2-(4-bromophenyl)-1'-oxo-4-phenyl-1',3'-dihydrospiro[cyclobutane-1,2'-indene]-3-carboxylate (Compound **190**)



Compound 190 is prepared using procedure C.

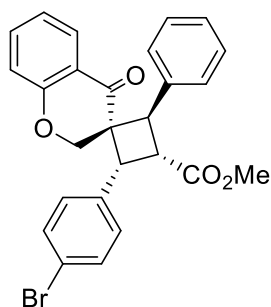
Isolated yield: 47% yield (silica gel, 1:20 = acetone:petroleum ether to 1:10 = acetone:petroleum ether, $R_F = 0.2$)

¹H NMR (500 MHz, CDCl₃) δ 7.58 – 7.51 (m, 2H), 7.42 – 7.35 (m, 3H), 7.35 – 7.28 (m, 3H), 7.27 – 7.22 (m, 1H), 7.17 – 7.12 (m, 2H), 7.12 – 7.08 (m, 2H), 5.13 (d, *J* = 11.8 Hz, 1H), 4.16 (dd, *J* = 11.9, 10.1 Hz, 1H), 3.87 (d, *J* = 10.2 Hz, 1H), 3.54 (s, 3H), 3.27 – 3.00 ppm (m, 2H).
¹³C NMR (126 MHz, CDCl₃) δ 202.55, 171.85, 151.05, 138.66, 136.00, 135.18, 134.76, 131.10, 130.63, 128.74, 127.78, 127.03, 126.96, 126.33, 124.07, 121.48, 57.73, 55.66, 51.86, 43.05, 41.63, 38.21 ppm.

HR-MS calculated for C₂₆H₂₂⁷⁹BrO₃: *m/z* (%): 461.0747 [M+H]⁺, found: 461.0749;
calculated for C₂₆H₂₂⁸¹BrO₃: *m/z* (%): 463.0726 [M+H]⁺, found: 463.0726.

IR ν_{max} (cm⁻¹) 1730, 1702, 1603, 1490, 1465, 1435, 1412, 1325, 1282, 1207, 1152, 1124, 1075, 1009, 927, 870, 834.

rac-Methyl (2'*R*,3*R*,3'*S*,4'*R*)-2'-(4-bromophenyl)-4-oxo-4'-phenylspiro[chromane-3,1'-cyclobutane]-3'-carboxylate (Compound **191**)



Compound 191 is prepared using procedure C.

Isolated yield: 42% yield (silica gel, 1:20 = acetone:petroleum ether to 1:10 = acetone:petroleum ether, R_F = 0.1)

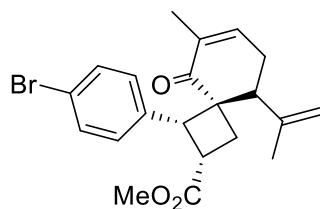
¹H NMR (500 MHz, CDCl₃) δ 7.46 (dd, *J* = 7.9, 1.7 Hz, 1H), 7.37 (ddd, *J* = 8.8, 7.2, 1.8 Hz, 1H), 7.32 (ddd, *J* = 7.6, 6.2, 1.3 Hz, 2H), 7.25 – 7.18 (m, 5H), 6.97 – 6.91 (m, 2H), 6.89 (dd, *J* = 8.5, 1.0 Hz, 1H), 6.84 (ddd, *J* = 8.1, 7.2, 1.1 Hz, 1H), 5.45 (d, *J* = 11.3 Hz, 1H), 4.29 (d, *J* = 12.2 Hz, 1H), 4.24 (d, *J* = 10.5 Hz, 1H), 4.21 – 4.13 (m, 1H), 3.99 (d, *J* = 12.1 Hz, 1H), 3.48 ppm (s, 3H).

¹³C NMR (126 MHz, CDCl₃) δ ¹³C NMR (126 MHz, CDCl₃) δ 190.73, 171.71, 160.44, 135.92, 135.85, 134.88, 131.14, 130.17, 128.66, 127.37, 127.23, 126.98, 121.51, 121.31, 120.47, 117.19, 71.88, 52.19, 51.93, 46.89, 40.36, 38.25 ppm.

HR-MS calculated for C₂₆H₂₂⁷⁹BrO₄: *m/z* (%): 477.0696 [M+H]⁺, found: 477.0695;
calculated for C₂₆H₂₂⁷⁹BrO₄: *m/z* (%): 479.0676 [M+H]⁺, found: 479.0674.

IR ν_{max} (cm⁻¹) 1733, 1687, 1605, 1490, 1475, 1465, 1315, 1208, 1143, 1034, 1010.

rac-Methyl (1*R*,2*S*,4*S*,9*R*)-1-(4-bromophenyl)-6-methyl-5-oxo-9-(prop-1-en-2-yl)spiro[3.5]non-6-ene-2-carboxylate (Compound **192**)



Compound 192 is prepared using procedure C.

Isolated yield: 44% (silica gel, 1:20 = acetone:petroleum ether to 1:10 = acetone:petroleum ether, $R_F = 0.2$)

$^1\text{H NMR}$ (500 MHz, CDCl_3) δ 7.29 (d, $J = 8.5$ Hz, 2H), 6.88 (d, $J = 8.5$ Hz, 2H), 6.19 (ddt, $J = 4.1, 2.7, 1.4$ Hz, 1H), 4.86 – 4.74 (m, 1H), 4.62 – 4.47 (m, 1H), 3.93 (dd, $J = 9.5, 2.3$ Hz, 1H), 3.69 – 3.57 (m, 2H), 3.40 (s, 3H), 3.21 – 3.08 (m, 1H), 3.01 – 2.90 (m, 1H), 2.35 (ddt, $J = 19.8, 5.6, 1.5$ Hz, 1H), 2.02 – 1.94 (m, 1H), 1.66 – 1.52 (m, 3H), 1.36 – 1.13 ppm (m, 3H).

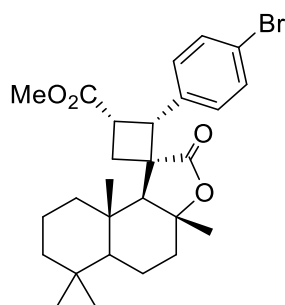
$^{13}\text{C NMR}$ (126 MHz, CDCl_3) δ 198.10, 172.90, 143.68, 139.09, 136.07, 135.50, 130.87, 130.48, 120.95, 114.56, 52.83, 51.79, 51.75, 51.57, 36.88, 27.05, 23.74, 22.00, 15.70 ppm.

HR-MS calculated for $\text{C}_{21}\text{H}_{24}^{79}\text{BrO}_3$: m/z (%): 403.0903 $[\text{M}+\text{H}]^+$, found: 403.0908;

calculated for $\text{C}_{21}\text{H}_{24}^{81}\text{BrO}_3$: m/z (%): 405.0883 $[\text{M}+\text{H}]^+$, found: 405.0883.

IR ν_{max} (cm^{-1}) 1730, 1663, 1489, 1435, 1353, 1201, 1156, 1076, 1010, 900, 847, 825.

rac-Methyl (2*R*,3*S*,3*a'**R*,9*a'**S*,9*b'**S*)-2-(4-bromophenyl)-3*a'*,6',6',9*a'*-tetramethyl-2'-oxodecahydro-2'*H*-spiro[cyclobutane-1,1'-naphtho[2,1-*b*]furan]-3-carboxylate (Compound **193**)



Compound 193 is prepared using procedure C.

Isolated yield: 40% (silica gel, 1:20 = acetone:petroleum ether to 1:10 = acetone:petroleum ether, $R_F = 0.2$)

$^1\text{H NMR}$ (500 MHz, CDCl_3) δ 7.32 (d, $J = 8.5$ Hz, 2H), 7.07 (d, $J = 8.4$ Hz, 2H), 4.36 (d, $J = 11.3$ Hz, 1H), 3.56 (s, 3H), 3.47 (ddd, $J = 11.3, 8.9, 5.1$ Hz, 1H), 2.94 – 2.73 (m, 2H), 2.05 –

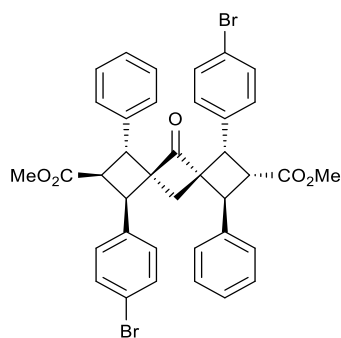
1.98 (m, 1H), 1.94 (dt, $J = 12.0, 3.4$ Hz, 1H), 1.80 (m, 2H), 1.73 – 1.62 (m, 1H), 1.60 – 1.46 (m, 3H), 1.42 – 1.33 (m, 2H), 1.31 (s, 3H), 1.22 – 1.15 (m, 1H), 1.12 (s, 3H), 0.95 (dd, $J = 12.5, 2.7$ Hz, 1H), 0.80 (s, 3H), 0.78 ppm (s, 3H).

^{13}C NMR (126 MHz, CDCl_3) δ 178.70, 172.14, 134.94, 131.17, 130.78, 121.07, 84.57, 61.39, 57.40, 53.72, 51.70, 48.72, 41.65, 40.30, 40.20, 39.27, 38.71, 33.52, 33.29, 28.73, 25.25, 21.04, 20.39, 18.13, 17.41 ppm.

HR-MS calculated for $\text{C}_{27}\text{H}_{36}^{79}\text{BrO}_4$: m/z (%): 503.1792 $[\text{M}+\text{H}]^+$, found: 503.1793; calculated for $\text{C}_{27}\text{H}_{36}^{81}\text{BrO}_4$: m/z (%): 505.1771 $[\text{M}+\text{H}]^+$, found: 505.1771;

IR ν_{max} (cm^{-1}) 1762, 1733, 1489, 1459, 1390, 1352, 1284, 1257, 1222, 1172, 1148, 1131, 1119, 1064, 1039, 1010, 971, 941, 914, 893, 878, 859, 830.

rac-Dimethyl (1*R*,2*S*,3*R*,4*R*,6*S*,7*S*,8*R*,9*S*)-1,7-bis(4-bromophenyl)-5-oxo-3,9-diphenyldispiro[3.1.36.14]decane-2,8-dicarboxylate (Compound **194**)



Compound **194** is prepared using procedure D.

Isolated yield: 36% (silica gel, 1:20 = acetone:petroleum ether to 1:10 = acetone:petroleum ether, $R_F = 0.1$)

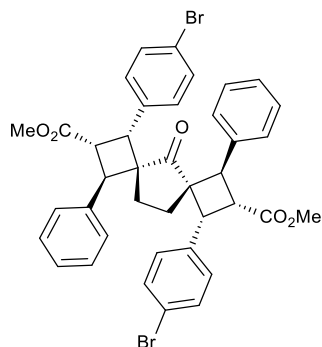
^1H NMR (500 MHz, CDCl_3) δ 7.52 – 7.42 (m, 4H), 7.34 – 7.28 (m, 6H), 7.20 – 7.16 (m, 4H), 6.87 – 6.84 (m, 4H), 4.60 (d, $J = 10.7$ Hz, 2H), 3.64 (t, $J = 10.7$ Hz, 2H), 3.47 (d, $J = 10.7$ Hz, 2H), 3.31 (s, 6H), 1.94 ppm (s, 2H).

^{13}C NMR (126 MHz, CDCl_3) δ 208.79, 170.92, 137.70, 135.10, 131.20, 130.64, 128.85, 127.49, 121.53, 64.74, 51.79, 51.69, 45.94, 41.89, 33.96 ppm.

HR-MS calculated for $\text{C}_{38}\text{H}_{33}^{79}\text{Br}^{79}\text{BrO}_5$: m/z (%): 727.0689 $[\text{M}+\text{H}]^+$, found: 727.0693; calculated for $\text{C}_{38}\text{H}_{33}^{79}\text{Br}^{81}\text{BrO}_5$: m/z (%): 729.06689 $[\text{M}+\text{H}]^+$, found: 729.0671; calculated for $\text{C}_{38}\text{H}_{33}^{81}\text{Br}^{81}\text{BrO}_5$: m/z (%): 731.0648 $[\text{M}+\text{H}]^+$, found: 731.0643.

IR ν_{max} (cm^{-1}) 1757, 1731, 1489, 1436, 1410, 1274, 1209, 1174, 1132, 1075, 1010, 963, 919, 853.

rac-Dimethyl (1*R*,2*S*,3*R*,4*R*,6*R*,7*R*,8*S*,9*R*)-1,7-bis(4-bromophenyl)-5-oxo-3,9-diphenyldispiro[3.1.36.24]undecane-2,8-dicarboxylate (Compound **195**)



Compound **195** is prepared using procedure D.

Isolated yield: 59% (silica gel, 1:20 = acetone:petroleum ether to 1:10 = acetone:petroleum ether, $R_F = 0.1$)

^1H NMR (500 MHz, CDCl_3) δ 7.56 – 7.39 (m, 4H), 7.23 – 7.17 (m, 6H), 6.98 (d, $J = 8.5$ Hz, 4H), 6.54 (dd, $J = 7.2, 2.3$ Hz, 4H), 4.54 (d, $J = 11.6$ Hz, 2H), 3.92 (dd, $J = 11.1, 11.1$ Hz, 2H), 3.48 (d, $J = 10.6$ Hz, 2H), 3.40 (s, 6H), 1.87 (d, $J = 8.1$ Hz, 2H), 1.57 ppm (d, $J = 8.2$ Hz, 2H).

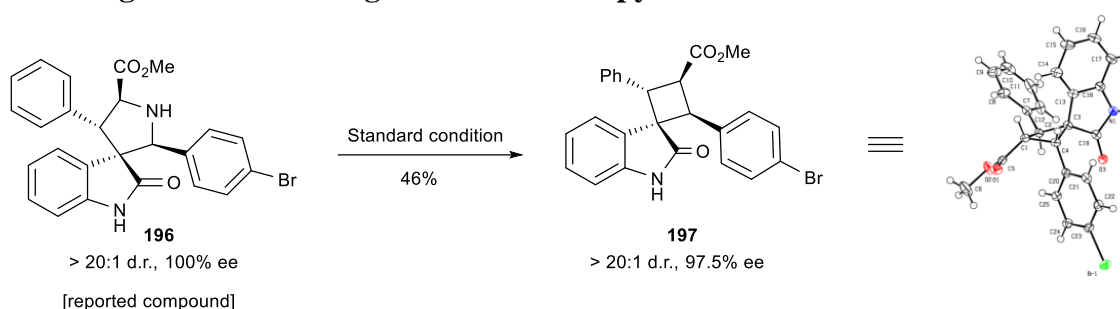
^{13}C NMR (126 MHz, CDCl_3) δ 211.22, 171.39, 137.20, 135.16, 131.24, 130.90, 128.44, 127.26, 126.95, 121.44, 57.46, 55.43, 51.72, 42.74, 41.38, 30.76 ppm.

HR-MS calculated for $\text{C}_{39}\text{H}_{35}^{79}\text{Br}^{79}\text{Br}$ O_5 : m/z (%): 741.0846 $[\text{M}+\text{H}]^+$, found: 741.0849; calculated for $\text{C}_{39}\text{H}_{35}^{79}\text{Br}^{81}\text{Br}$ O_5 : m/z (%): 743.0825 $[\text{M}+\text{H}]^+$, found: 743.0831; calculated for $\text{C}_{39}\text{H}_{35}^{81}\text{Br}^{81}\text{Br}$ O_5 : m/z (%): 745.0805 $[\text{M}+\text{H}]^+$, found: 745.0804.

IR ν_{max} (cm^{-1}) 1730, 1489, 1435, 1412, 1312, 1203, 1160, 1075, 1010, 843.

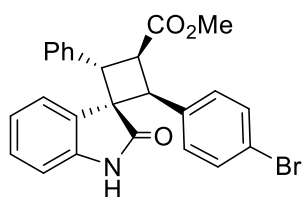
5.7 Further investigation of contractive synthesis of cyclobutanes from pyrrolidines

5.7.1 Ring contraction using enantioenriched pyrrolidine



Scheme S1. Retention of stereochemistry in ring contraction. Enantioenriched pyrrolidine was prepared according to ref. 1.

Methyl (1*R*,2*R*,3*S*,4*R*)-2-(4-bromophenyl)-2'-oxo-4-phenylspiro[cyclobutane-1,3'-indoline]-3-carboxylate (Compound **197**)



Compound 197 is prepared using procedure C.

Isolated yield: 46% (yellow solid), 97.5% *ee*

(silica gel, 1:20 = acetone:petroleum ether to 1:10 = acetone:petroleum ether, $R_F = 0.1$)

^1H NMR (700 MHz, CDCl_3) δ 7.42 (d, $J = 8.5$ Hz, 2H), 7.27 (s, 2H), 7.16 (t, $J = 7.6$ Hz, 2H), 7.13 – 7.08 (m, 2H), 7.02 (d, $J = 7.5$ Hz, 1H), 6.90 (d, $J = 8.1$ Hz, 2H), 6.87 (t, $J = 7.6$ Hz, 1H), 6.75 (d, $J = 7.7$ Hz, 1H), 5_{jj} 10.8 Hz, 1H), 3.57 ppm (s, 3H).

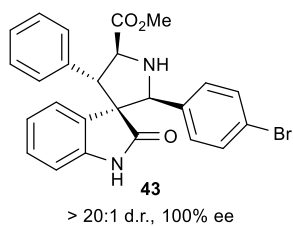
^{13}C NMR (126 MHz, CDCl_3) δ 178.70, 172.14, 134.94, 131.17, 130.78, 121.07, 84.57, 61.39, 57.40, 53.72, 51.70, 48.72, 41.65, 40.30, 40.20, 39.27, 38.71, 33.52, 33.29, 28.73, 25.25, 21.04, 20.39, 18.13, 17.41 ppm.

HR-MS calculated for $\text{C}_{25}\text{H}_{21}^{79}\text{BrNO}_3$: m/z (%): 462.0699 $[\text{M}+\text{H}]^+$, found: 462.0702; calculated for $\text{C}_{25}\text{H}_{21}^{81}\text{BrNO}_3$: m/z (%): 464.0679 $[\text{M}+\text{H}]^+$, found: 464.0680;

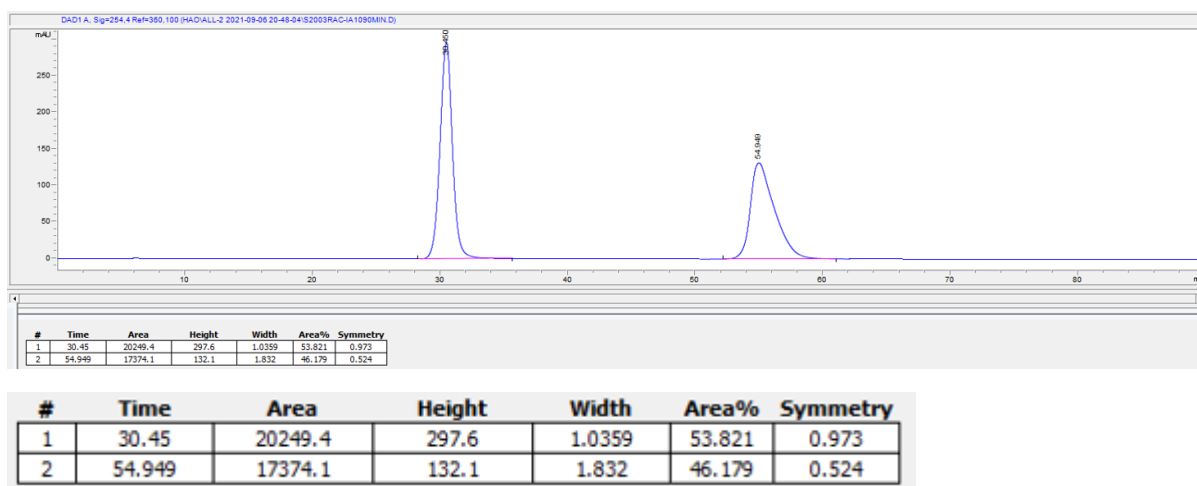
IR ν_{max} (cm^{-1}) 1706, 1617, 1489, 1470, 1329, 1262, 1210, 1109, 1074, 1010, 830. $[\alpha]_D^{20} - 62$ (c 0.10, CHCl_3)

HPLC conditions: CHIRALPAK IA column, *iso*-propanol/ *iso*-hexane = 10/90, flow rate = 0.5 mL min, minor enantiomer: $t_R = 31.67$ min; major enantiomer: $t_R = 49.61$ min; (60% *ee*);

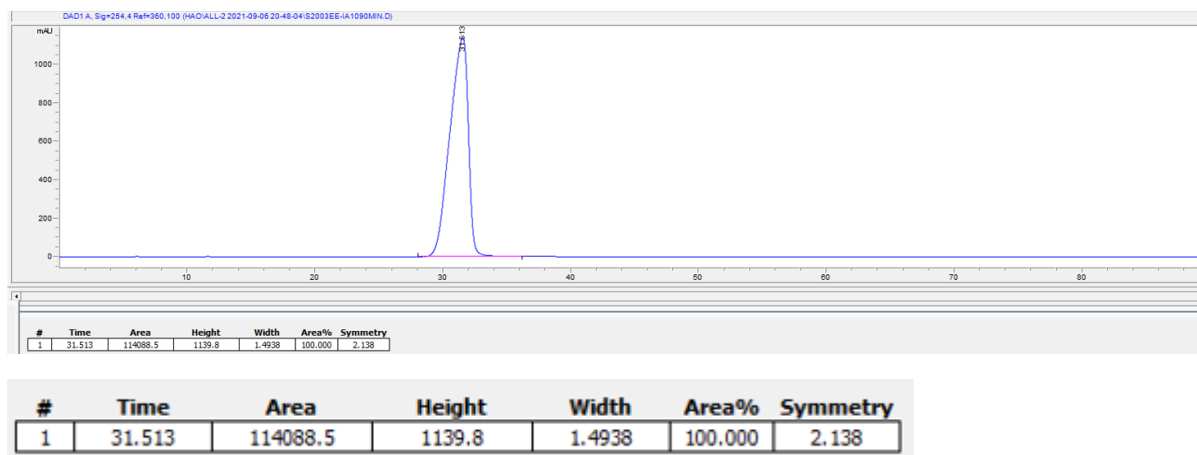
HPLC traces (compound 196)



racemic

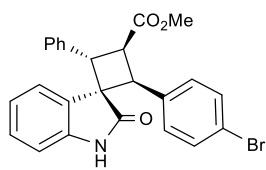


chiral



Method IA 10C: CHIRALPAK IA column, *iso*-propanol/ *iso*-hexane = 10/90, flow rate = 0.5 mL min

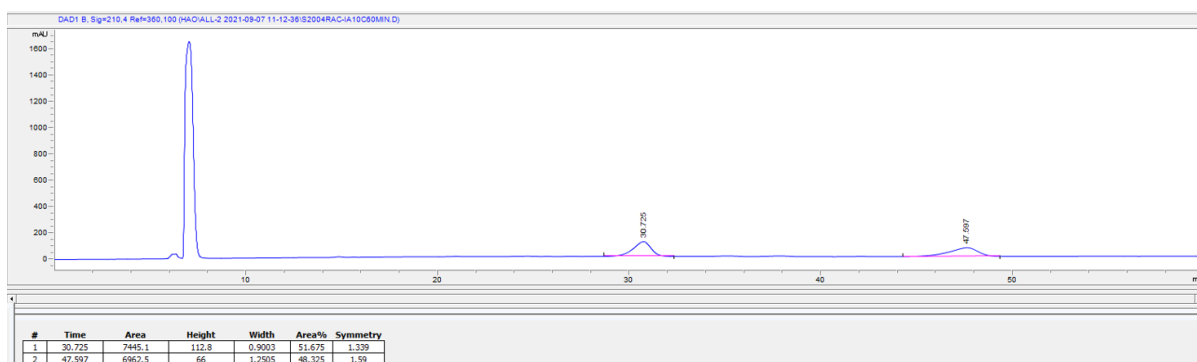
HPLC traces (compound 197)



44

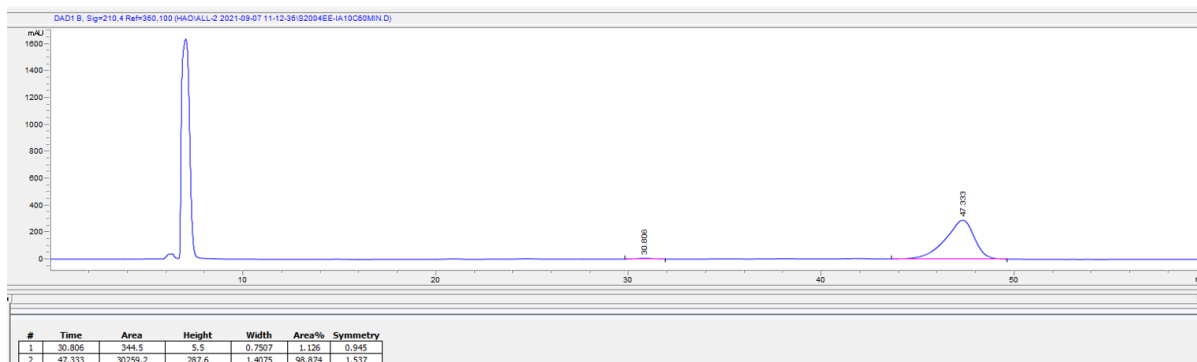
> 20:1 d.r., 97.5% ee

racemic



#	Time	Area	Height	Width	Area%	Symmetry
1	30.725	7445.1	112.8	0.9003	51.675	1.339
2	47.597	6962.5	66	1.2505	48.325	1.59

chiral



#	Time	Area	Height	Width	Area%	Symmetry
1	30.806	344.5	5.5	0.7507	1.126	0.945
2	47.333	30259.2	287.6	1.4075	98.874	1.537

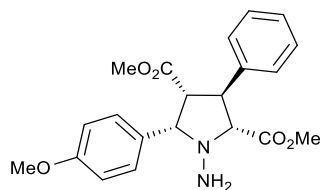
Method IA 10C: CHIRALPAK IA column, *iso*-propanol/ *iso*-hexane = 10/90, flow rate = 0.5 mL min

5.72 Ring contraction of *N*-aminopyrrolidine

Synthesis of *N*-aminopyrrolidine (compound **200**)

Under ambient condition, the pyrrolidine **167** (0.5 g, 1.35 mmol), NaNO₂ (0.187 g, 2.71 mmol, 2 eq.) and were dissolved in 100 ml DCM at 0°C. Then acetic acid (0.116 ml, 2.03 mmol, 1.5 eq.) and water (0.122 ml, 6.77 mmol, 5 eq.) were added to the reaction mixture. Ice-water bath was removed and the reaction was stirred for 5 hours in room temperature, in which the complete consumption of starting material can be monitored by TLC. The crude reaction mixture was transferred to the separation funnel and was diluted with DCM. Saturated aqueous sodium bicarbonate was added. Repeat extraction of the aqueous phase using DCM (100 ml) for three times. Combined organic phase was then dried by MgSO₄. Solvent were evaporated under vacuum to give the *N*-nitrosylation product as a yellow solid. Flash chromatography of this crude product gave the *N*-nitrosylated pyrrolidine in 68% yield (367 mg, 0.92 mmol) in the form of yellow solid (eluent: from 10:1 to 2:1 petroleum ether: ethyl acetate). *N*-nitrosylated pyrrolidine (367 mg, 0.92 mmol) was dissolved in MeOH and was cooled down to 0°C. Zinc (0.602 g, 9.21 mmol, 10 eq.) and NH₄Cl (0.739 g, 13.82 mmol, 15 eq.) were added to the reaction. Reaction mixture was stirred at 0°C for 1h. The crude reaction mixture was filtered through a pad of celite. The filtrate was evaporated and the crude mixture was purified by flash chromatography to give the *N*-aminopyrrolidine **200** as a white solid. (210 mg, 0.55 mmol 59% yield)

rac-Dimethyl (2*R*,3*S*,4*R*,5*S*)-1-amino-5-(4-methoxyphenyl)-3-phenylpyrrolidine-2,4-dicarboxylate (compound **200**)



Isolated yield: 59% (white solid) (silica gel, 1:10 = ethyl acetate:petroleum ether to 1:5 = ethyl acetate:petroleum ether, R_F= 0.1)

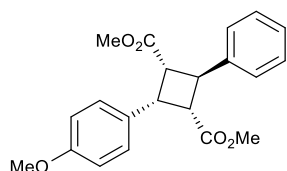
¹H NMR (700 MHz, CD₂Cl₂) δ 7.50 – 7.30 (m, 4H), 7.30 – 7.22 (m, 3H), 6.88 (d, *J* = 8.7 Hz, 2H), 4.06 (d, *J* = 10.8 Hz, 1H), 4.04 – 4.00 (m, 1H), 3.79 (s, 3H), 3.67 (s, 3H), 3.55 (d, *J* = 10.4 Hz, 1H), 3.44 (dd, *J* = 10.8, 8.6 Hz, 1H), 3.09 ppm (s, 3H).

¹³C NMR (176 MHz, CD₂Cl₂) δ 172.21, 171.91, 160.06, 140.01, 130.63, 130.04, 129.30, 128.36, 127.90, 114.05, 76.89, 75.11, 56.08, 55.78, 52.51, 51.92, 48.34 ppm.

HR-MS calculated for C₂₁H₂₅N₂O₅: m/z (%): 385.1758 [M+H]⁺, found: 385.1767.

IR ν_{max} (cm⁻¹) 1735, 1610, 1511, 1435, 1384, 1245, 1210, 1168, 1106, 1030, 929, 843, 817.

Dimethyl (1*R*,2*S*,3*S*,4*S*)-2-(4-methoxyphenyl)-4-phenylcyclobutane-1,3-dicarboxylate (compound **169**)



Compound **169** is prepared using procedure C.

Isolated yield: 25% (white solid) (silica gel, 1:50 = acetone:petroleum ether to 1:20 = acetone:petroleum ether, , R_F= 0.1)

¹H NMR (500 MHz, CDCl₃) δ 7.39 – 7.30 (m, 4H), 7.25 – 7.19 (m, 3H), 6.85 – 6.78 (m, 2H), 4.77 (dd, *J* = 10.7, 10.7 Hz, 1H), 4.16 (dd, *J* = 10.0, 10.0 Hz, 1H), 3.79 (s, 3H), 3.66 (dd, *J* = 10.4, 10.4 Hz, 2H), 3.39 ppm (s, 6H).

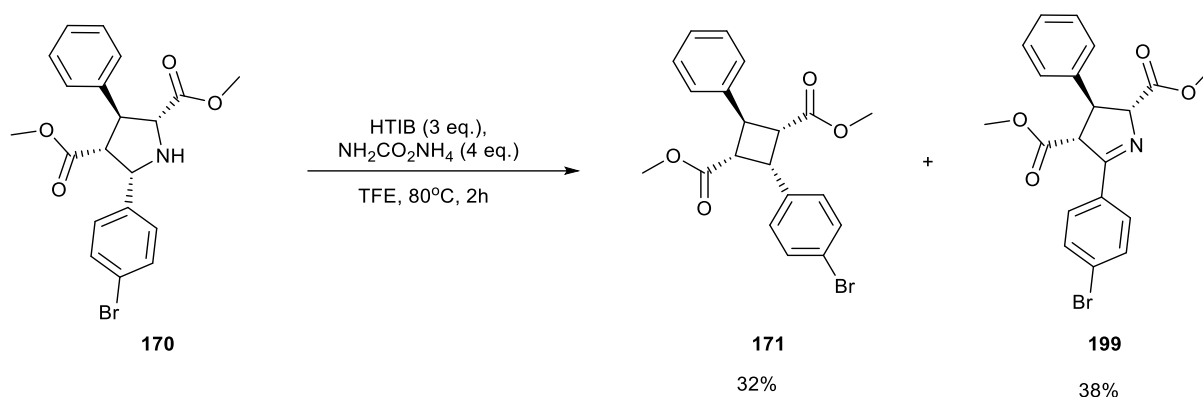
¹³C NMR (126 MHz, CDCl₃) δ 171.82, 158.61, 141.82, 129.41, 129.29, 128.59, 126.81, 126.45, 113.63, 55.15, 51.65, 43.78, 41.59 ppm.

HR-MS calculated for C₂₁H₂₄O₅: m/z (%): 355.1540 [M+H]⁺, found: 355.1543.

IR ν_{max} (cm⁻¹) 1728, 1611, 1514, 1435, 1249, 1201, 1181, 1031, 836.

5.73 Oxidation of pyrrolidine as side reaction

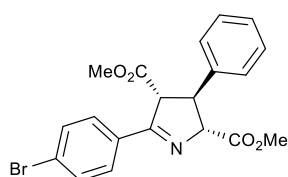
Synthesis of compound **171**



Scheme S2. Oxidation of pyrrolidine was observed when 4 eq. of ammonium carbamate was used.

Under ambient atmosphere, HTIB (98 mg, 0.25 mmol, 2.5 eq.), ammonium carbamate (62 mg, 0.8 mmol, 4 eq.) and pyrrolidine (0.1 mmol, 1 eq.) were dissolved in 1 mL 2,2,2-trifluoroethanol and stirred at 80°C for two hours. The reaction vial was cooled down to room temperature and the vial cap was opened slowly. The reaction mixture was filtered through a cotton wool and the filtrate was concentrated under vacuum. The crude mixture was directly charged onto silica gel and the imine was isolated using petroleum ether / acetone (10:1 v:v) as eluent.

rac-Dimethyl (2*R*,3*S*,4*R*)-5-(4-bromophenyl)-3-phenyl-3,4-dihydro-2*H*-pyrrole-2,4-dicarboxylate (compound **199**)



Isolated yield: 38% (white solid) (silica gel, 1:50 = acetone:petroleum ether, , $R_F=0.1$)

^1H NMR (500 MHz, CD_2Cl_2) δ 7.86 – 7.70 (m, 2H), 7.59 (d, $J = 8.7$ Hz, 2H), 7.39 – 7.30 (m, 4H), 7.27 – 7.19 (m, 1H), 4.97 (dd, $J = 6.1, 1.6$ Hz, 1H), 4.41 – 4.28 (m, 1H), 4.14 (t, $J = 6.3$ Hz, 1H), 3.78 (s, 3H), 3.65 ppm (s, 3H).

^{13}C NMR (126 MHz, CD_2Cl_2) δ 171.16, 170.98, 169.81, 141.11, 131.85, 131.77, 131.12, 129.67, 129.08, 127.57, 127.03, 81.58, 62.45, 52.69, 52.47, 52.31 ppm.

HR-MS calculated for C₂₀H₁₉⁷⁹BrNO₄: m/z (%): 416.0492, [M+H]⁺, found: 416.0498;

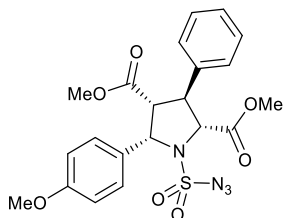
calculated for C₂₀H₁₉⁸¹BrNO₄: m/z (%): 418.0472, [M+H]⁺, found: 418.0474;

IR ν_{\max} (cm⁻¹) 1735, 1617, 1589, 1489, 1434, 1396, 1262, 1197, 1161, 1072, 1009, 827.

5.74 Synthesis of *N*-sulfamoyl azide

Synthesis of compound **166**¹³²

A solution of pyrrolidine **167** (1 eq.) and DBU (1.5 eq) in CH₂Cl₂ was added to the solution of N₃SO₂N₃ (2 eq.) in CH₂Cl₂. After the reaction mixture was stirred for 2 h, water (15 mL) was added and the aqueous solution was extracted with ethyl acetate for three times. The combined organic layer was dried over Na₂SO₄ and concentrated under vacuum. The crude product **166** was purified by flash chromatography (ethyl acetate: PE = 1:10 to 1:5 v:v).

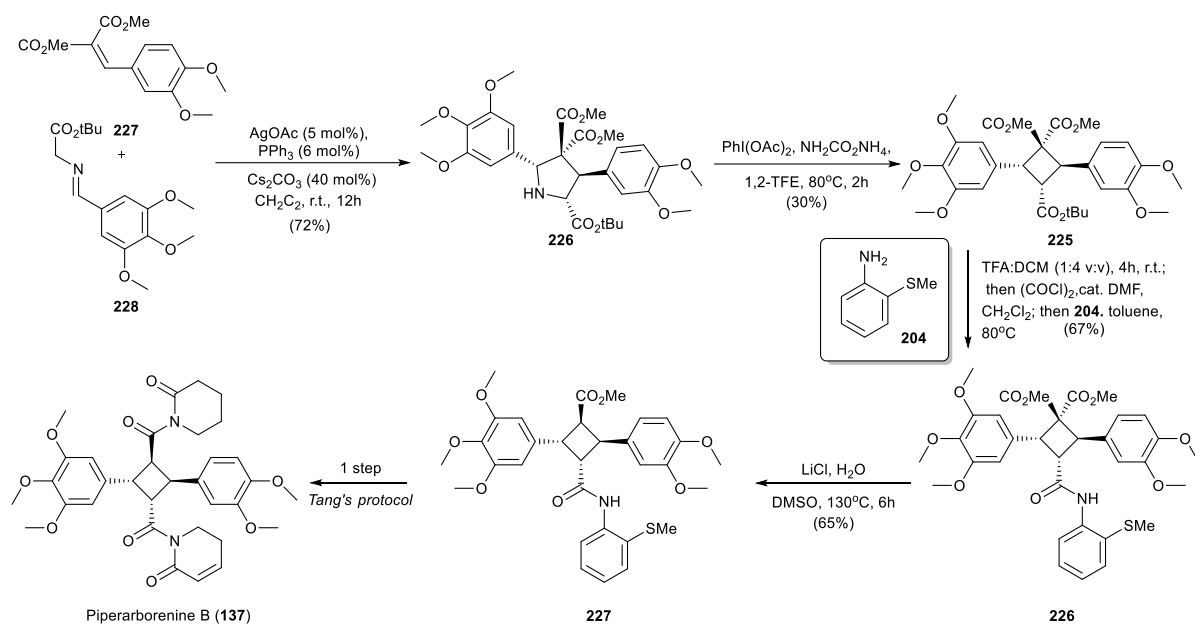


¹H NMR (400 MHz, Chloroform-*d*) δ 7.53 (d, *J* = 8.7 Hz, 1H), 7.27 (dq, *J* = 12.2, 7.6 Hz, 3H), 6.89 (d, *J* = 8.7 Hz, 1H), 5.40 (d, *J* = 9.2 Hz, 1H), 4.49 (d, *J* = 10.4 Hz, 1H), 4.23 – 4.04 (m, 1H), 3.77 (d, *J* = 5.1 Hz, 1H), 3.75 (s, 2H), 3.67 (s, 2H), 3.23 (s, 2H).

¹³C NMR (101 MHz, cdcl₃) δ 170.98, 168.17, 160.11, 135.34, 129.32, 128.97, 128.65, 128.18, 127.98, 114.22, 68.72, 65.80, 56.13, 55.47, 55.45, 52.21, 49.51.

ESI-MS calculated for C₂₁H₂₃N₄O₇S: m/z (%): 475.1282 [M+H]⁺, found: 475.1287.

5.8 Formal synthesis of piperarborenine B

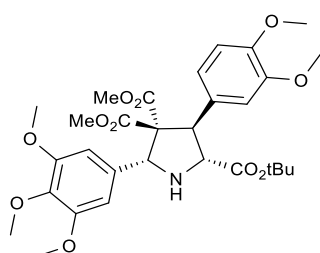


Scheme S4. Formal synthesis of piperarborenine B (**137**) (*this work*)

5.9 Synthesis and characterization of synthetic intermediates

rac-2-(tert-butyl) 4,4-dimethyl (2*R*,3*R*,5*R*)-3-(3,4-dimethoxyphenyl)-5-(3,4,5-trimethoxyphenyl)pyrrolidine-2,4,4-tricarboxylate (Compound **226**)¹⁵¹

A solution of AgOAc (0.02 mmol, 0.1 equiv.) and PPh₃ (0.03 mmol, 0.12 equiv.) in DCM (0.5 mL) was stirred for 30 minutes at room temperature. Cs₂CO₃ (0.04 mmol, 0.2 equiv.), imine **228** and dimethyl benzylidenemalonate **227**¹⁵⁴ were added sequentially into the solution and stirred overnight. The solvent was removed under reduced pressure. Compound **226** were purified by silica gel chromatography using petroleum ether and acetone from 10:1 (v:v) to 5:1 (v:v).



Isolated yield: 72% (white solid) (silica gel, 1:5 = acetone:petroleum ether, R_F= 0.1)

¹H NMR (400 MHz, CDCl₃) δ 6.94 – 6.77 (m, 3H), 6.71 (s, 2H), 5.21 (s, 1H), 4.25 (d, *J* = 7.9 Hz, 1H), 4.08 (d, *J* = 7.6 Hz, 1H), 4.04 (m, 3H), 3.90 – 3.85 (m, 9H), 3.82 (d, *J* = 1.3 Hz, 3H), 3.26 (d, *J* = 1.4 Hz, 3H), 3.21 (s, 3H), 1.37 ppm (s, 9H).

¹³C NMR (101 MHz, CDCl₃) δ 171.57, 169.74, 152.97, 148.51, 148.35, 137.69, 134.28, 130.64, 120.97, 112.25, 110.75, 104.68, 81.76, 71.43, 68.45, 66.29, 60.85, 56.33, 56.20, 55.99, 55.86, 52.21, 52.12, 27.94 ppm.

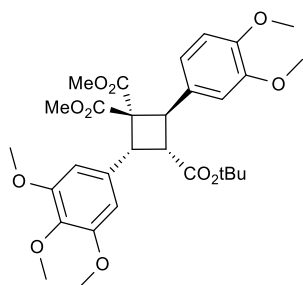
HR-MS calculated for C₃₀H₄₀NO₁₁: *m/z* (%): 590.2596 [M+H]⁺, found: 590.2599.

IR ν_{max} (cm⁻¹) 2950, 2839, 2349, 2326, 1726, 1591, 1517, 1463, 1423, 1367, 1328, 1249, 1157, 1126, 1027, 1008, 848.

rac-3-(tert-butyl) 1,1-dimethyl (2*R*,3*S*,4*R*)-2-(3,4-dimethoxyphenyl)-4-(3,4,5-trimethoxyphenyl)cyclobutane-1,1,3-tricarboxylate (Compound **225**)

Under ambient atmosphere, PIDA (2.5 eq.), ammonium carbamate (8 eq.), pyrrolidine **226** (0.1 mmol, 1 eq.) were dissolved in 1 mL TFE and stirred at 80°C for two hours. The reaction vial was cooled down to room temperature and the vial cap was opened slowly. The reaction mixture was filtered through a cotton wool and the filtrate was concentrated under vacuum.

The crude product **225** was purified by column chromatography using petroleum ether and acetone from 20:1 (v:v) to 10:1 (v:v). to give the cyclobutene product.



Isolated yield: 30% (yellow solid) (silica gel, 1:10 = acetone:petroleum ether, $R_F=0.1$)

$^1\text{H NMR}$ (400 MHz, CDCl_3) δ 6.94 (d, $J = 1.8$ Hz, 1H), 6.88 – 6.76 (m, 2H), 6.52 (s, 2H), 5.00 (d, $J = 11.4$ Hz, 1H), 4.41 (d, $J = 10.7$ Hz, 1H), 3.98 (dd, $J = 11.0, 11.0$ Hz, 1H), 3.89 (s, 3H), 3.85 (s, 9H), 3.78 (s, 3H), 3.36 (s, 3H), 3.30 (s, 3H), 1.08 ppm (s, 9H).

$^{13}\text{C NMR}$ (101 MHz, CDCl_3) δ 170.31, 169.89, 169.64, 152.96, 148.78, 148.49, 137.37, 132.78, 129.98, 119.30, 111.32, 110.83, 105.80, 80.90, 62.43, 60.96, 56.23, 55.98, 52.68, 52.41, 47.52, 45.41, 43.26, 27.77 ppm.

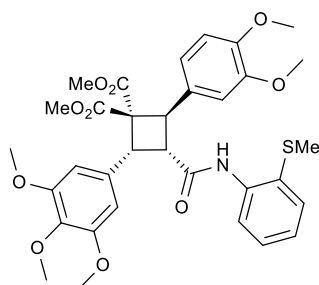
HR-MS calculated for $\text{C}_{30}\text{H}_{39}\text{O}_{11}$: m/z (%): 575.2487 $[\text{M}+\text{H}]^+$, found: 575.2487.

IR ν_{max} (cm^{-1}) 2349, 1726, 1589, 1516, 1462, 1424, 1367, 1345, 1247, 1156, 1124, 1060, 1027, 909, 846.

rac-Dimethyl (2R,3S,4R)-2-(3,4-dimethoxyphenyl)-3-((2-(methylthio)phenyl)carbamoyl)-4-(3,4,5-trimethoxyphenyl)cyclobutane-1,1-dicarboxylate (Compound **226**)

Cyclobutane **225** (0.03 mmol, 0.12 equiv.) was dissolved in DCM (1 mL). Trifluoroacetic acid (0.25ml) was added slowly to the solution at room temperature and stirred for 4 – 6h at that temperature. Solvents and acid were removed under vacuum and the residue was purified by column chromatography using petroleum ether/acetone (silica gel, 10:1 to 5:1 v:v). Carboxylic acid was collected and the solvent were evaporated. This acid was dissolved in DCM. Oxalyl chloride was added slowly to this solution at room temperature. Catalytic amount of DMF (0.1 eq.) was added into the reaction mixture and stirred for 1h. Solvent was removed under vacuum. To the dried reaction mixture, toluene, aniline **204** and molecular sieve were added sequentially. Reaction was put into a pre-heated oil bath at 80°C and stirred for 12h. The reaction was cooled

to room temperature and was filtered through a filter paper to remove the molecular sieve. Filtrate was dried under reduced pressure. Compound **226** were purified by silica gel chromatography using petroleum ether and acetone (silica gel, 10:1 to 5:1 v:v).



Isolated yield: 89% (yellow solid) (silica gel, 1:5 = acetone:petroleum ether, R_F = 0.1)

$^1\text{H NMR}$ (500 MHz, CDCl_3) δ 8.27 – 8.06 (m, 2H), 7.37 (d, J = 7.3 Hz, 1H), 7.23 – 7.13 (m, 1H), 7.03 – 6.94 (m, 1H), 6.91 (dd, J = 8.3, 1.9 Hz, 1H), 6.83 (d, J = 8.4 Hz, 1H), 6.57 (s, 2H), 5.21 (d, J = 11.6 Hz, 1H), 4.60 (d, J = 10.4 Hz, 1H), 4.28 – 4.21 (m, 1H), 3.92 (s, 3H), 3.87 (s, 3H), 3.78 (s, 6H), 3.70 (s, 3H), 3.34 (s, 3H), 3.32 (s, 3H), 2.02 ppm (s, 3H).

$^{13}\text{C NMR}$ (126 MHz, CDCl_3) δ 169.64, 169.18, 152.93, 148.77, 148.54, 137.32, 133.53, 131.51, 129.45, 129.18, 124.45, 124.22, 119.84, 119.27, 111.15, 110.76, 105.79, 62.42, 60.79, 56.13, 55.92, 55.90, 52.74, 52.32, 47.38, 45.11, 44.03, 19.02 ppm.

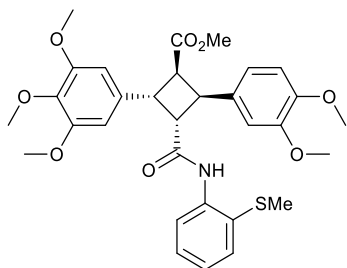
HR-MS calculated for $\text{C}_{33}\text{H}_{38}\text{NO}_{10}\text{S}$: m/z (%): 640.2211 $[\text{M}+\text{H}]^+$, found: 640.2212.

IR ν_{max} (cm^{-1}) 2397, 2344, 2310, 2172, 2154, 2141, 2023, 2007, 1978, 1725, 1685, 1587, 1509, 1429, 1236, 1120, 1026.

rac-Methyl (1*S*,2*S*,3*S*,4*S*)-2-(3,4-dimethoxyphenyl)-3-((2-(methylthio)phenyl)carbamoyl)-4-(3,4,5-trimethoxyphenyl)cyclobutane-1-carboxylate (Compound **227**)

Compound **226** (13mg, 0.02mmol, 1 eq.) in DMSO (1 mL) was added lithium chloride (9 mg, 0.21 mmol, 10 eq.) and water (4ml, 0.021 mmol, 10 eq.). The reaction vial was purged with argon gas for 10 seconds before closing tightly with the cap. The reaction vial was put into the pre-heated metal block at 130°C for 6h with vigorous stirring. After 6h, the reaction vial was cooled down to the room temperature. Reaction mixture was added 2ml of water and was extracted with 3 ml of ethyl acetate (3 ml x 3 times). The combined organic phase was dried by sodium sulfate and the solvent was evaporated to give a reaction mixture as yellow, crude

oil. This mixture was subjected to flash chromatography (silica gel, petroleum ether: acetone from 10:1 to 3:2 v:v) and gave compound **227** in 65% yield.



Isolated yield: 65% (yellow foam) (silica gel, 1:5 = acetone:petroleum ether, $R_F = 0.1$)

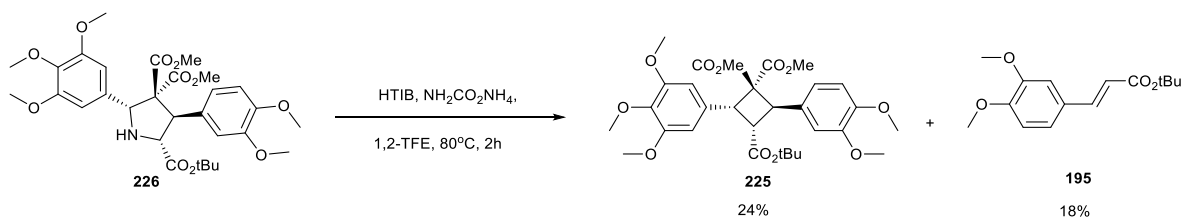
$^1\text{H NMR}$ (700 MHz, CD_2Cl_2) δ 8.17 – 8.03 (m, 1H), 7.37 (dd, $J = 7.7, 1.5$ Hz, 1H), 7.19 (d, $J = 1.3$ Hz, 1H), 7.00 (t, $J = 7.5$ Hz, 1H), 6.97 – 6.93 (m, 1H), 7.02 – 6.70 (m, 2H), 6.58 (s, 2H), 4.53 (dd, $J = 10.8, 6.3$ Hz, 1H), 4.42 (t, $J = 9.1, 9.1$ Hz, 1H), 3.94 (dd, $J = 10.9, 7.6$ Hz, 1H), 3.91 – 3.88 (m, 1H), 3.87 (s, 3H), 3.83 (s, 3H), 3.75 (s, 6H), 3.59 (s, 3H), 3.38 (s, 3H), 2.15 ppm (s, 3H).

$^{13}\text{C NMR}$ (176 MHz, CD_2Cl_2) δ 172.89, 169.93 (d, $J = 15.0$ Hz), 153.84, 149.60, 148.98, 137.89, 134.89, 133.38, 132.19, 129.09, 125.75, 125.65, 124.70, 120.47, 120.39, 119.93, 112.22, 111.84, 105.56, 60.85, 56.57, 56.46, 56.32, 52.00, 50.12, 47.95, 43.19, 41.57 (d, $J = 2.7$ Hz), 19.20 ppm.

HR-MS calculated for $\text{C}_{31}\text{H}_{35}\text{NO}_8\text{S}$: m/z (%): 582.2156 $[\text{M}+\text{H}]^+$, found: 582.2170.

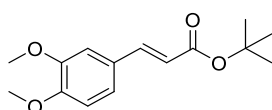
IR ν_{max} (cm^{-1}) 1729, 1681, 1587, 1511, 1462, 1334, 1250, 1124, 1026.

5.91 Observation of olefinic side products using general procedure C



Scheme 5. Olefinic side product observed when standard condition using HTIB was applied.

tert-Butyl (*E*)-3-(3,4-dimethoxyphenyl)acrylate (Compound **195**)



Using general procedure C

Isolated yield: 18% (colorless oil) (silica gel, 1:20 = acetone:petroleum ether, $R_F = 0.3$)

(silica gel, 1:100 acetone:petroleum ether to 1:50 = acetone:petroleum ether)

$^1\text{H NMR}$ (500 MHz, CDCl_3) δ 7.53 (d, $J = 15.9$ Hz, 1H), 7.16 – 6.99 (m, 2H), 6.85 (d, $J = 8.3$ Hz, 1H), 6.24 (d, $J = 15.9$ Hz, 1H), 3.91 (s, 6H), 1.53 ppm (s, 9H).

$^{13}\text{C NMR}$ (126 MHz, CDCl_3) δ 166.61, 150.82, 149.13, 143.50, 127.64, 122.47, 117.90, 110.95, 109.38, 80.35, 55.96, 55.87, 28.25 ppm.

HR-MS calculated for $\text{C}_{15}\text{H}_{21}\text{O}_4$: m/z (%): 265.1434 $[\text{M}+\text{H}]^+$, found: 265.1429.

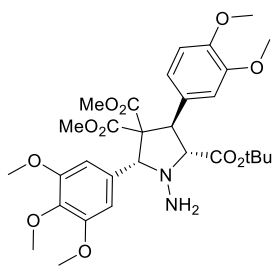
IR ν_{max} (cm^{-1}) 1702, 1632, 1599, 1513, 1465, 1421, 1367, 1308, 1264, 1138, 1025, 980, 912, 847.

5.92 Synthesis of *N*-aminopyrrolidine

Synthesis of compound **231**

The condition used below was reported by Kurti and co-workers originally for organocatalytic nitrogen transfer to unactivated olefins via transient oxaziridines. ¹⁵⁵

HOSA (1.5 equiv.), Cs₂CO₃ (3.0 equiv.), HFIP (5 mL), ethyl trifluoroacetate (20 mol%) and the pyrrolidine were sequentially added into the reaction vial. The resulting mixture was stirred at room temperature for 12 h, then quenched with saturated aqueous Na₂CO₃ and extracted with CH₂Cl₂. The combined organic layer was dried over anhydrous Na₂SO₄, filtered and concentrated under reduced pressure. The residue was purified by flash column chromatography using ethyl acetate and petroleum ether (2:1 v:v) to afford the corresponding product.



Isolated yield: 59% (white solid)

¹H NMR (500 MHz, CD₂Cl₂) δ 6.79 (s, 2H), 6.78 (s, 1H), 6.68 (s, 2H), 5.33 (s, 1H), 4.59 (s, 1H), 4.38 (d, *J* = 11.1 Hz, 1H), 3.84 (s, 6H), 3.81 (s, 3H), 3.80 (s, 3H), 3.74 (s, 3H), 3.70 (d, *J* = 11.1 Hz, 1H), 3.20 (s, 3H), 3.12 (s, 3H), 1.27 (s, 9H).

¹³C NMR (126 MHz, CD₂Cl₂) δ 170.73, 170.45, 169.37, 153.61, 149.22, 149.14, 138.21, 134.92, 129.06, 121.73, 113.22, 111.38, 81.55, 77.95, 74.15, 69.32, 60.91, 56.60, 56.33, 56.24, 52.75, 52.58, 51.63, 28.16.

ESI-MS calculated for C₃₀ H₄₁ O₁₁ N₂: *m/z* (%): 605.2705 [M+H]⁺, found: 605.2722.

5.10 X-ray diffraction (XRD) analysis

The crystal structures of compounds of **171**, **189**, **192**, **195**, **197**, **167** and **199** was determined using the *Bruker D8 Venture* four-circle diffractometer equipped with a *PHOTON II* CPAD detector by *Bruker AXS GmbH*. The X-ray radiation was generated by the *I μ S* microfocus source Mo ($\lambda = 0.71073 \text{ \AA}$) from *Incoatec GmbH* equipped with HELIOS mirror optics and a single-hole collimator by *Bruker AXS GmbH*. The selected single crystal of **171**, **189**, **192**, **195**, **197**, **167** and **199** were covered with an inert oil (perfluoropolyalkyl ether) and mounted on the *MicroMount* from *MiTeGen*. The APEX 3 Suite (v.2019.1-0) software integrated with SAINT (integration) and SADABS (adsorption correction) programs by *Bruker AXS GmbH* were used for data collection. The processing and finalization of the crystal structure were performed using the Olex2 program.¹⁵⁶ The crystal structures were solved by the ShelXT¹⁵⁷ structure solution program using the Intrinsic Phasing option, which were further refined by the ShelXL¹⁵⁸ refinement package using Least Squares minimization. The non-hydrogen atoms were anisotropically refined. The C-bound H atoms were placed in geometrically calculated positions, and a fixed isotropic displacement parameter was assigned to each atom according to the riding-model: C_{sp3}-H = 0.95–1.00 \AA with $U_{\text{iso}}(\text{H}) = 1.5U_{\text{eq}}(\text{CH}_3)$ and $1.2U_{\text{eq}}(\text{CH}_2, \text{CH})$ for other hydrogen atoms. The N-bound hydrogen atoms were located on the Difference-Fourier-Map and refined independently in every structure. The crystallographic data for the structures of **171**, **189**, **192**, **195**, **197**, **167** and **199** has been published as supplementary publication number 2080159 (**B1484**), 2080166 (**B1681**), 2080174 (**B1692**), 2080185 (**B1808**), 2080194 (**B1832**), 2080203 (**B1956**) and 2080204 (**B2074**) in the Cambridge Crystallographic Data Centre. A copy of these data can be obtained for free by applying to CCDC, 12 Union Road, Cambridge CB2 IEZ, UK, fax: 144-(0)1223-336033 or e-mail: deposit@ccdc.cam.ac.uk.

X-ray structure of compound **167** (CCDC: 2080159)

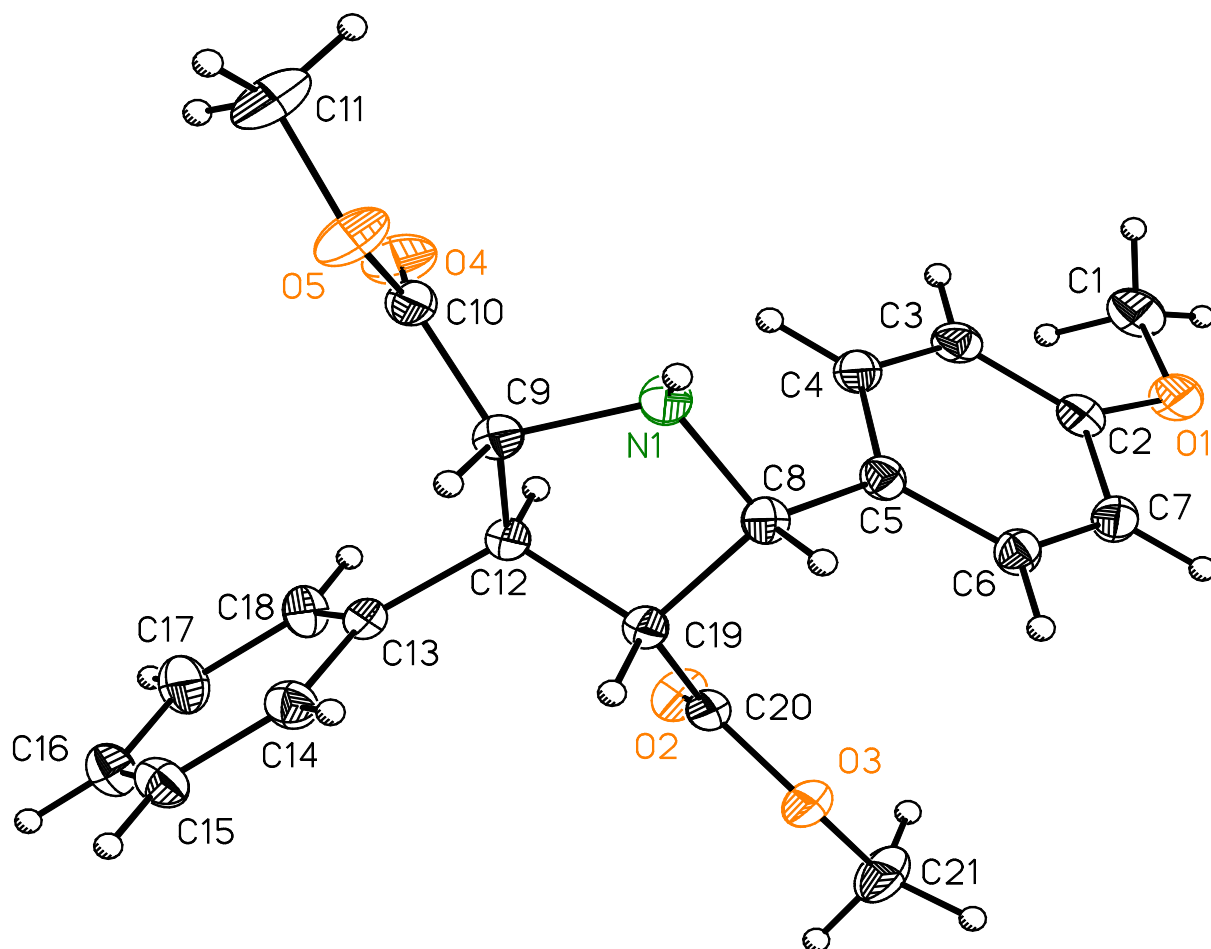
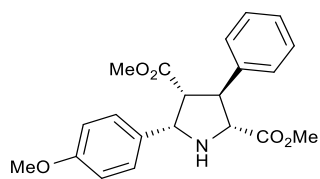


Figure S1 Ortep plot of the molecular structure in the crystal of compound **167** (**B1484**).¹⁵⁹ The displacement ellipsoids are drawn at the 50% probability level. Co-crystallized solvent has been omitted for clarity.



Compound 167

Table Crystallographic data of compound **167 (B1484)**.

Compound	167 (B1484)
Empirical formula	C ₂₁ H ₂₃ NO ₅
Formula weight	369.40
Temperature/K	100.0
Crystal system	monoclinic
Space group	<i>P</i> 2 ₁ / <i>n</i>
<i>a</i> /Å	5.7105(3)
<i>b</i> /Å	36.9090(18)
<i>c</i> /Å	8.9359(4)
<i>α</i> /°	90
<i>β</i> /°	90.225(2)
<i>γ</i> /°	90
Volume/Å ³	1883.39(16)
<i>Z</i>	4
$\rho_{\text{calc}}/\text{cm}^3$	1.303
μ/mm^{-1}	0.093
F(000)	784.0
Crystal size/mm ³	0.782 × 0.347 × 0.245
Radiation	MoK α ($\lambda = 0.71073$)
2 θ range for data collection/°	5.064 to 61.098
Index ranges	-8 ≤ <i>h</i> ≤ 8, -52 ≤ <i>k</i> ≤ 52, -12 ≤ <i>l</i> ≤ 12
Reflections collected	52374
Independent reflections	5742 [<i>R</i> _{int} = 0.0389, <i>R</i> _{sigma} = 0.0230]
Data/restraints/parameters	5742/0/251
Goodness-of-fit on F ²	1.189
Final <i>R</i> indexes [<i>I</i> >= 2 σ (<i>I</i>)]	<i>R</i> ₁ = 0.0558, <i>wR</i> ₂ = 0.1377
Final <i>R</i> indexes [all data]	<i>R</i> ₁ = 0.0571, <i>wR</i> ₂ = 0.1383
Largest diff. peak/hole / e Å ⁻³	0.53/-0.21
Flack parameter	—

X-ray structure of compound **171** (CCDC: 2080174)

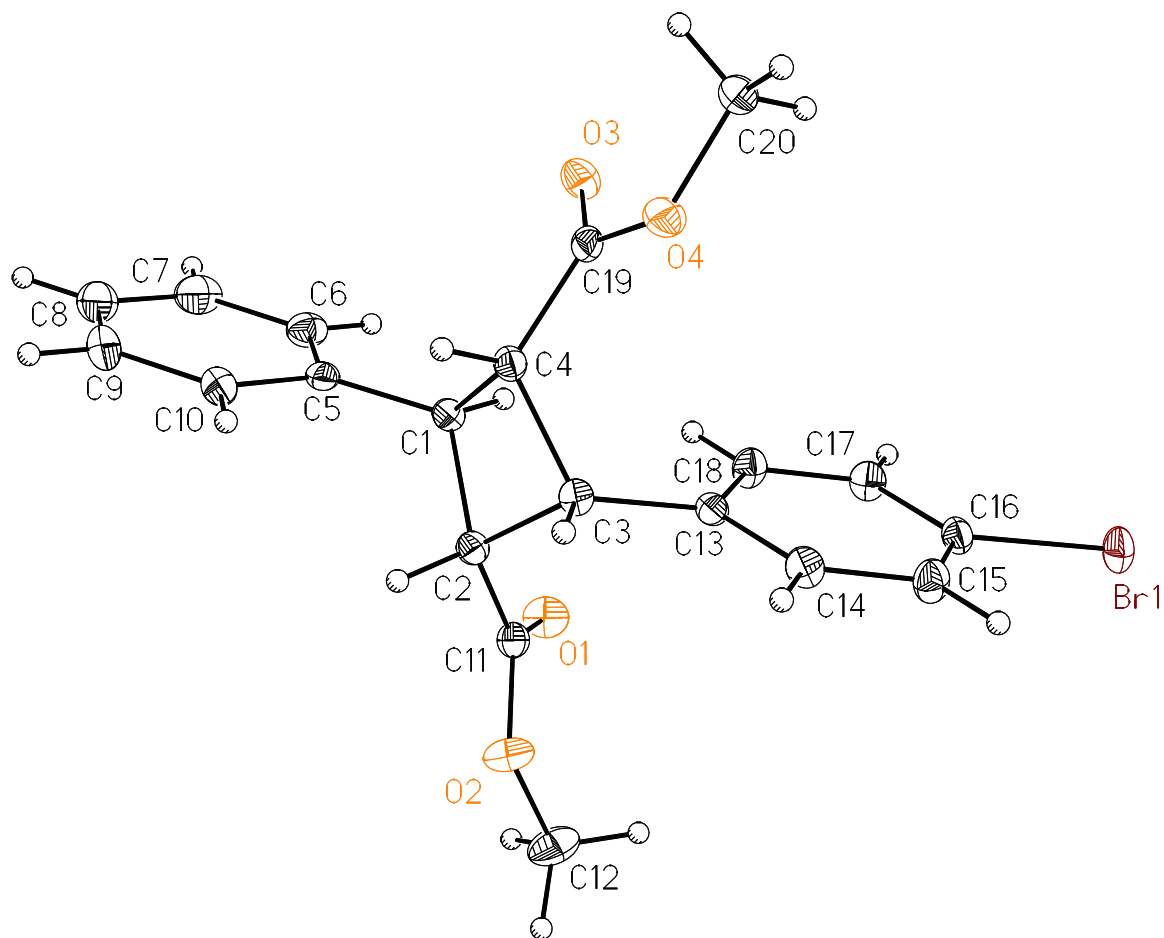
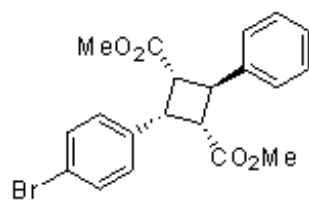


Figure S2 Ortep plot of the molecular structure in the crystal of compound **171 (B1692)**.¹⁵⁹ The displacement ellipsoids are drawn at the 50% probability level.



Compound 171

Table Crystallographic data of compound **171 (B1692)**.

Compound	171 (B1692)
Empirical formula	C ₂₀ H ₁₉ BrO ₄
Formula weight	403.26
Temperature/K	100.0
Crystal system	monoclinic
Space group	<i>P</i> 2 ₁ / <i>n</i>
<i>a</i> /Å	5.683(3)
<i>b</i> /Å	21.449(9)
<i>c</i> /Å	14.809(5)
<i>α</i> /°	90
<i>β</i> /°	97.565(16)
<i>γ</i> /°	90
Volume/Å ³	1789.4(14)
<i>Z</i>	4
$\rho_{\text{calc}}/\text{cm}^3$	1.497
μ/mm^{-1}	2.319
F(000)	824.0
Crystal size/mm ³	0.336 × 0.082 × 0.066
Radiation	MoK α (λ = 0.71073)
2 θ range for data collection/°	5.55 to 59.996
Index ranges	-7 ≤ <i>h</i> ≤ 7, -30 ≤ <i>k</i> ≤ 30, -20 ≤ <i>l</i> ≤ 20
Reflections collected	52874
Independent reflections	5196 [<i>R</i> _{int} = 0.0397, <i>R</i> _{sigma} = 0.0205]
Data/restraints/parameters	5196/0/228
Goodness-of-fit on F ²	1.037
Final <i>R</i> indexes [<i>I</i> ≥ 2 σ (<i>I</i>)]	<i>R</i> ₁ = 0.0255, <i>wR</i> ₂ = 0.0579
Final <i>R</i> indexes [all data]	<i>R</i> ₁ = 0.0316, <i>wR</i> ₂ = 0.0604
Largest diff. peak/hole / e Å ⁻³	0.48/-0.32
Flack parameter	—

X-ray structure of compound **189** (CCDC: 2080166)

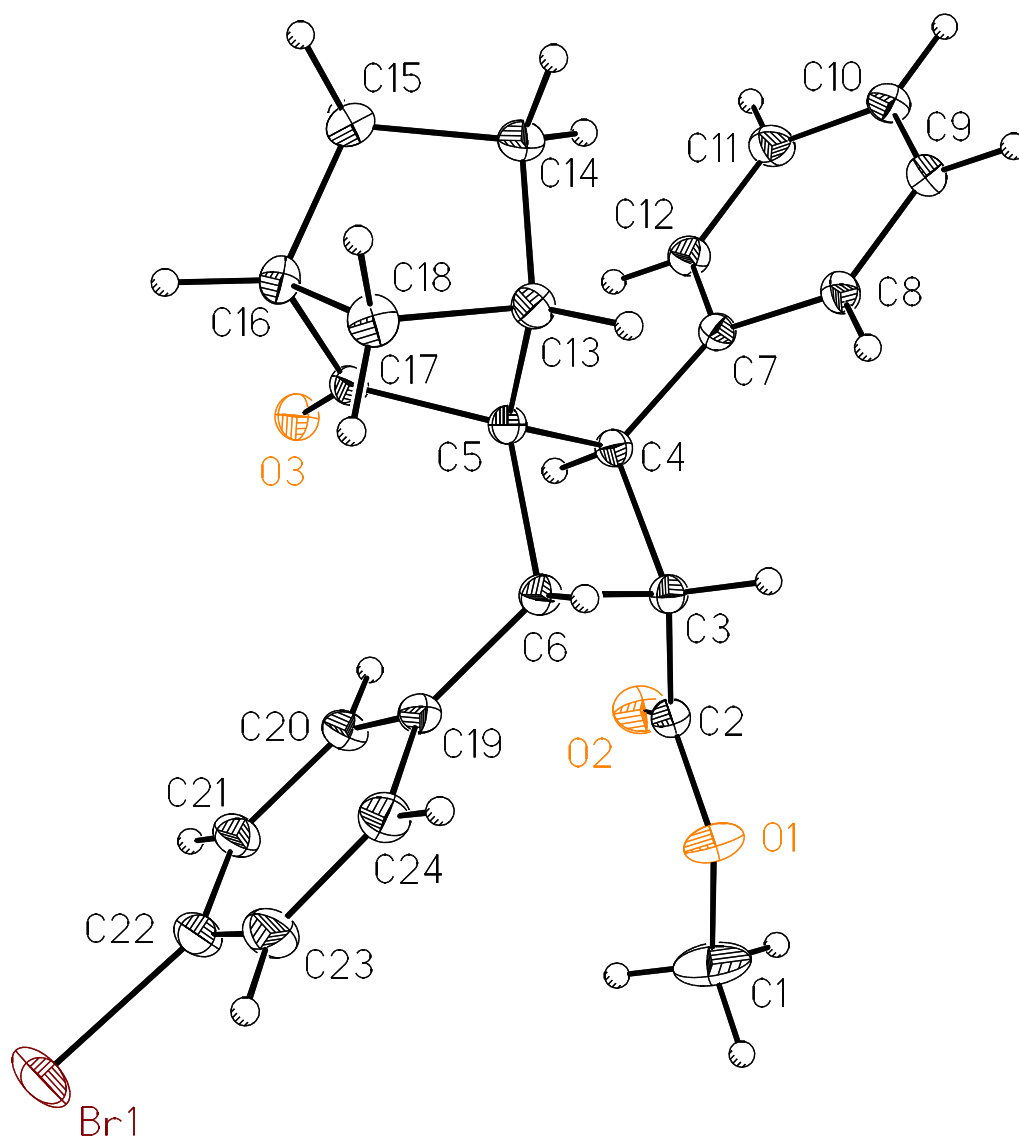
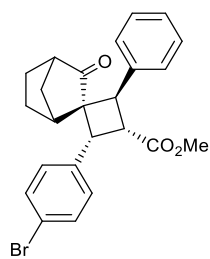


Figure S3 Ortep plot of the molecular structure in the crystal of compound **189(B1681)**. ¹⁵⁹The displacement ellipsoids are drawn at the 50% probability level.



Compound 189

Table Crystallographic data of compound **189 (B1681)**.

Compound	161r(B1681)
Empirical formula	C ₂₄ H ₂₃ BrO ₃
Formula weight	439.33
Temperature/K	100.0
Crystal system	triclinic
Space group	<i>P</i> -1
<i>a</i> /Å	6.1786(4)
<i>b</i> /Å	7.7074(5)
<i>c</i> /Å	22.9571(12)
<i>α</i> /°	84.833(2)
<i>β</i> /°	85.296(2)
<i>γ</i> /°	70.319(2)
Volume/Å ³	1023.63(11)
<i>Z</i>	2
$\rho_{\text{calc}}/\text{cm}^3$	1.425
μ/mm^{-1}	2.030
F(000)	452.0
Crystal size/mm ³	0.433 × 0.294 × 0.092
Radiation	MoK α (λ = 0.71073)
2 θ range for data collection/°	5.354 to 69.998
Index ranges	-9 ≤ <i>h</i> ≤ 9, -12 ≤ <i>k</i> ≤ 12, -37 ≤ <i>l</i> ≤ 37
Reflections collected	106331
Independent reflections	9005 [<i>R</i> _{int} = 0.0361, <i>R</i> _{sigma} = 0.0134]
Data/restraints/parameters	9005/0/254
Goodness-of-fit on F ²	1.031
Final <i>R</i> indexes [<i>I</i> >= 2 σ (<i>I</i>)]	<i>R</i> ₁ = 0.0292, <i>wR</i> ₂ = 0.0783
Final <i>R</i> indexes [all data]	<i>R</i> ₁ = 0.0323, <i>wR</i> ₂ = 0.0801
Largest diff. peak/hole / e Å ⁻³	0.92/-0.84
Flack parameter	—

X-ray structure of compound **192** (CCDC: 2080203)

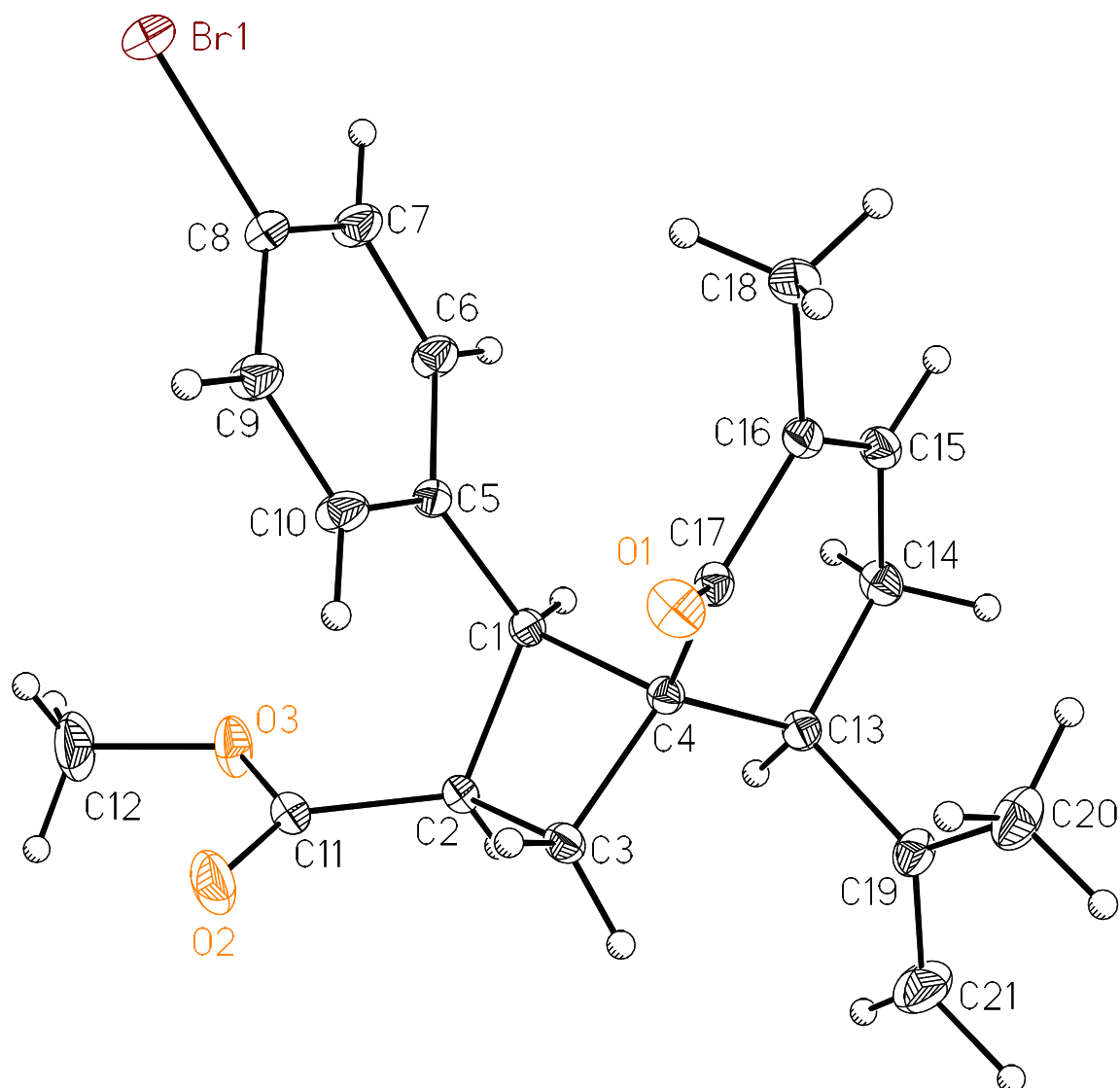
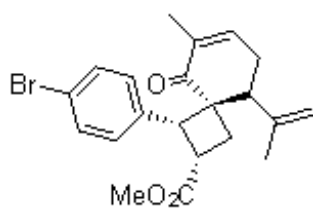


Figure S4 Ortep plot of the molecular structure in the crystal of compound **192 (B1956)**.¹⁵⁹ The displacement ellipsoids are drawn at the 50% probability level. Co-crystallized solvent has been omitted for clarity.



Compound **192**

Table Crystallographic data of compound **192 (B1956)**.

Compound	192 (B1956)
Empirical formula	C ₂₁ H ₂₃ BrO ₃
Formula weight	403.30
Temperature/K	100.0
Crystal system	trigonal
Space group	<i>P</i> 3 ₁
<i>a</i> /Å	10.3555(5)
<i>b</i> /Å	10.3555(5)
<i>c</i> /Å	15.2451(9)
<i>α</i> /°	90
<i>β</i> /°	90
<i>γ</i> /°	120
Volume/Å ³	1415.80(16)
<i>Z</i>	3
$\rho_{\text{calc}}/\text{cm}^3$	1.419
μ/mm^{-1}	2.194
F(000)	624.0
Crystal size/mm ³	0.334 × 0.396 × 0.312
Radiation	MoK α (λ = 0.71073)
2 Θ range for data collection/°	4.542 to 72.674
Index ranges	-17 ≤ <i>h</i> ≤ 17, -17 ≤ <i>k</i> ≤ 17, -25 ≤ <i>l</i> ≤ 25
Reflections collected	257036
Independent reflections	9159 [<i>R</i> _{int} = 0.0515 <i>R</i> _{sigma} = 0.0146]
Data/restraints/parameters	9159/1/238
Goodness-of-fit on F ²	1.038
Final <i>R</i> indexes [<i>I</i> ≥ 2 σ (<i>I</i>)]	<i>R</i> ₁ = 0.0175, <i>wR</i> ₂ = 0.0468
Final <i>R</i> indexes [all data]	<i>R</i> ₁ = 0.0184, <i>wR</i> ₂ = 0.0472
Largest diff. peak/hole / e Å ⁻³	0.34/-0.23
Flack parameter	-0.0029(13)

X-ray structure of compound **195** (CCDC: 2080185)

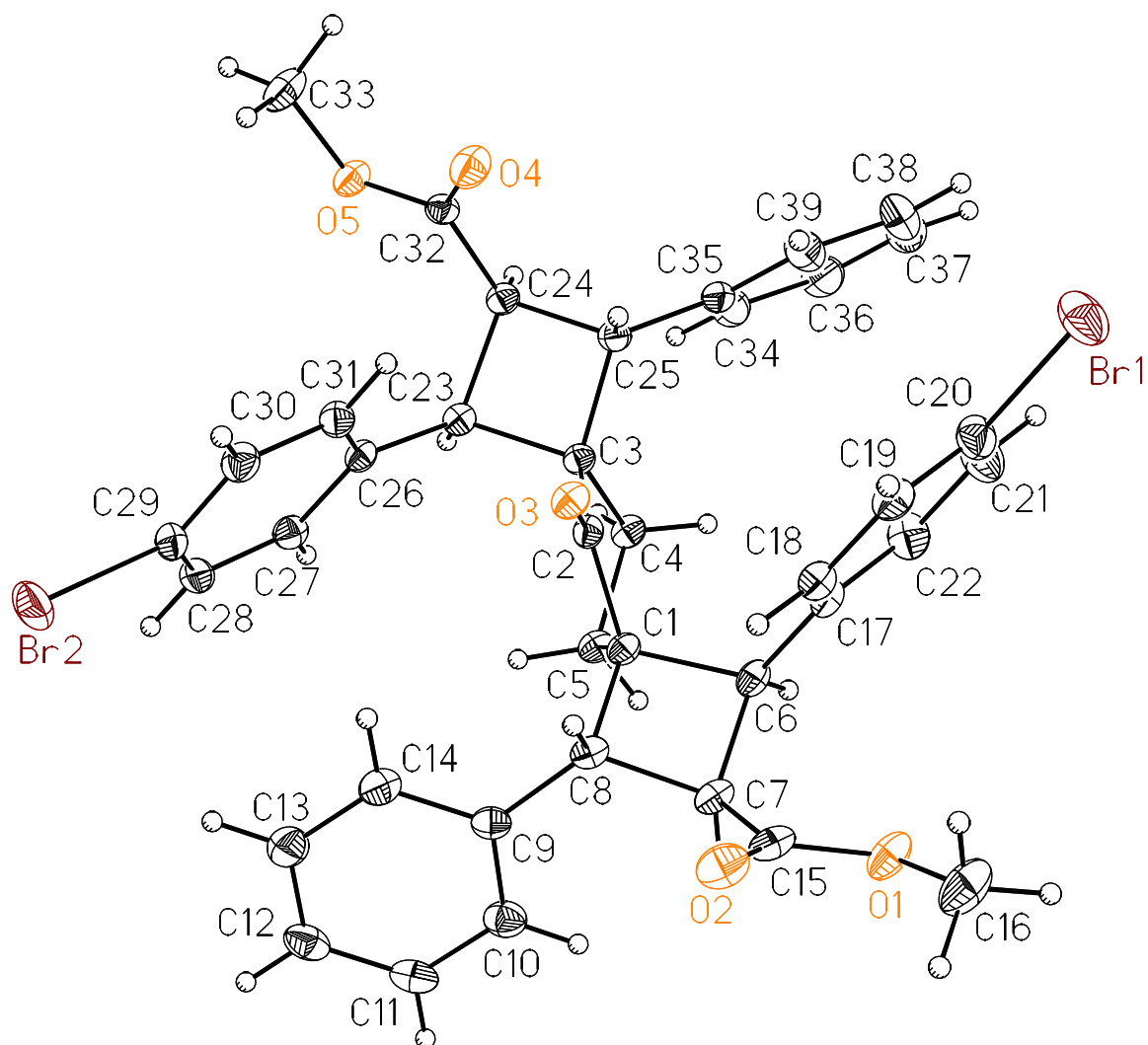
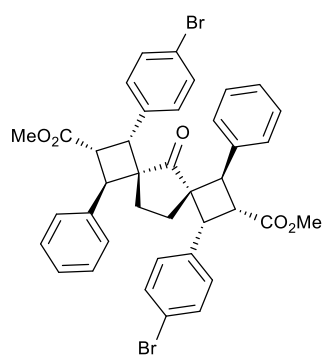


Figure S5 Ortep plot of the molecular structure in the crystal of compound **195 (B1808)**.¹⁵⁹ The displacement ellipsoids are drawn at the 50% probability level.



Compound 195

Table Crystallographic data of compound **195 (B1808)**.

Compound	195 (B1808)
Empirical formula	C ₃₉ H ₃₄ Br ₂ O ₅
Formula weight	742.48
Temperature/K	100.0
Crystal system	monoclinic
Space group	<i>P</i> 2 ₁ / <i>c</i>
<i>a</i> /Å	11.456(16)
<i>b</i> /Å	23.373(18)
<i>c</i> /Å	13.367(11)
<i>α</i> /°	90
<i>β</i> /°	112.38(4)
<i>γ</i> /°	90
Volume/Å ³	3310(6)
<i>Z</i>	4
$\rho_{\text{calc}}/\text{cm}^3$	1.490
μ/mm^{-1}	2.493
F(000)	1512.0
Crystal size/mm ³	0.514 × 0.129 × 0.035
Radiation	MoK α (λ = 0.71073)
2 Θ range for data collection/°	4.222 to 61.16
Index ranges	-16 ≤ <i>h</i> ≤ 16, -32 ≤ <i>k</i> ≤ 33, -19 ≤ <i>l</i> ≤ 19
Reflections collected	105668
Independent reflections	10155 [<i>R</i> _{int} = 0.0461, <i>R</i> _{sigma} = 0.0247]
Data/restraints/parameters	10155/0/417
Goodness-of-fit on F ²	1.023
Final <i>R</i> indexes [<i>I</i> ≥ 2 σ (<i>I</i>)]	<i>R</i> ₁ = 0.0307, <i>wR</i> ₂ = 0.0691
Final <i>R</i> indexes [all data]	<i>R</i> ₁ = 0.0456, <i>wR</i> ₂ = 0.0747
Largest diff. peak/hole / e Å ⁻³	0.73/-1.04
Flack parameter	—

X-ray structure of compound **197** (CCDC: 2080204)

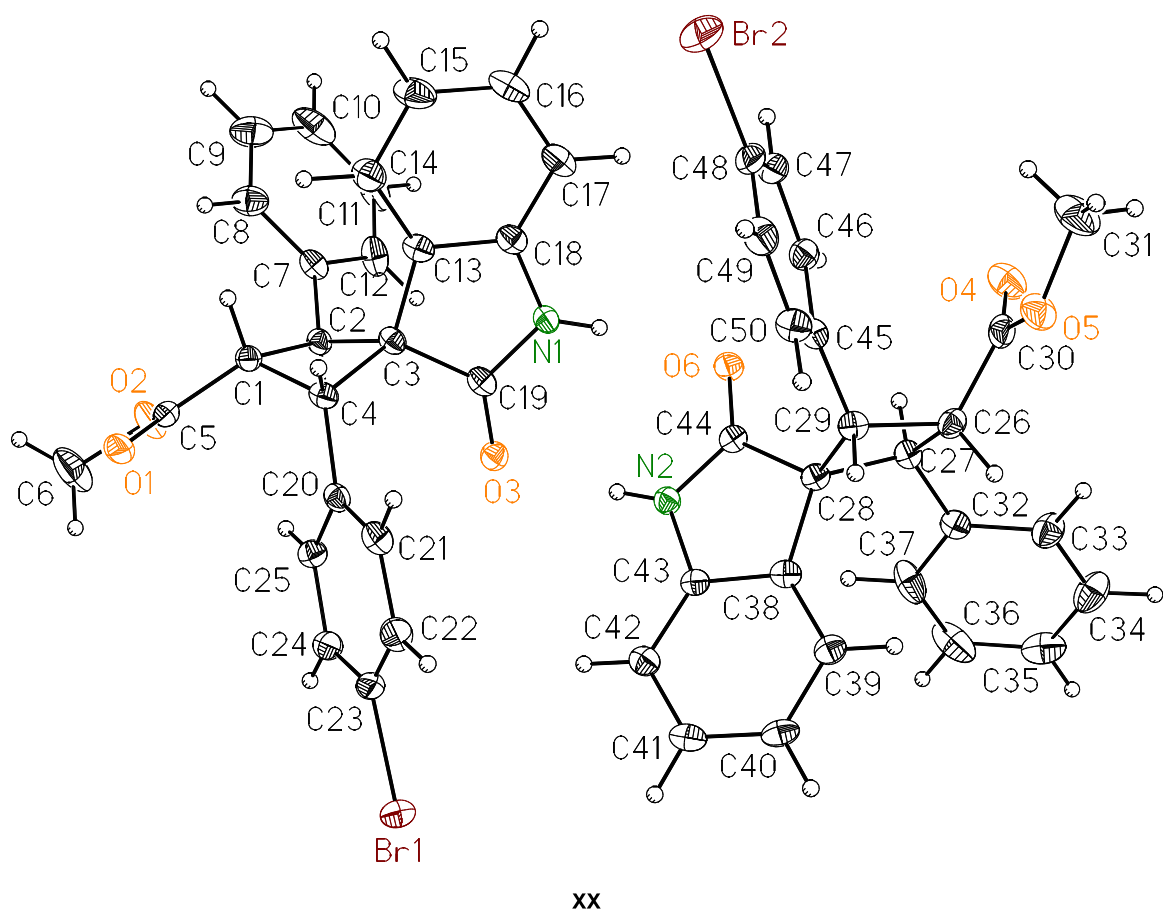
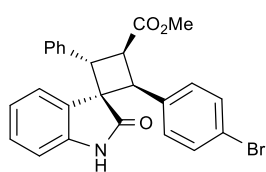


Figure S6 Ortep plot of the molecular structure in the crystal of compound **197 (B2074)**.¹⁵⁹The displacement ellipsoids are drawn at the 50% probability level. Co-crystallized solvent has been omitted for clarity.



Compound 197

Table Crystallographic data of compound **197 (B2074)**.

Compound	197 (B2074)
Empirical formula	C ₂₅ H ₂₀ BrNO ₃
Formula weight	462.33
Temperature/K	100.0
Crystal system	orthorhombic
Space group	<i>P</i> 2 ₁ 2 ₁ 2 ₁
<i>a</i> /Å	11.150(3)
<i>b</i> /Å	16.942(8)
<i>c</i> /Å	22.754(5)
α /°	90
β /°	90
γ /°	90
Volume/Å ³	4298(2)
<i>Z</i>	8
ρ_{calc} /cm ³	1.429
μ /mm ⁻¹	1.939
F(000)	1888.0
Crystal size/mm ³	0.845 × 0.053 × 0.027
Radiation	MoK α (λ = 0.71073)
2 Θ range for data collection/°	4.068 to 60.992
Index ranges	-15 ≤ <i>h</i> ≤ 15, -24 ≤ <i>k</i> ≤ 24, -32 ≤ <i>l</i> ≤ 32
Reflections collected	56317
Independent reflections	13094 [<i>R</i> _{int} = 0.0406, <i>R</i> _{sigma} = 0.0374]
Data/restraints/parameters	13094/0/551
Goodness-of-fit on F ²	1.023
Final <i>R</i> indexes [<i>I</i> ≥ 2 σ (<i>I</i>)]	<i>R</i> ₁ = 0.0322, <i>wR</i> ₂ = 0.0654
Final <i>R</i> indexes [all data]	<i>R</i> ₁ = 0.0440, <i>wR</i> ₂ = 0.0695
Largest diff. peak/hole / e Å ⁻³	0.69/-0.59
Flack parameter	-0.007(2)

X-ray structure of compound **199** (CCDC: 2080194)

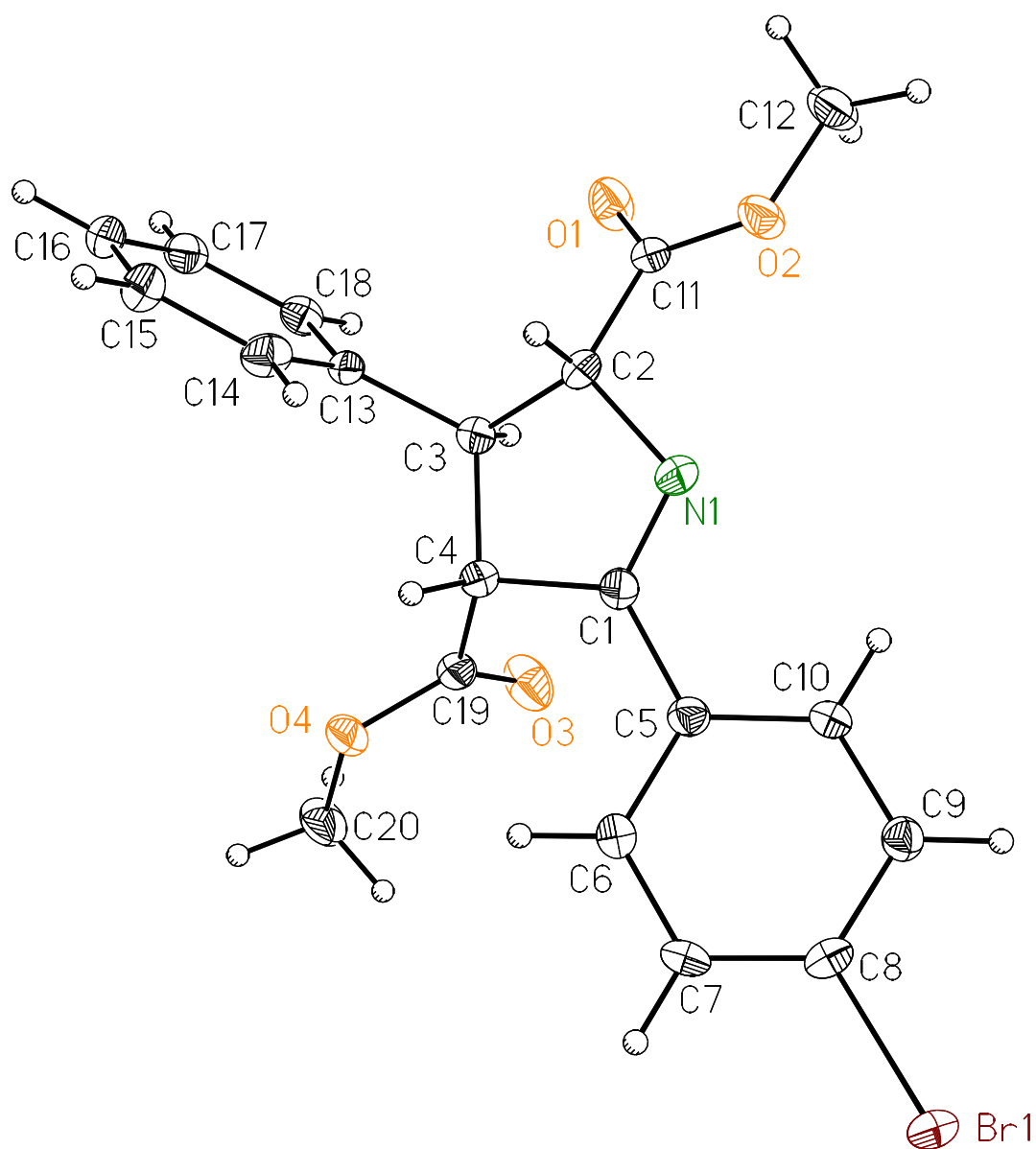
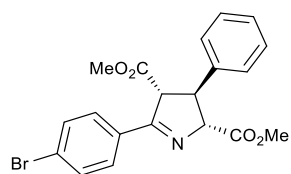


Figure S7 Ortep plot of the molecular structure in the crystal of compound **199** (**B1832**).¹⁵⁹ The displacement ellipsoids are drawn at the 50% probability level. Co-crystallized solvent has been omitted for clarity.



Compound **199**

Table Crystallographic data of compound **199 (B1832)**.

Compound	199 (B1832)
Empirical formula	C ₂₀ H ₁₈ BrNO ₄
Formula weight	416.26
Temperature/K	100.0
Crystal system	monoclinic
Space group	<i>Pn</i>
<i>a</i> /Å	5.8234(8)
<i>b</i> /Å	9.4036(19)
<i>c</i> /Å	16.355(3)
<i>α</i> /°	90
<i>β</i> /°	96.446(6)
<i>γ</i> /°	90
Volume/Å ³	890.0(3)
<i>Z</i>	2
ρ_{calc} /cm ³	1.553
μ /mm ⁻¹	2.335
F(000)	424.0
Crystal size/mm ³	0.519 × 0.057 × 0.048
Radiation	MoK α (λ = 0.71073)
2 Θ range for data collection/°	4.332 to 55.012
Index ranges	-7 ≤ <i>h</i> ≤ 7, -12 ≤ <i>k</i> ≤ 10, -21 ≤ <i>l</i> ≤ 21
Reflections collected	11658
Independent reflections	4093 [<i>R</i> _{int} = 0.0408, <i>R</i> _{sigma} = 0.0485]
Data/restraints/parameters	4093/2/237
Goodness-of-fit on F ²	1.039
Final <i>R</i> indexes [<i>I</i> ≥ 2 σ (<i>I</i>)]	<i>R</i> ₁ = 0.0324, <i>wR</i> ₂ = 0.0598
Final <i>R</i> indexes [all data]	<i>R</i> ₁ = 0.0392, <i>wR</i> ₂ = 0.0627
Largest diff. peak/hole / e Å ⁻³	0.32/-0.33
Flack parameter	0.009(5)

X-ray structure of compound **163**

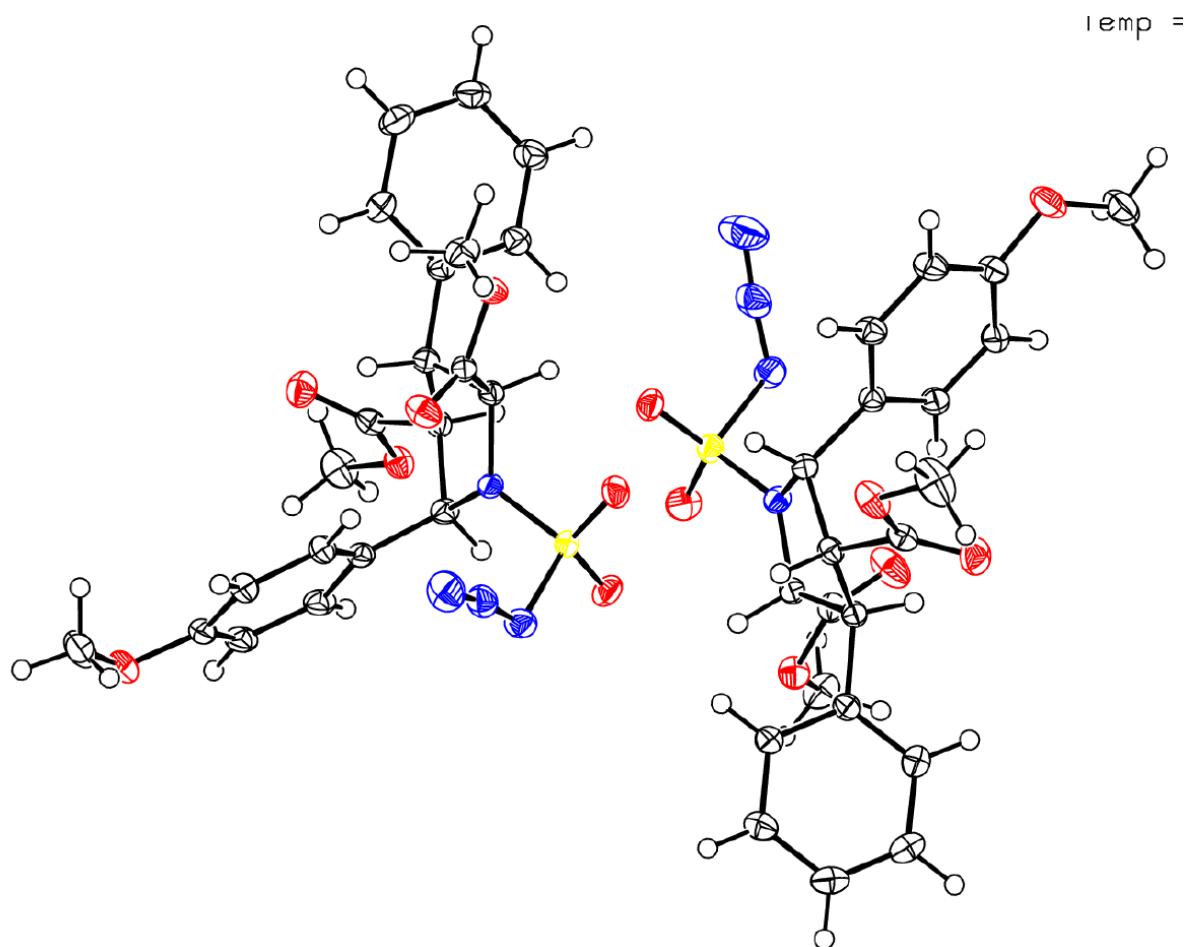
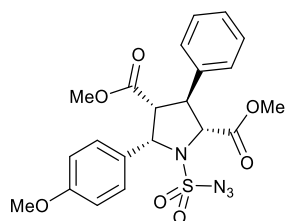


Figure S8 Ortep plot of the molecular structure in the crystal of compound **163**.¹⁵⁹ The displacement ellipsoids are drawn at the 50% probability level. Co-crystallized solvent has been omitted for clarity.



Compound **163**

Table Crystallographic data of compound **163 (C0109)**.

Compound	163 (C0109)
Empirical formula	C ₂₁ H ₂₂ N ₄ O ₇ S
Formula weight	474.48
Temperature/K	100.0
Crystal system	triclinic
Space group	<i>P</i> -1
<i>a</i> /Å	10.8593(10)
<i>b</i> /Å	12.3348(12)
<i>c</i> /Å	18.8823(16)
<i>α</i> /°	85.354(3)
<i>β</i> /°	77.294(3)
<i>γ</i> /°	66.639(3)
Volume/Å ³	2265.0(4)
<i>Z</i>	4
ρ_{calc} /cm ³	1.391
μ /mm ⁻¹	0.193
F(000)	992.0
Crystal size/mm ³	1.585 × 0.462 × 0.325
Radiation	MoK α (λ = 0.71073)
2 θ range for data collection/°	5.22 to 60
Index ranges	-15 ≤ <i>h</i> ≤ 15, , -17 ≤ <i>k</i> ≤ 17, -26 ≤ <i>l</i> ≤ 26
Reflections collected	255327
Independent reflections	13182 [Rint = 0.0474, Rsigma = 0.0161]
Data/restraints/parameters	13182/0/601
Goodness-of-fit on F ²	1.044
Final <i>R</i> indexes [<i>I</i> ≥ 2 σ (<i>I</i>)]	<i>R</i> ₁ = 0.0389, <i>wR</i> ₂ = 0.1048
Final <i>R</i> indexes [all data]	<i>R</i> ₁ = 0.0434, <i>wR</i> ₂ = 0.1091
Largest diff. peak/hole / e Å ⁻³	0.97/-0.51

X-ray structure of compound **169**

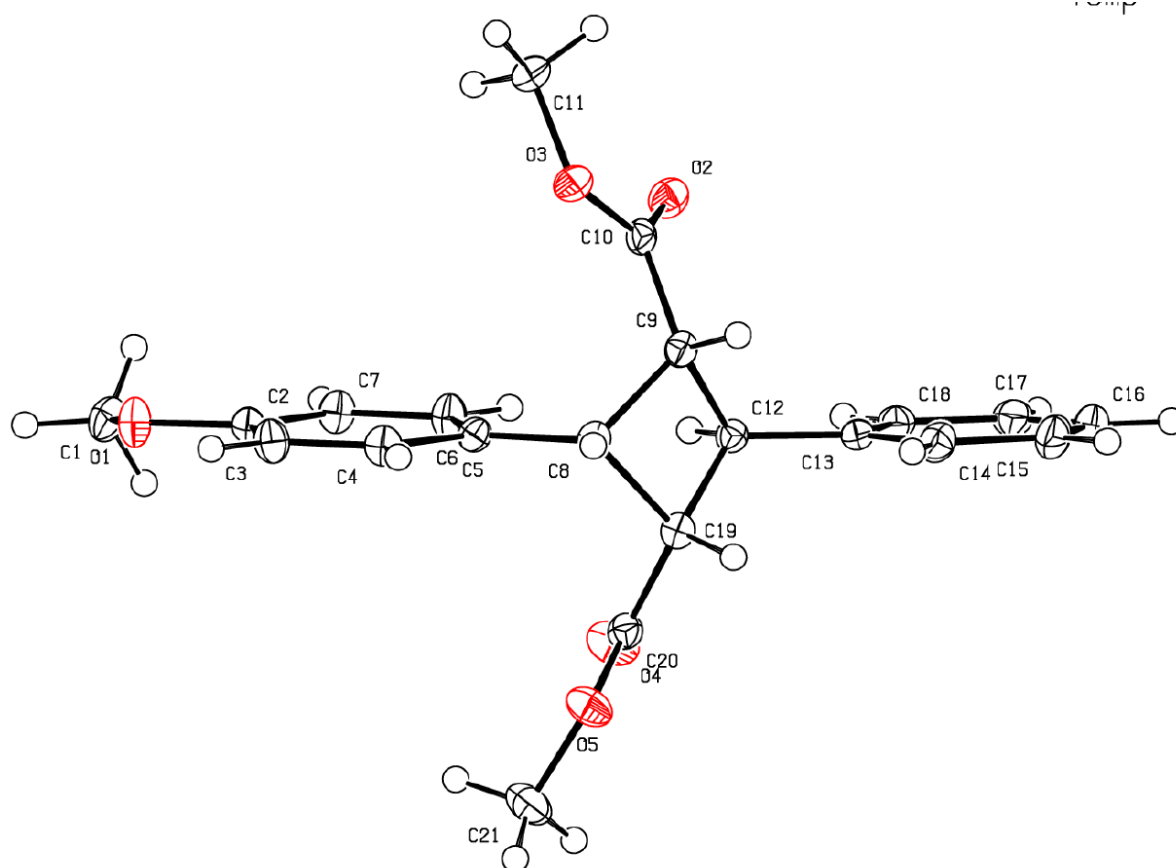
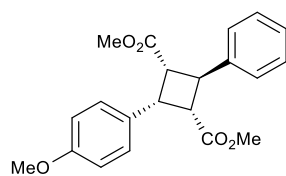


Figure S9 Ortep plot of the molecular structure in the crystal of compound **169**.¹⁵⁹ The displacement ellipsoids are drawn at the 50% probability level. Co-crystallized solvent has been omitted for clarity.



Compound 169

Table Crystallographic data of compound **163 (C0121)**.

Compound	163 (C0121)
Empirical formula	C ₂₁ H ₂₂ O ₅
Formula weight	354.38
Temperature/K	99.99
Crystal system	monoclinic
Space group	<i>P2₁/n</i>
<i>a</i> /Å	5.9332(10)
<i>b</i> /Å	21.251(5)
<i>c</i> /Å	14.580(4)
<i>α</i> /°	90
<i>β</i> /°	96.559(5)
<i>γ</i> /°	90
Volume/Å ³	1826.3(7)
Z	4
ρ _{calc} /cm ³	1.289
μ/mm ⁻¹	0.091
F(000)	752
Crystal size/mm ³	0.993 × 0.112 × 0.086
Radiation	MoKα (λ = 0.71073)
2θ range for data collection/°	5.626 to 58
Index ranges	-7 ≤ h ≤ 8, -28 ≤ k ≤ 28, -19 ≤ l ≤ 19
Reflections collected	29466
Independent reflections	4810 [<i>R</i> _{int} = 0.0329, <i>R</i> _{sigma} = 0.0217]
Data/restraints/parameters	4810/0/239
Goodness-of-fit on F ²	1.034
Final <i>R</i> indexes [<i>I</i> ≥ 2σ (<i>I</i>)]	<i>R</i> ₁ = 0.0366, <i>wR</i> ₂ = 0.0899
Final <i>R</i> indexes [all data]	<i>R</i> ₁ = 0.0447, <i>wR</i> ₂ = 0.0964
Largest diff. peak/hole / e Å ⁻³	0.37/-0.18

6. Reference

1. C. N. Ungarean, E. H. Southgate and D. Sarlah, *Organic & Biomolecular Chemistry*, 2016, **14**, 5454-5467.
2. Z. G. Brill, M. L. Condakes, C. P. Ting and T. J. Maimone, *Chemical Reviews*, 2017, **117**, 11753-11795.
3. V. A. D'yakonov, O. g. A. Trapeznikova, A. de Meijere and U. M. Dzhemilev, *Chemical Reviews*, 2014, **114**, 5775-5814.
4. R. Long, J. Huang, J. X. Gong and Z. Yang, *Natural Product Reports*, 2015, **32**, 1584-1601.
5. M. Buschleb, S. Dorich, S. Hanessian, D. Tao, K. B. Schenthal and L. E. Overman, *Angewandte Chemie-International Edition*, 2016, **55**, 4156-4186.
6. Y. Xu, M. L. Conner and M. K. Brown, *Angewandte Chemie-International Edition*, 2015, **54**, 11918-11928.
7. P. A. Wender, V. A. Verma, T. J. Paxton and T. H. Pillow, *Accounts of Chemical Research*, 2008, **41**, 40-49.
8. R. A. Shenvi, D. P. O'Malley and P. S. Baran, *Accounts of Chemical Research*, 2009, **42**, 530-541.
9. I. S. Young and P. S. Baran, *Nature Chemistry*, 2009, **1**, 193-205.
10. B. M. Trost, *Science*, 1991, **254**, 1471-1477.
11. N. Z. Burns, P. S. Baran and R. W. Hoffmann, *Angewandte Chemie-International Edition*, 2009, **48**, 2854-2867.
12. B. M. Trost, *Science*, 1983, **219**, 245-250.
13. R. W. Hoffmann, *Synthesis-Stuttgart*, 2006, DOI: 10.1055/s-2006-950311, 3531-3541.
14. T. Newhouse, P. S. Baran and R. W. Hoffmann, *Chemical Society Reviews*, 2009, **38**, 3010-3021.
15. T. Gaich and P. S. Baran, *Journal of Organic Chemistry*, 2010, **75**, 4657-4673.
16. T. Bach and J. P. Hehn, *Angewandte Chemie-International Edition*, 2011, **50**, 1000-1045.
17. K. E. O. Ylijoki and J. M. Stryker, *Chemical Reviews*, 2013, **113**, 2244-2266.
18. S. Poplata, A. Troster, Y. Q. Zou and T. Bach, *Chemical Reviews*, 2016, **116**, 9748-9815.
19. X. Y. Liu and Y. Qin, *Natural Product Reports*, 2017, **34**, 1044-1050.
20. Z. S. Yin, Y. He and P. Chiu, *Chemical Society Reviews*, 2018, **47**, 8881-8924.
21. D. J. Edmonds, D. Johnston and D. J. Procter, *Chemical Reviews*, 2004, **104**, 3371-3403.
22. K. Gilmore and I. V. Alabugin, *Chemical Reviews*, 2011, **111**, 6513-6556.
23. N. Krause and C. Winter, *Chemical Reviews*, 2011, **111**, 1994-2009.
24. L. Li, Z. Chen, X. W. Zhang and Y. X. Jia, *Chemical Reviews*, 2018, **118**, 3752-3832.
25. K. Q. Ma, B. S. Martin, X. L. Yin and M. J. Dai, *Natural Product Reports*, 2019, **36**, 174-219.
26. A. Furstner, *Angewandte Chemie-International Edition*, 2013, **52**, 2794-2819.
27. M. R. Becker, R. B. Watson and C. S. Schindler, *Chemical Society Reviews*, 2018, **47**, 7867-7881.
28. C. Lecourt, S. Dhambri, L. Allievi, Y. Sanogo, N. Zeghib, R. Ben Othman, M. I. Lannou, G. Sorin and J. Ardisson, *Natural Product Reports*, 2018, **35**, 105-124.
29. R. A. Yoder and J. N. Johnston, *Chemical Reviews*, 2005, **105**, 4730-4756.
30. K. C. Nicolaou and J. S. Chen, *Chemical Society Reviews*, 2009, **38**, 2993-3009.
31. J. Poulin, C. M. Grise-Bard and L. Barriault, *Chemical Society Reviews*, 2009, **38**, 3092-3101.
32. C. Grondal, M. Jeanty and D. Enders, *Nature Chemistry*, 2010, **2**, 167-178.
33. A. C. Jones, J. A. May, R. Sarpong and B. M. Stoltz, *Angewandte Chemie-International Edition*, 2014, **53**, 2556-2591.
34. M. P. Plesniak, H. M. Huang and D. J. Procter, *Nature Reviews Chemistry*, 2017, **1**.
35. K. Hung, X. R. Hu and T. J. Maimone, *Natural Product Reports*, 2018, **35**, 174-202.
36. P. S. Baran, T. J. Maimone and J. M. Richter, *Nature*, 2007, **446**, 404-408.

37. J. M. Ready, S. E. Reisman, M. Hirata, M. M. Weiss, K. Tamaki, T. V. Ovaska and J. L. Wood, *Angewandte Chemie-International Edition*, 2004, **43**, 1270-1272.
38. S. E. Reisman, J. M. Ready, A. Hasuoka, C. J. Smith and J. L. Wood, *Journal of the American Chemical Society*, 2006, **128**, 1448-1449.
39. S. E. Reisman, J. M. Ready, M. M. Weiss, A. Hasuoka, M. Hirata, K. Tamaki, T. V. Ovaska, C. J. Smith and J. L. Wood, *Journal of the American Chemical Society*, 2008, **130**, 2087-2100.
40. M. Tiffeneau and J. Levy, *Comptes rendus*, 1923, **176**, 312.
41. Z. L. Song, C. A. Fan and Y. Q. Tu, *Chemical Reviews*, 2011, **111**, 7523-7556.
42. B. M. Wang and Y. Q. Tu, *Accounts of Chemical Research*, 2011, **44**, 1207-1222.
43. T. J. Snape, *Chemical Society Reviews*, 2007, **36**, 1823-1842.
44. F. A. Davis, J. C. Towson, D. B. Vashi, R. ThimmaReddy, J. P. McCauley, M. E. Harakal and D. J. Gosciniak, *The Journal of Organic Chemistry*, 1990, **55**, 1254-1261.
45. G. D. Artman, A. W. Grubbs and R. M. Williams, *Journal of the American Chemical Society*, 2007, **129**, 6336-6342.
46. T. J. Greshock, A. W. Grubbs, S. Tsukamoto and R. M. Williams, *Angew Chem Int Edit*, 2007, **46**, 2262-2265.
47. Z. G. Bian, C. C. Marvin and S. F. Martin, *Journal of the American Chemical Society*, 2013, **135**, 10886-10889.
48. Z. G. Bian, C. C. Marvin, M. Pettersson and S. F. Martin, *Journal of the American Chemical Society*, 2014, **136**, 14184-14192.
49. E. V. Mercado-Marin and R. Sarpong, *Chemical Science*, 2015, **6**, 5048-5052.
50. B. X. Zhang, W. F. Zheng, X. Q. Wang, D. Q. Sun and C. Z. Li, *Angewandte Chemie-International Edition*, 2016, **55**, 10435-10438.
51. A. R. Angeles, D. C. Dorn, C. A. Kou, M. A. Moore and S. J. Danishefsky, *Angew Chem Int Edit*, 2007, **46**, 1451-1454.
52. A. R. Angeles, S. P. Waters and S. J. Danishefsky, *Journal of the American Chemical Society*, 2008, **130**, 13765-13770.
53. K. Maruoka, M. Hasegawa, H. Yamamoto, K. Suzuki, M. Shimazaki and G. Tsuchihashi, *Journal of the American Chemical Society*, 1986, **108**, 3827-3829.
54. C. Marti and Erick M. Carreira, *European Journal of Organic Chemistry*, 2003, **2003**, 2209-2219.
55. J. M. Conia and J. P. Barnier, *Tetrahedron Letters*, 1971, **12**, 4981-4984.
56. C. Ebner and E. M. Carreira, *Chemical Reviews*, 2017, **117**, 11651-11679.
57. J. D. Sunderhaus, T. J. McAfoos, J. M. Finefield, H. Kato, S. Y. Li, S. Tsukamoto, D. H. Sherman and R. M. Williams, *Organic Letters*, 2013, **15**, 22-25.
58. M. T. Hovey, D. T. Cohen, D. M. Walden, P. H. Cheong and K. A. Scheidt, *Angew Chem Int Edit*, 2017, **56**, 9864-9867.
59. C. K. Jana, R. Scopelliti and K. Gademann, *Chemistry – A European Journal*, 2010, **16**, 7692-7695.
60. A. J. E. Novak, C. E. Grigglesome and D. Trauner, *Journal of the American Chemical Society*, 2019, **141**, 15515-15518.
61. L. Min, X. H. Lin and C. C. Li, *Journal of the American Chemical Society*, 2019, **141**, 15773-15778.
62. S. A. Snyder and E. J. Corey, *Journal of the American Chemical Society*, 2006, **128**, 740-742.
63. J. Deng, R. Li, Y. Luo, J. Li, S. Zhou, Y. Li, J. Hu and A. Li, *Org Lett*, 2013, **15**, 2022-2025.
64. J. Deng, S. Zhou, W. Zhang, J. Li, R. Li and A. Li, *Journal of the American Chemical Society*, 2014, **136**, 8185-8188.
65. R. Meier and D. Trauner, *Angew Chem Int Edit*, 2016, **55**, 11251-11255.
66. C. Liu, R. Chen, Y. Shen, Z. Liang, Y. Hua and Y. Zhang, *Angew Chem Int Edit*, 2017, **56**, 8187-8190.

67. A. Y. Hong, M. R. Krout, T. Jensen, N. B. Bennett, A. M. Harned and B. M. Stoltz, *Angew Chem Int Edit*, 2011, **50**, 2756-2760.
68. A. Y. Hong and B. M. Stoltz, *Angew Chem Int Edit*, 2012, **51**, 9674-9678.
69. A. D. Rodríguez, J.-G. Shi and S. D. Huang, *The Journal of Organic Chemistry*, 1998, **63**, 4425-4432.
70. Z. Yang, Y. Li and G. Pattenden, *Tetrahedron*, 2010, **66**, 6546-6549.
71. H. Weinstabl, T. Gaich and J. Mulzer, *Organic Letters*, 2012, **14**, 2834-2837.
72. G. Xu, M. Elkin, D. J. Tantillo, T. R. Newhouse and T. J. Maimone, *Angewandte Chemie International Edition*, 2017, **56**, 12498-12502.
73. B. Gaspar and E. M. Carreira, *Angewandte Chemie International Edition*, 2008, **47**, 5758-5760.
74. P. A. Wender, J.-M. Kee and J. M. Warrington, *Science*, 2008, **320**, 649.
75. G. Tong, Z. Liu and P. Li, *Chem*, 2018, **4**, 2944-2954.
76. A. Padwa and H. Ku, *The Journal of Organic Chemistry*, 1980, **45**, 3756-3766.
77. W. Xu, S. Wu, L. Zhou and G. Liang, *Organic Letters*, 2013, **15**, 1978-1981.
78. M. S. Kirillova, M. E. Muratore, R. Dorel and A. M. Echavarren, *Journal of the American Chemical Society*, 2016, **138**, 3671-3674.
79. J. Kim and M. Movassaghi, *Journal of the American Chemical Society*, 2011, **133**, 14940-14943.
80. S. P. Lathrop and M. Movassaghi, *Chemical Science*, 2014, **5**, 333-340.
81. S. P. Lathrop, M. Pompeo, W.-T. T. Chang and M. Movassaghi, *Journal of the American Chemical Society*, 2016, **138**, 7763-7769.
82. P. Lindovska and M. Movassaghi, *Journal of the American Chemical Society*, 2017, **139**, 17590-17596.
83. J. A. Berson, C. D. Duncan and L. R. Corwin, *Journal of the American Chemical Society*, 1974, **96**, 6175-6177.
84. R. D. Little and G. W. Muller, *Journal of the American Chemical Society*, 1979, **101**, 7129-7130.
85. T. Kang, W.-Y. Kim, Y. Yoon, B. G. Kim and H.-Y. Lee, *Journal of the American Chemical Society*, 2011, **133**, 18050-18053.
86. T. Kang, S. B. Song, W.-Y. Kim, B. G. Kim and H.-Y. Lee, *Journal of the American Chemical Society*, 2014, **136**, 10274-10276.
87. H. Lee, T. Kang and H.-Y. Lee, *Angewandte Chemie International Edition*, 2017, **56**, 8254-8257.
88. M. A. Beniddir, L. Evanno, D. Joseph, A. Skiredj and E. Poupon, *Natural Product Reports*, 2016, **33**, 820-842.
89. M. T. Pirnot, Y.-M. Wang and S. L. Buchwald, *Angewandte Chemie International Edition*, 2016, **55**, 48-57.
90. J. Miao, N. G. J. Richards and H. Ge, *Chemical Communications*, 2014, **50**, 9687-9689.
91. J. L. Jat, M. P. Paudyal, H. Gao, Q.-L. Xu, M. Yousufuddin, D. Devarajan, D. H. Ess, L. Kürti and J. R. Falck, *Science*, 2014, **343**, 61.
92. M. P. Paudyal, A. M. Adebessin, S. R. Burt, D. H. Ess, Z. Ma, L. Kürti and J. R. Falck, *Science*, 2016, **353**, 1144.
93. C. G. Espino, K. W. Fiori, M. Kim and J. Du Bois, *Journal of the American Chemical Society*, 2004, **126**, 15378-15379.
94. B. Darses, R. Rodrigues, L. Neuville, M. Mazurais and P. Dauban, *Chemical Communications*, 2017, **53**, 493-508.
95. M. Zenzola, R. Doran, L. Degennaro, R. Luisi and J. A. Bull, *Angew Chem Int Edit*, 2016, **55**, 7203-7207.
96. T. Glachet, H. Marzag, N. Saraiva Rosa, J. F. P. Colell, G. Zhang, W. S. Warren, X. Franck, T. Theis and V. Reboul, *Journal of the American Chemical Society*, 2019, **141**, 13689-13696.

97. C. Iacobucci, S. Reale and F. De Angelis, *Angewandte Chemie International Edition*, 2016, **55**, 2980-2993.
98. K. W. Fiori, C. G. Espino, B. H. Brodsky and J. Du Bois, *Tetrahedron*, 2009, **65**, 3042-3051.
99. N. A. Romero, K. A. Margrey, N. E. Tay and D. A. Nicewicz, *Science*, 2015, **349**, 1326.
100. V. N. Telvekar and K. A. Sasane, *Synlett*, 2010, **2010**, 2778-2780.
101. R. M. Moriarty, M. Sultana and Y.-Y. Ku, *Journal of the Chemical Society, Chemical Communications*, 1985, DOI: 10.1039/C39850000974, 974-975.
102. M. Ciaccia and S. Di Stefano, *Organic & Biomolecular Chemistry*, 2015, **13**, 646-654.
103. R. R. Mondal, S. Khamarui and D. K. Maiti, *Org Lett*, 2017, **19**, 5964-5967.
104. R. D. Richardson, M. Desai and T. Wirth, *Chemistry – A European Journal*, 2007, **13**, 6745-6754.
105. L. Lykke, K. S. Halskov, B. D. Carlsen, V. X. Chen and K. A. Jørgensen, *Journal of the American Chemical Society*, 2013, **135**, 4692-4695.
106. L. P. Conway, A. M. Jadhav, R. A. Homan, W. Li, J. S. Rubiano, R. Hawkins, R. M. Lawrence and C. G. Parker, *Chemical Science*, 2021, **12**, 7839-7847.
107. T. Glachet, H. Marzag, N. S. Rosa, J. F. P. Colell, G. Zhang, W. S. Warren, X. Franck, T. Theis and V. Reboul, *Journal of the American Chemical Society*, 2019, **141**, 13689-13696.
108. J. S. Li, K. Gao, M. Bian and H. F. Ding, *Org Chem Front*, 2020, **7**, 136-154.
109. E. N. Hancock and M. K. Brown, *Chemistry-a European Journal*, 2021, **27**, 565-576.
110. B. Alcaide, P. Almendros and C. Aragoncillo, *Chemical Society Reviews*, 2010, **39**, 783-816.
111. Y. J. Hong and D. J. Tantillo, *Chemical Society Reviews*, 2014, **43**, 5042-5050.
112. K. G. Wen, Y. Y. Peng and X. P. Zeng, *Org Chem Front*, 2020, **7**, 2576-2597.
113. N. Zhao, S. Q. Yin, S. L. Xie, H. Yan, P. Ren, G. Chen, F. Chen and J. Xu, *Angewandte Chemie-International Edition*, 2018, **57**, 3386-3390.
114. C. Shu, A. Noble and V. K. Aggarwal, *Angewandte Chemie-International Edition*, 2019, **58**, 3870-3874.
115. L. M. Chapman, J. C. Beck, L. L. Wu and S. E. Reisman, *Journal of the American Chemical Society*, 2016, **138**, 9803-9806.
116. R. Meier and D. Trauner, *Angewandte Chemie International Edition*, 2016, **55**, 11251-11255.
117. C. Liu, R. Chen, Y. Shen, Z. Liang, Y. Hua and Y. Zhang, *Angewandte Chemie International Edition*, 2017, **56**, 8187-8190.
118. C. G. Overberger, J. G. Lombardino and R. G. Hiskey, *Journal of the American Chemical Society*, 1958, **80**, 3009-3012.
119. H. Takemura, T. Shinmyozu and T. Inazu, *Tetrahedron Letters*, 1988, **29**, 1031-1032.
120. S. E. Denmark, W.-T. T. Chang, K. N. Houk and P. Liu, *The Journal of Organic Chemistry*, 2015, **80**, 313-366.
121. R. L. Hinman and K. L. Hamm, *Journal of the American Chemical Society*, 1959, **81**, 3294-3297.
122. D. M. Lemal and T. W. Rave, *Journal of the American Chemical Society*, 1965, **87**, 393-394.
123. M. G. Horner, M. J. Rudolph, S. Wolff and W. C. Agosta, *Journal of the American Chemical Society*, 1992, **114**, 6034-6037.
124. B. F. Strick, D. A. Mundal and R. J. Thomson, *Journal of the American Chemical Society*, 2011, **133**, 14252-14255.
125. W. D. Hinsberg and P. B. Dervan, *Journal of the American Chemical Society*, 1978, **100**, 1608-1610.
126. P. G. Schultz and P. B. Dervan, *Journal of the American Chemical Society*, 1980, **102**, 878-880.
127. P. G. Schultz and P. B. Dervan, *Journal of the American Chemical Society*, 1981, **103**, 1563-1564.
128. P. G. Schultz and P. B. Dervan, *Journal of the American Chemical Society*, 1982, **104**, 6660-6668.

129. W. D. Hinsberg, P. G. Schultz and P. B. Dervan, *Journal of the American Chemical Society*, 1982, **104**, 766-773.
130. S. H. Kennedy, B. D. Dherange, K. J. Berger and M. D. Levin, *Nature*, 2021, **593**, 223-227.
131. H. Qin, W. Cai, S. Wang, T. Guo, G. Li and H. Lu, *Angewandte Chemie International Edition*, 2021, **n/a**.
132. X. Zou, J. Zou, L. Yang, G. Li and H. Lu, *The Journal of Organic Chemistry*, 2017, **82**, 4677-4688.
133. H. Lu, H. Jiang, L. Wojtas and X. P. Zhang, *Angewandte Chemie International Edition*, 2010, **49**, 10192-10196.
134. S. Chaabouni, J. F. Lohier, A. L. Barthelemy, T. Glachet, E. Anselmi, G. Dagousset, P. Diter, B. Pegot, E. Magnier and V. Reboul, *Chemistry-a European Journal*, 2018, **24**, 17006-17010.
135. M. Zenzola, R. Doran, L. Degennaro, R. Luisi and J. A. Bull, *Angewandte Chemie International Edition*, 2016, **55**, 7203-7207.
136. A. Yoshimura and V. V. Zhdankin, *Chemical Reviews*, 2016, **116**, 3328-3435.
137. P. Hu, H. M. Chi, K. C. DeBacker, X. Gong, J. H. Keim, I. T. Hsu and S. A. Snyder, *Nature*, 2019, **569**, 703-707.
138. W.-X. Wei, Y. Li, Y.-T. Wen, M. Li, X.-S. Li, C.-T. Wang, H.-C. Liu, Y. Xia, B.-S. Zhang, R.-Q. Jiao and Y.-M. Liang, *Journal of the American Chemical Society*, 2021, **143**, 7868-7875.
139. N. J. Truax and D. Romo, *Natural Product Reports*, 2020, **37**, 1436-1453.
140. A. P. Antonchick, C. Gerding-Reimers, M. Catarinella, M. Schürmann, H. Preut, S. Ziegler, D. Rauh and H. Waldmann, *Nature Chemistry*, 2010, **2**, 735-740.
141. W. Nie, J. Gong, Z. Chen, J. Liu, D. Tian, H. Song, X.-Y. Liu and Y. Qin, *Journal of the American Chemical Society*, 2019, **141**, 9712-9718.
142. Z. Zhou, A. X. Gao and S. A. Snyder, *Journal of the American Chemical Society*, 2019, **141**, 7715-7720.
143. R. Andres, Q. Wang and J. Zhu, *Journal of the American Chemical Society*, 2020, **142**, 14276-14285.
144. F. P. Lee, Y. C. Chen, J. J. Chen, I. L. Tsai and I. S. Chen, *Helvetica Chimica Acta*, 2004, **87**, 463-468.
145. W. R. Gutekunst and P. S. Baran, *Journal of the American Chemical Society*, 2011, **133**, 19076-19079.
146. R. A. Panish, S. R. Chintala and J. M. Fox, *Angewandte Chemie-International Edition*, 2016, **55**, 4983-4987.
147. J. L. Hu, L. W. Feng, L. J. Wang, Z. W. Xie, Y. Tang and X. G. Li, *Journal of the American Chemical Society*, 2016, **138**, 13151-13154.
148. W. R. Gutekunst and P. S. Baran, *J Am Chem Soc*, 2011, **133**, 19076-19079.
149. R. A. Panish, S. R. Chintala and J. M. Fox, *Angewandte Chemie International Edition*, 2016, **55**, 4983-4987.
150. J.-L. Hu, L.-W. Feng, L. Wang, Z. Xie, Y. Tang and X. Li, *Journal of the American Chemical Society*, 2016, **138**, 13151-13154.
151. Z.-Y. Xue, T.-L. Liu, Z. Lu, H. Huang, H.-Y. Tao and C.-J. Wang, *Chemical Communications*, 2010, **46**, 1727-1729.
152. A. P. Antonchick, C. Gerding-Reimers, M. Catarinella, M. Schürmann, H. Preut, S. Ziegler, D. Rauh and H. Waldmann, *Nat Chem*, 2010, **2**, 735-740.
153. J. F. Zhou, J. M. Xu, H. Wei and L. L. Zhang, *Chinese Journal of Organic Chemistry*, 2001, **21**, 322-324.
154. S. D. Sanders, A. Ruiz-Olalla and J. S. Johnson, *Chemical Communications*, 2009, DOI: 10.1039/B911765B, 5135-5137.
155. Q.-Q. Cheng, Z. Zhou, H. Jiang, J. H. Siitonen, D. H. Ess, X. Zhang and L. Kürti, *Nature Catalysis*, 2020, **3**, 386-392.

156. O. V. Dolomanov, L. J. Bourhis, R. J. Gildea, J. A. K. Howard and H. Puschmann, *Journal of Applied Crystallography*, 2009, **42**, 339-341.
157. G. Sheldrick, *Acta Crystallographica Section A*, 2015, **71**, 3-8.
158. G. Sheldrick, *Acta Crystallographica Section C*, 2015, **71**, 3-8.
159. L. Farrugia, *Journal of Applied Crystallography*, 1997, **30**, 565.

7. Appendix

7.1 List of abbreviations

Ac	acetyl
AcOH	acetic acid
AgOAc	silver acetate
aq.	aqueous
BEMP	2-tert-Butylimino-2-diethylamino-1,3-dimethylperhydro-1,3,2-diazaphosphorine
Bn	benzyl
CA	cycloaddition
calcd	calculated
cat.	catalyst
Cs ₂ CO ₃	cesium carbonate
COMAS	Compound Management and Screening Center
conc.	concentration
DBU	1,8-diazabicyclo[5.4.0]undec-7-ene
DCE	1,2-dichloroethane
DCM	dichloromethane
DEAD	diethyl azodicarboxylate
DIPEA	diisopropylethylamine
DMAP	4-(Dimethylamino)pyridine
DMF	dimethylformamide
DMSO	dimethylsulfoxide
d.r.	<i>diastereomeric ratio</i>
e.e.	<i>enantiomeric excess</i>
ESI	electrospray ionization
Et	ethyl
Et ₃ N	triethylamine
Et ₂ O	diethylether
EtOAc	ethylacetate
equiv.	equivalent
EWG	electron withdrawing group

FT-IR	Fourier-Transform Infrared spectroscopy
h	hour
HFIP	Hexafluoroisopropanol
HOSA	Hydroxylamine-O-sulfonic acid
HPLC	high-performance liquid chromatography
HRMS	high resolution mass spectrometry
HTIB	[Hydroxy(tosyloxy)iodo]benzene
Hz	Hertz
IBX	2-Iodoxybenzoic acid
IC ₅₀	half-maximal inhibitory concentration
<i>i</i> Bu	<i>iso</i> -butyl
<i>i</i> Pr	iso-propyl
<i>J</i>	coupling constants
LDA	lithium diisopropylamide
LUMO	lowest unoccupied molecular orbital
<i>m</i>	meta
Me	methyl
MeCN	acetonitrile
MLCK1	Myosin light chain kinase
NMR	nuclear magnetic resonance
n.d.	not detected
NP	Natural product
Nu	Nucleophile
<i>o</i>	ortho
OAc	acetate
Oxone	potassium peroxymonosulfate
<i>p</i>	para
PIDA	(Diacetoxyiodo)benzene
PIFA	[Bis(trifluoroacetoxy)iodo]benzene
Ph	phenyl
PPh ₃	triphenylphosphine
ppm	parts per million

PPTS	pyridinium <i>p</i> -toluenesulfonate
rt	room temperature
<i>p</i> TsOH	para toluenesulfonic acid
R_f	Retention factor
Sat.	saturated
TBAF	tetra- <i>n</i> -butylammonium fluoride
TBDPS	<i>tert</i> -Butyldiphenylsilyl
<i>t</i> Bu	<i>tert</i> -butyl
TBS	<i>tert</i> -butyldimethylsilyl.
Temp.	temperature
TFE	2,2,2-trifluoroethanol
TMS	trimethylsilyl
TIPS	triisopropylsilyl
THF	tetrahydrofuran
t_R	retention time
Ts	<i>p</i> -toluenesulfonyl
TsCl	Para toluenesulfonyl chloride
XeF ₂	xenon fluoride

7.2 Acknowledgement

First of all, I am extremely grateful to Prof. Dr. Herbert Waldmann and would like to thank him for giving me the opportunity to work in such an excellent scientific environment and his invaluable advice, continuous support during my PhD study. I am also deeply grateful to him for being my first examiner.

I would like to express my gratitude to Prof. Dr. Andrey Antonchick for all his help and invaluable advice during my PhD study. His in-depth understanding in organic chemistry, especially in new method development, helps fast identification problem and hence accelerate the progress of my PhD project. Importantly, his patience and trust provides me the room to explore and verify more scientific ideas. and I am also deeply grateful to him for being my second examiner.

I would like to thank all analytic departments involved in the characterization of the synthesized compounds emphasizing my gratitude to Miss. Svetlana Gerdt for the maintenance of the analytical HPLCs, Dr. Petra Janning and Miss. Christiane Heitbrink for HRMS measurements as well as Mr. Bernhard Griewel and the NMR-Team of the TU Dortmund for all NMR experiments. I would like to express my gratitude to Prof. Dr. Carsten Strohmann and Mr. Lukas Brieger for carrying out the X-ray analysis.

I would like to thank my colleagues for helpful and inspiring discussion in my PhD research project, including Dr. Houhua, Li, Dr. Chunfa, Xu , Dr. Yusheng, Xie, Dr. Michael Grigalunas and Dr. Saad Shaaban.

I would like to thank the whole department IV for the great working atmosphere that made me enjoy my PhD every day. I want to especially name Vicky, Mahesh, Okan, Jie, Lin, Jianing and Sukdev.

Finally, my deepest appreciation goes to my family for their continuous support and encouragement.